The G protein-coupled receptor GPR30 signalosome - A novel G protein-independent mechanism regulating cAMP signaling and receptor trafficking

Broselid, Stefan

2014

The G protein-coupled receptor GPR30 signalosome

A novel G protein-independent mechanism regulating cAMP signaling and receptor trafficking

by
Stefan Broselid

LUND
UNIVERSITY

DOCTORAL DISSERTATION

With the approval from the Faculty of Medicine, Lund University, the public defense of this thesis will be defended on January 9, 2015, at 13:00 in Segerfalksalen, Biomedicinskt centrum, Sölvegatan 19, Lund.

Faculty opponent
Professor Graeme Milligan
University of Glasgow

Organization: LUND UNIVERSITY	Document name: DOCTORAL DISSERTATION
	Date of issue
Author(s): Stefan Broselid	Sponsoring organization

Title and subtitle

The G protein-coupled receptor GPR30 signalosome

A novel G protein-independent mechanism regulating cAMP signaling and receptor trafficking

Abstract

The large protein family called G Protein-coupled receptors (GPCRs) has co-evolved with life throughout evolution; from single cell organisms all the way to complex beings such as us humans. The fact that GPCRs are involved in essentially every physiological event, and that ~50% of drugs on the current market are either directly or indirectly targeted towards the function of GPCRs, we can be certain of their considerable importance.

This thesis is dedicated solely to one particular GPCR, GPR30. This receptor is shrouded in uncertainty with contradictory results and opposing views on effectors and subcellular localization. The aim of this thesis was to elucidate the signaling and membrane trafficking of GPR30 in addition to look for any binding partners.

My primary findings were:

(1) GPR30 constitutively internalizes without any need for ligand binding.
(2) GPR30 associates with cytokeratin filaments
(3) GPR30 expression in ER^+ breast cancer is a favorable prognostic marker for distant-disease-free survival.
(4) GPR30 confer some constitutive pro-apoptotic signaling but also readily sensitizes the cells to other apoptotic stimuli.
(5) GPR30 directly associates with RAMP3 in-vivo and in-vitro and RAMP3 expression has an impact on GPR30 subcellular localization in the murine heart.
(6) GPR30 constitutively form a signalosome with Membrane associated guanylate kinase proteins (MAGUKs) and A Kinase Anchoring Protein 5 (AKAP5) through its C-terminal PDZ-motif. PKA-RII, which directly binds to AKAP5, is responsible for the attenuation of cAMP in response to cAMP-elevating agents.

Key words

GPER, GPER1, GPR30, estrogen signaling, G1, MAGUK, AKAP5, PDZ, cAMP

Classification system and/or index terms (if any)

Supplementary bibliographical information	Language ENGLISH
ISSN and key title 1652-8220	ISBN 978-91-7619-082-1
Recipient's notes / Number of pages 100	Price
	Security classification

Signature  Date 2014-12-05

The G protein-coupled receptor GPR30 signalosome

A novel G protein-independent mechanism regulating cAMP signaling and receptor trafficking

by

Stefan Broselid

Group of Drug Target Discovery
Department of Experimental Medical Science
Faculty of Medicine
2015

LUND
UNIVERSITY

Cover image:
MDCK cells, fixed and stained with anti-GPR30 antibody, followed by alexa488 anti-donkey antibody for visualization.

Lund University, Faculty of Medicine Doctoral Dissertation Series 2015:2

ISBN 978-91-7619-082-1
ISSN 1652-8220

Printed in Sweden by Media-Tryck, Lund University
Lund 2014

I can do science, me!

Table of contents

Abbreviations

4-OHT	4-hydroxy-tamoxifen
5HT2AR	5-HT_{2a} Receptor
5HT2CR	5-HT_{2c} Receptor
7TMR	7-transmembrane-receptor
ADP	Adenosine diphosphate
AKAP	A kinase-anchoring protein
AT_1R	Angiotensin II Receptor, type I
ATP	Adenosine triphosphate
BPA	Bisphenol A
cAMP	cyclic Adenosine Mono Phosphate
CCL-18	Chemokine ligand 18
CTGF	Connective Tissue Growth Factor
CXCR4	C-X-C chemokine receptor type 4
D1R	Dopamine Receptor D_1
DAG	Diacylglycerol
EGFR	Epidermal growth factor receptor
E2	17-β-estradiol
EEA1	Early endosomal antigen 1
EP_1R	Prostaglandin E receptor 1
ER	Endoplasmatic reticulum
ERK	Extracellular signal regulated protein kinase
ERα	Estrogen receptor α
FCS	Fetal calf serum
G protein	Guanine nucleotide regulatory protein
GDP	Guanosine diphosphate
GEF	Guanine nucleotide exchange factor
GPCR	G protein-coupled receptor
GPER	G protein-coupled estrogen receptor
GRK	GPCR-regulated protein kinase
GTP	Guanosine triphosphate
HEK293	Human embryonic kidney 293 cells
HRP	Horseradish peroxidase

IL8-R	Interleukin 8 Receptor
IP_3	Inositol trisphosphate
M3R	Muscarinic acetylcholine receptor M3
MAGI-2	membrane-associated guanylate kinase inverted 2
MAGUK	Membrane-associated guanylate kinase
MAPK	Mitogen Activated Protein Kinase
MAPK	Mitogen-activated protein kinase
MCF-7	Michigan Cancer Foundation-7 cells (ER^+ breast cancer cell)
MDCK	Madin Darby canine kidney cells
mGlu2R	Metabotropic glutamate receptor 2
PARP	Poly ADP ribose polymerase
PBS	Phosphate-buffered saline
PDZ	Post-synaptic-density-protein 95 Drosophila disc-large tumor suppressor (DlgA) Zo-1 protein
PI3K	Phosphatidylinositol 3-kinase
PIP2	Phosphatidylinositol 4,5-bisphosphate
PKA	Protein Kinase A
PKC	Protein Kinase C
PLC	Phospholipase C
PNGase F	Protein N-glycosidase
PP1	Protein Phosphatase 1
PP2B	Protein Phosphatase 2B/Calcineurin
PSD-95	Post-synaptic density protein 95
RAMP	Receptor activity modifying protein
SAP97	Synapse associated protein 97
SSTR5	Somatostatin receptor type 5
β1AR	β1-adrenergic receptor
β2AR	β2-adrenergic receptor
γOR	γ Opioid Receptor
δOR	δ Opioid Receptor

List of included publications

Paper I

G protein-coupled estrogen receptor 1/G protein-coupled receptor 30 localizes in the plasma membrane and traffics intracellularly on cytokeratin intermediate filaments.
Sandén C*, Broselid S*, Cornmark L, Andersson K, Daszkiewicz-Nilsson J, Mårtensson UE, Olde B, Leeb-Lundberg LM.
Mol Pharmacol. 2011 Mar;79(3):400-10

Paper II

G protein-coupled estrogen receptor is apoptotic and correlates with increased distant disease-free survival of estrogen receptor-positive breast cancer patients.
Broselid S*, Cheng B*, Sjöström M*, Lövgren K, Klug-De Santiago HL, Belting M, Jirström K, Malmström P, Olde B, Bendahl PO, Hartman L, Fernö M, Leeb-Lundberg LM.
Clin Cancer Res. 2013 Apr 1;19(7):1681-92

Paper III

G-protein-coupled receptor 30 interacts with receptor activity-modifying protein 3 and confers sex-dependent cardioprotection.
Lenhart PM, Broselid S, Barrick CJ, Leeb-Lundberg LM, Caron KM.
J Mol Endocrinol. 2013 Jul 3;51(1):191-202

Paper IV

G protein-coupled Receptor 30 (GPR30) Forms a Plasma Membrane Complex with Membrane-associated Guanylate Kinases (MAGUKs) and Protein Kinase A-anchoring Protein 5 (AKAP5) That Constitutively Inhibits cAMP Production
Broselid S, Berg K, Chavera T, Kahn R, Clarke W, Olde B, Leeb-Lundberg LM
J Biol Chem. 2014 Aug 8;289(32):22117-27

*** Shared first authorship**

Preface

This thesis is all about a single protein, the enigmatic receptor GPR30.

This receptor is associated with multiple cancer forms and reported to be activated by multiple endogenous ligands. Notably, the female sex hormone estrogen is proposed to be the cognate ligand by what looks like the majority of GPR30 researchers. This has given the receptor the (controversial) name G Protein coupled Estrogen Receptor (GPER), a name I have chosen to not use in this thesis because of reasons that will become apparent to the reader as he/she reads on.

It is undeniable that the conflicting reports are numerous with regards to GPR30 signaling, agonist specificity, receptor localization, its potential role in cancer, as well as other fundamental parts of its pharmacology and function. This has made the research area of GPR30 a tough field to navigate, to say the least. Apparently, incoherent results, unfortunate unusual methodology and irreproducibility all haunt what makes up existing knowledge. The only conclusion must be, that, even today, some 18 years after its discovery, there is a considerable amount of missing information about how this receptors functions at the cellular and molecular level.

To try to resolve the discrepancy, I have dedicated my Ph. D. years to study this atypical receptor. In doing so, I have learned a significant amount and also enjoyed contributing to the growing knowledge of GPR30. My research has resulted in four published articles, in which I present novel results and insights regarding GPR30 signaling, subcellular localization, membrane trafficking and multiple newly discovered interacting proteins and more. These articles make up the basis of this thesis. Enjoy!

/Stefan Broselid, Ph.D.

Introduction

This thesis describes my work with a controversial seven-trans-membrane receptor (7TMR) called GPR30. It is purported to be activated by estrogen and is therefore also called G Protein Estrogen Receptor (GPER). It is also reported to be activated by aldosterone, genistein, BPA, CCL-18 and not to mention the "GPR30-specific" synthetic compound G1. A lot of "what is known" about GPR30 is built upon frail ground and unrepeatable results obtained through obscure methods. To overcome most of these obstacles I have eventually come to study the effects that the receptor confers by itself, just by being expressed in a cell.

G protein-coupled receptors (GPCRs)

The protein family we call G protein-coupled receptors (GPCRs), to which my receptor of interest, G Protein-coupled receptor 30 (GPR30) is a member of, is currently the most important family of targets for clinically useful drugs, and is expected to remain so for the foreseeable future. How so? These receptor proteins are the initiators of complex intracellular signaling involved in essentially all physiological events. Faulty receptor signaling can manifest itself in disease, emphasizing the importance of this field of science. The fact that there are so many different GPCRs and that they have remained and co-evolved during evolution and are thus found in early organisms such as bacteria, yeast, plants, insects as well as more advanced organisms such as vertebrates and mammals (Schiöth and Fredriksson, 2005) speaks for their importance by itself.

Still today, as pharmaceutical companies and academia around the world have worked for half a century to try to understand and identify these receptors, there are believed to be more than 200 so called orphan receptors remaining in humans. Orphan receptors are those receptors to which no endogenous ligand has yet been identified (Jassal *et al.,* 2010). The total amount of GPCRs in the human genome is unknown but predicted to be around 800 (Jassal *et al.,* 2010). Thus, one in four GPCRs in the human genome remain classified as orphan receptors.

Is it possible that there is a subset of GPCRs that do not necessarily couple and signal through G proteins?

The original definition of these receptor types (before there was any knowledge of G proteins) were 7TMRs but the name is not as commonly adapted as GPCRs. The name 7TMR has the advantage of not assuming that G proteins inherently must be involved in the signaling of the receptor, something that some researchers may at first have a hard time to grasp.

There are many GPCRs that, aside from classical G protein-mediated signaling, are known to signal through G protein-independent pathways. Even though I have nothing to back this up with, I would not rule out the possibility that some GPCRs may have evolved without the need for an extracellular ligand or associated G protein. Instead these 7TMRs might signal through other mechanisms by acting as membrane-bound docking proteins and associating with G protein-coupled receptor interacting proteins (GIPs) and in many cases being part of larger protein complexes or signalosomes. My point has hopefully been made and semantics and nomenclature aside, henceforth I will refer to the receptors as GPCRs to avoid any further confusion.

The superfamily of proteins known as GPCRs is one of the largest groups of proteins in the vertebrate genome with members found in all eukaryotic cells. Indeed, they constitute the largest single gene family in the human genome and it is worth repeating that there are more than 800 genes coding for different GPCRs identified therein. Of further importance, GPCRs are involved in essentially every physiological response. Furthermore, about 40-50% of all drugs used clinically today, target the function of these receptors either directly or indirectly (Jacoby *et al., 2006*), indicating that they also constitute the most important drug targets known.

Despite their extreme diversity in function, all GPCRs share the superstructural feature of spanning the plasma membrane seven times, which is why they are sometimes referred to as 7TMRs (see *Figure 1).* As the name suggests, this means that all mature GPCRs have an extracellular N-terminal tail, three intracellular loops, three extracellular loops and a C-terminal intracellular tail. In between the loops are seven hydrophobic regions that allow the receptor to reside within the lipid bilayer that makes up the plasma membrane. Aside from the shared 7TM structural homology, the sequential homology in the tails and loops of different GPCRs is remarkably low, likely reflecting their large functional diversity.

A simplified analogy useful to describe GPCRs is that they act as "molecular antennae" mostly residing in the plasma membrane awaiting specific extracellular stimuli (lipid, peptide- or steroid hormone, neurotransmitter etc.), which they subsequently convert into intracellular signals, resulting in receptor-specific responses. These antennae vary in their ligand-specificity, i.e. what they bind and respond to.

Some receptors are highly specific and recognize only a single endogenous ligand, whereas other receptors have a broader ligand recognition profile.

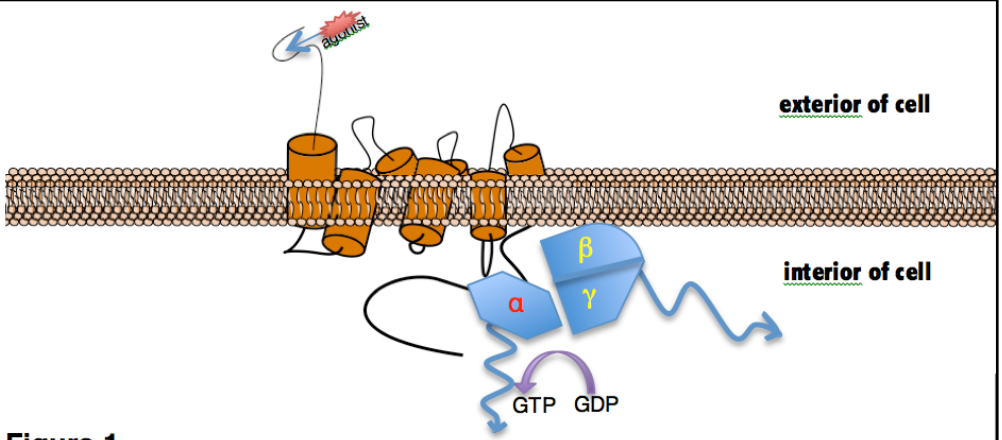

Figure 1
A schematic representation of a GPCR in the plasma membrane, getting activated by an agonist as in the classical model off GPCR signaling. Agonist binding to the receptor jostles the receptor slightly, so that the weak interaction with its associated G protein is altered. As a consequence, the dissociation of GDP and subsequent reassociation of GTP from and to the α-subunit of the associated G protein leads to the activation of two effectors. The activated cytoplasmic α subunit and the activated membrane-bound βγ-subunits are so thus free to influence further signaling downstream. Which pathways that will be affected and what response will occur as a consequence depend on the specific set of α- and βγ-subunits.

An example of the complexity and variability of GPCRs can be made of the adrenergic subfamily of GPCRs. Numerous variants exist and all react to the catecholamines adrenaline or noradrenaline and thus together mediate the sympathetic nervous system activity. Stimulation of these receptors leads to different effects in different parts of the body depending on what specific subtype of adrenergic receptor present. Adrenaline causes an increase in heart rate (mainly through β-adrenergic receptors which are ubiquitous and the predominant types of adrenergic receptors in the heart). At the same time in other tissues, other adrenergic receptors redistribute blood flow and promote optimal oxygenation of skeletal muscle while simultaneously reducing intestinal motility (mainly through α-adrenergic receptors). The combined effects of adrenaline and noradrenaline acting on all the different adrenergic receptors found in the different tissues of the body lead to an increase in what we often call the "fight and flight"-response.

Another example of the high variability within the family of GPCRs is the highly atypical receptor rhodopsin, which is expressed in the rod cells in the retina of the eye and also was the very first GPCR to be crystallized (Rasmussen et al., 2007). Activation of this GPCR is not initiated by the binding of a ligand to the receptor;

instead rhodopsin is activated directly by specific wavelengths of light. An integral part of rhodopsin is called retinal and has the ability to absorb the energy of photons and cause a conformational change in the receptor, thus triggering its activation and initiation of signal transduction.

GPCRs are thought to exist in an equilibrium between inactivate and a series of active conformational states. The degree of activation is tightly regulated by both ligand-dependent and ligand-independent factors. Anything that has the ability to bind the receptor can potentially alter the equilibrium and stabilize a specific conformational state with a specific intrinsic activity. The endogenous cognate ligand of a receptor normally stabilizes the receptor conformation in a state very close to the theoretical R* state, thus promoting receptor-mediated signaling, classifying the cognate ligand as a full agonist (see *Figure 2*).

From many years of studying ligand binding to GPCRs, primarily by the pharmaceutical industry for therapeutic benefit, a multitude of different types of synthetic ligands have been developed. Because of this endeavor, it is known that ligands can also be classified as partial agonists, which are thought to stabilize partially active receptor conformational states and neutral antagonists, which do not perturb the basal equilibrium of receptor states. In addition, there are inverse agonists, which stabilizes inactive receptor conformational states and thus inhibit any constitutive receptor activity (see *Figure 2).*

Figure 2
Current classification system of ligands and the two state-model of GPCR pharmacaology

The functions of GPCRs are classically thought to be mediated by G proteins, which interact with the intracellular part of the receptor (see *Figure 1*) and become active G protein subunits conferring the GPCR-mediated signaling. This classical model is perhaps not entirely wrong, though arguably obsolete.

A new concept has emerged during the last decade or so. It is the notion that some receptors, possibly the majority of them, have specific intracellular protein-protein-interaction domains made up from specific amino acid sequences, which make them the outermost part of a larger intracellular multi-protein structure, often dubbed signalosome or receptosome. These signalosomes are made up of a multitude of different proteins and enzymes, often with opposing effects such as kinases and phosphatases, allowing for a very tight regulation of receptor signaling, both spatially and temporally.

GPCR signaling

GPCR-G protein-mediated signaling

As the name indicates, GPCRs couple to G proteins, which occurs through their intracellular domains. Therefore, most receptor signaling has been studied through these "molecular switches". G proteins are made up of three subunits, the α-, β- and γ subunit. These in turn make up two functional subunits, the α- and the βγ-subunit. There are 20 different α-subunits, 6 β-subunits and 12 γ-subunits found (Clapman and Neer, 1997:37) creating an astounding 1440 theoretical combinations, again in line with the impressive functional diversity of GPCRs. G protein classes are defined based on the function and sequence of their Gα-subunits, the most common being $G\alpha_S$, $G\alpha_i$ and $G\alpha_Q$.

$G\alpha_S$ activation leads to an increase in the second messenger cAMP through direct activation of specific adenylate cyclases, whereas $G\alpha_i$ causes an inhibition of adenylate cyclase. On the other hand, $G\alpha_Q$ causes activation of phospholipase C (PLC) and the production of two different second messengers through hydrolysis of PIP_2 into DAG and IP_3. IP_3 then freely diffuses to IP_3 receptors in the endoplasmatic reticulum (ER), which releases Ca^{2+} into the cytosol and DAG activates protein kinase C (PKC).

The binding of an agonist to a GPCR causes a small but significant conformational shift, allowing for a tighter binding to associated G proteins. This tighter binding between the GPCR and a G protein releases the GDP from the α-subunit of the G protein, allowing the more freely available GTP to bind. The GTP-bound α-subunit then dissociates, activating the effector enzyme, while the activated βγ-subunit mainly resides and affect substrates within the membrane. Re-association of the αβγ complex happens quickly when the GTP is hydrolyzed into GDP. GEFs (Guanine nucleotide exchange factors) are able to influence the speed of this process. Agonist stimulation

of a many GPCRs also commonly triggers receptor internalization, which is a way for the cell to regulate the number of available receptors at any given time or for the receptor to access additional effectors. Internalized receptors can either be stored intracellularly, recycled back to the membrane, or degraded either via the endosomal-lysosomal- or proteosomal degradation pathway.

Receptor activity states and agonist-dependent- and –independent function

Most GPCRs do not function as simple switches waiting for agonists to press the button that starts the signaling process. Instead, research has shown that many GPCRs confer ligand-independent signaling just by being expressed at the cell surface. In a simplified scheme, a GPCR is thought of to exist in an equilibrium between different conformational states, an inactive conformation, R, and an active conformation, R*.

The R* state is considered to be responsible for effective G-protein activation. The equilibrium between R and R* determines the level of ongoing constitutive GPCR signaling. Because of the structural limitations, the equilibrium usually lies closer towards the R state than R*. Agonist binding or site-specific mutations in the GPCRs can shift the equilibrium towards R* leading to increased constitutive GPCR activity. Agonists and antagonists are thought to stabilize different conformations of GPCRs; agonists stabilize conformations closer to R* whereas antagonists stabilize conformations closer to R. Dynamic phosphorylation and dephosphorylation of the GPCR by kinases and phosphatases are also thought to stabilize different conformations with different intrinsic activities. Another class of ligands that are able to modulate the state of activation of GPCRs is called allosteric modulators. Allosteric modulators bind to the receptor at a different site than the orthosteric binding-site and are thus able to fine-tune a receptor response even in presence of a ligand at the orthosteric binding-site.

By increasing receptor density, the absolute amount of R* will increase, making recombinant overexpression a valid strategy to use when investigating both agonist dependent- and independent GPCR signaling. The understanding of intrinsic constitutive signaling led to the reclassification of many substances and compounds previously considered antagonists as inverse agonists, because when intrinsic GPCR activity was investigated, it was found to be inhibited by these compounds.

GPCR oligomerization and GPCR-interacting proteins (GIPs)

GPCRs were previously thought to exist and couple to G proteins primarily as monomers, but research now favors the concept that many receptors have the capacity to oligomerize, thus forming multimeric complexes (Milligan, 2007). GPCRs have been found to form both homodimers and heterodimers with other GPCRs.

Oligomerization has been shown to influence various receptor events such as receptor surface maturation, internalization, ligand binding, and G protein coupling (Somvanshi et al., 2011); (Prinster, 2005). The discovery of hetero-dimerization of different GPCRs has unveiled a new dimension of cross talk between different signaling pathways and possibly pharmacological entities. Notable hetero-oligomers include β2AR-M3R, β2AR-EP_1R, β1AR-SSTR5, γOR-δOR, 5HT2CR-D1R, 5HT2AR-mGlu2R (Barnes, 2006).

Research has shown that the C-terminal domain of GPCRs is the predominant site for protein-protein interactions and regulation of GPCR effects (Bockaert et al., 2004) with more than 50 different GIPs identified at this site. Many GPCR splice variants also show sequence variation primarily in the C-terminal tail. In addition, this domain is also the primary site for a number of important post-translational modifications such as palmitoylation and phosphorylation and such modifications can influence G protein-coupling, ligand binding, internalization, resensitization and localization (Leeb-Lundberg et al., 2005); (Ryan et al., 2008). Important GIPs include G protein-coupled Receptor Kinases (GRKs), which commonly phosphorylate C-terminal serine-residues following receptor activation. Such phosphorylation facilitates the binding of β-arrestins, which subsequently promote receptor internalization through endocytosis (Luttrell and Lefkowitz, 2002).

Arrestins have also been shown to function as scaffold proteins; notably it is well established that β-arrestins can function as scaffolds for components of the Mitogen-activated protein kinase (MAPK)-cascade thus mediating MAPK activation by various GPCRs (Luttrell and Lefkowitz, 2002). Other notable GIPs are proteins with PDZ domains (Olalla et al., 2001). Many GPCRs have PDZ (PSD95-disc large-Zonula occludens) recognition motifs (a.k.a. PDZ ligands) at their extreme C-terminus. These motifs constitute important protein-protein interaction motifs and allows for proteins with PDZ domains to bind and influence the pharmacology and/or receptor localization of a given GPCR. Three hundred and twenty-eight different PDZ domain proteins have been identified in the mouse genome (Lee and Zheng, 2010). PDZ domains can be categorized into three different subtypes based on recognition specificity: class I domains interact with C-terminal motifs X-S/T-X-Φ (where Φ indicates a hydrophobic amino acid and X indicates any amino acid), class II domains with Φ-X-Φ motif and class III domains with D/E-X-Φ motifs. Most GPCRs with C-terminal PDZ motifs are able to bind to a number of different PDZ proteins, often with dramatically different effects. For instance β1AR, which has a type I PDZ-motif in its C-terminal tail (E-S-K-V), interacts with six different PDZ domain-containing proteins, among those the membrane-associated guanylate kinases (MAGUKs) PSD-95 and SAP97, and another PDZ protein, MAGI-2 (He et al., 2006). PSD-95 retains the receptor in the cell membrane in response to agonist stimulation whereas MAGI-2 promotes receptor internalization in response to agonist. A schematic representation of a MAGUK is seen in *Figure* 3 below. As different PDZ domain-containing

proteins are expressed in different tissues, the importance of knowing the expression status of these proteins in for example tumors can not be understated, especially since many of them have been shown to be potent tumor suppressors and involved in GPCR signaling and G protein-switching.

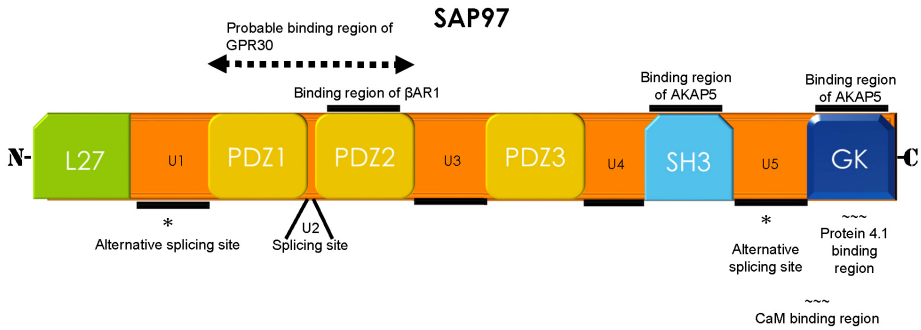

Figure 3
A schematic representation of SAP97, A MAGUK and also a GIP with several PDZ domains as well as other anchoring and interaction domains.

Not a GIP in its literal sense, but PKA-anchoring proteins (AKAPs) are known to dock to MAGUK proteins such as PSD-95 and SAP-97 (Colledge, 2000). One particular AKAP might be of interest since it is known to be involved in β1AR signaling which has a similar extreme C-terminus as GPR30 and that is AKAP5, which is seen in *Figure 4*.

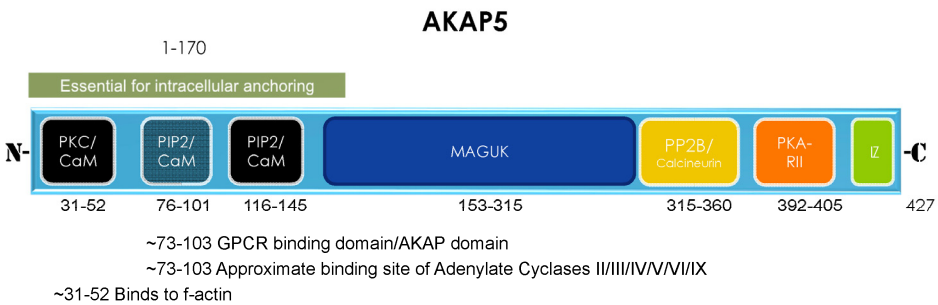

Figure 4
A schematic representation of A Kinase Anchoring protein 5 (AKAP5). AKAP5 constitutively associates with different MAGUKs such as SAP97.

GPR30

GPR30, also known as GPER (G protein-coupled estrogen receptor), is a GPCR that was first cloned in Lund and subsequently in several labs around the world in 1996-1998 (Owman et al., 1996); (Kvingedal and Smeland, 1997); (O'Dowd et al., 1998). Based on sequence homology, its closest relatives are the IL8-R and the AT_1-R. Therefore, it was initially speculated that GPR30 was most likely activated by an endogenously expressed peptide. Catusse *et al.* presented some evidence that the chemokine CCL-18 regulates CXCR4 responsiveness in a GPR30-dependent manner (Catusse et al., 2010) but no consensus regarding this has been established in the scientific community.

In one of the cloning approaches used, HUVECs (Human Umbilical Vein Endothelial Cells) were found to have GPR30 upregulated 8-fold by shear stress (Takada et al., 1997). Another study, investigating GPR30 expression in breast cancer cell lines, found that GPR30 correlated with ERα expression, suggesting that the expression of the two receptors might be regulated by the same transcription factors (Carmeci et al., 1997). Furthermore, in $ER\alpha^+$ MCF-7 cells, progestins were found to enhance GPR30 mRNA expression, and GPR30 had an antiproliferative effect with $GPR30^+$ cells prone be inhibited in the G0/G1 phase. Interestingly, this effect was completely independent of the presence of any steroid hormones such as 17β-estradiol (E2).

GPR30 was, perhaps prematurely, deorphanized by two independent research groups in 2005 (Revankar et al., 2005); (Thomas et al., 2005). Revankar *et al.* reported that GPR30-GFP directly bound a fluorescent Alexa-estradiol-derivative in the ER, whereas Thomas *et al.* reported GPR30-dependent tritiated estradiol binding in plasma membrane fractions. Both these studies have caveats with lacking controls, low amounts of specific binding as well as the use of non-standard methods. Interestingly, they also reported that tamoxifen and ICI-182780, two of the most clinically used anti-estrogens worldwide, apparently acted as agonists through GPR30, in sharp contrast to their antagonistic effects on nuclear ERs. These findings led to a number of publications where the effects of E2, which could not be abrogated by tamoxifen or ICI-182780, were directly attributed to GPR30. Revankar *et al.* also reported sustained Ca^{2+} signals through a PI3K-mediated pathway in response to estrogen, whereas Thomas *et al.* reported a very modest cAMP response and GTPγS binding in GPR30-transfected cells upon E2 stimulation.

In 2004, Maggiolini *et al.* performed gene expression analysis of ER^- SKBr3 cells and found that C-fos and CTGF genes were specifically upregulated in response to micromolar concentrations of E2, and that the C-fos induction was inhibited when an anti-sense vector against GPR30 was used to silence endogenous GPR30

expression (Maggiolini et al., 2004). Using ERK-inhibitors and EGFR-inhibitors, they also provided evidence that the C-fos induction involved transactivation of the EGFR, which subsequently induced a MAPK-response. In the same article, they reported that they were unable to induce any C-fos expression in SKBr3 cells when stimulated with ICI-182780 or 4-hydroxy-tamoxifen (4-OHT). In 2009 however, the same researchers found that 10uM 4-OHT (an extremely high concentration) induced C-fos and CTGF in the same SkBr3 cells (Pandey et al., 2009), a strange contradiction to their work five years earlier for which they gave no explanation. Langer *et al.* (2010) points out additional caveats to their studies (Langer et al., 2010), including that the 4-OHT concentrations were unusually high, and that the genomic changes seen in response to E2 and 4-OHT are very similar to a receptor-independent stress response, a response that has been shown to occur with 4-OHT in such high concentrations (Morley and Whitfield, 1994).

The lack of a reliable antibody against human or murine GPR30 has made the studying of its expression and localization a challenge. Because of this, other less sensitive methods have been used to investigate the subcellular localization of GPR30. Revankar *et al.* (2005) made use of a GFP-GPR30 fusion-protein that they found to be retained in the ER when ectopically overexpressed in COS-7 cells lacking endogenous GPR30. Revankar *et al.* reported no plasma membrane localization of endogenous GPR30 in any of the investigated cell lines, including MCF7, SKBr3, MDA-MB231, JEG and Hec50 when using an antiserum produced against the C-terminus of GPR30. In stark contrast, later studies by many different research groups have shown plasma membrane localization of GPR30 in the same cell lines. Another group showed that HeLa cells transiently transfected with N-terminally flag-tagged GPR30, a less disruptive tag compared to GFP-tagging, do have GPR30 in the cell membrane (Funakoshi et al., 2006). The same group also identified endogenous GPR30 in the cell membrane of pyramidal neurons with their in house-produced polyclonal antibody. Similar results have also surfaced from another group regarding HA-tagged GPR30 in HEK293 cells and endogenous SKBr3 cells (Thomas et al., 2005). The discrepancies in receptor localization can be explained by the different methods employed and by the use of unspecific antibodies, a common problem in GPCR research (Michel et al., 2009). The use of a GFP-GPCR fusion protein is particularly controversial, as the covalent attachment of a GFP-moiety to the C-terminal end of a GPCR, as used by Revankar *et al. (2005),* will most likely interfere with GIPs that normally bind to the C-terminus of untagged endogenous receptors. Careful comparison of GFP-fusion proteins and epitope-tagged proteins with endogenous untagged protein should always be performed, something that unfortunately has not always been taken in to consideration in GPR30 research.

In 2006, Bologa *et al.* identified G1 as a GPR30 specific agonist through a virtual in-silico screening. Its effects were evaluated using Alexa-labelled E2 and GPR30-GFP in

COS-7 cells with all the mentioned caveats. G1 caused a dose-dependent sustained Ca^{2+} signal in transfected cells that was not detected in wild-type COS-7 cells. G15, a structurally very similar analog of G1, was later developed as a specific antagonist for GPR30 based on its ability to inhibit G1 effects (Dennis et al., 2009).

In 2010, Kang *et al.* presented compelling evidence that G1 might not be GPR30-specific but instead an agonist for ERα36, a splice variant of ERα. GPR30 expression was found to induce the expression of ERα36, and specific binding of G1 to SKBr3 cells with silenced GPR30 but functional ERα36 was shown. Subsequently, Wang *et al. (*2012) presented additional evidence for GPR30-independent effects of G1 as they observed suppression of cell proliferation and pro-apoptotic signaling in both native and recombinant cell lines independent of GPR30 expression. Other research groups have reported numerous GPR30-independent effects of G1 such as microtubule reorganization (Holm et al., 2012), antiproliferation and apoptotic signaling (Wang et al., 2012).

Taken together, the signaling through GPR30 is far from elucidated and caution should be used when interpreting data obtained through the use of the proposed agonist G1 and antagonist G15, both of which are routinely used in labs all over the world as a means to detect GPR30-specific effects.

GPR30 and cancer

Given that GPR30 is reportedly activated by tamoxifen, and the fact that one in four breast cancer patients with ER^+ tumors do not respond to anti-estrogens (Wittliff, 1984), GPR30 expression has been studied in breast cancer biopsies in a number of studies. Filardo *et al.* (2006) investigated GPR30 expression in 321 cases of primary breast cancer as well as in normal breast tissue and found that the receptor is expressed both in healthy and cancerous mammary tissue. They also found that GPR30 expression positively correlates with ER expression, PGR expression, Her2 expression, tumor size, and with metastasis. Later studies have confirmed GPR30 correlation with ER, PGR and Her2 (Sjöström et al., 2014).

The prognostic value of GPR30 in different cancers is however not yet fully understood as there are conflicting reports regarding survival and GPR30 expression levels. GPR30 expression has been evaluated in cancers from other estrogenic tissues asides from breast cancer, for instance ovarian cancer, where the authors could not see any correlation of GPR30 with any clinicopathological factors (Kolkova et al., 2012). The fact that tamoxifen possibly works as an agonist through GPR30 could offer an explanation to the existence of tamoxifen-resistant ER^+ cancer as when a tumor becomes more advanced, it tends to lose its ER expression.

.

References

Akama, K.T., Thompson, L.I., Milner, T.A., McEwen, B.S., 2013. Post-synaptic density-95 (PSD-95) binding capacity of G-protein-coupled receptor 30 (GPR30), an estrogen receptor that can be identified in hippocampal dendritic spines. J. Biol. Chem. 288, 6438–6450. doi:10.1074/jbc.M112.412478

Barnes, P.J., 2006. Receptor heterodimerization: a new level of cross-talk. Journal of Clinical Investigation 116, 1210–1212. doi:10.1172/JCI28535

Bockaert, J., G. Roussignol, C. Bécamel, S. Gavarini, L. Joubert, A. Dumuis, L. Fagni, and P. Marin. "GPCR-Interacting Proteins (GIPs): Nature and Functions." *Biochemical Society Transactions* 32, no. Pt 5 (November 2004): 851–55. doi:10.1042/BST0320851.

Carmeci, C., D. A. Thompson, H. Z. Ring, U. Francke, and R. J. Weigel. "Identification of a Gene (GPR30) with Homology to the G-Protein-Coupled Receptor Superfamily Associated with Estrogen Receptor Expression in Breast Cancer." *Genomics* 45, no. 3 (November 1, 1997): 607–17. doi:10.1006/geno.1997.4972.

Catusse, J., S. Wollner, M. Leick, P. Schröttner, I. Schraufstätter, and M. Burger. "Attenuation of CXCR4 Responses by CCL18 in Acute Lymphocytic Leukemia B Cells." *Journal of Cellular Physiology* 225, no. 3 (November 2010): 792–800. doi:10.1002/jcp.22284.

Clapham, David E., and Eva J. Neer. "G PROTEIN Bγ SUBUNITS." *Annual Review of Pharmacology and Toxicology* 37, no. 1 (April 1997): 167–203. doi:10.1146/annurev.pharmtox.37.1.167.

Colledge, M., 2000. Targeting of PKA to Glutamate Receptors through a MAGUK-AKAP Complex. Neuron 27, 107–119. doi:10.1016/S0896-6273(00)00013-1

Dennis, Megan K., Ritwik Burai, Chinnasamy Ramesh, Whitney K. Petrie, Sara N. Alcon, Tapan K. Nayak, Cristian G. Bologa, et al. "In Vivo Effects of a GPR30 Antagonist." *Nature Chemical Biology* 5, no. 6 (June 2009): 421–27. doi:10.1038/nchembio.168.

Filardo, Edward J., Carl T. Graeber, Jeffrey A. Quinn, Murray B. Resnick, Dilip Giri, Ronald A. DeLellis, Margaret M. Steinhoff, and Edmond Sabo. "Distribution of GPR30, a Seven Membrane-Spanning Estrogen Receptor, in Primary Breast Cancer and Its Association with Clinicopathologic Determinants of Tumor Progression." *Clinical Cancer Research: An Official Journal of the American Association for Cancer Research* 12, no. 21 (November 1, 2006): 6359–66. doi:10.1158/1078-0432.CCR-06-0860.

Funakoshi, Takeshi, Akie Yanai, Koh Shinoda, Michio M. Kawano, and Yoichi Mizukami. "G Protein-Coupled Receptor 30 Is an Estrogen Receptor in the Plasma Membrane." *Biochemical and Biophysical Research Communications* 346, no. 3 (August 4, 2006): 904–10. doi:10.1016/j.bbrc.2006.05.191.

He, J., Bellini, M., Inuzuka, H., Xu, J., Xiong, Y., Yang, X., Castleberry, A.M., Hall, R.A., 2006. Proteomic analysis of beta1-adrenergic receptor interactions with PDZ scaffold proteins. J. Biol. Chem. 281, 2820–2827. doi:10.1074/jbc.M509503200

Holm, Anders, Per-Olof Grände, Richard F. Ludueña, Björn Olde, Veena Prasad, L. M. Fredrik Leeb-Lundberg, and Bengt-Olof Nilsson. "The G Protein-Coupled Oestrogen Receptor 1 Agonist G-1 Disrupts Endothelial Cell Microtubule Structure in a Receptor-Independent Manner." *Molecular and Cellular Biochemistry* 366, no. 1–2 (July 2012): 239–49. doi:10.1007/s11010-012-1301-3.

Jacoby, Edgar, Rochdi Bouhelal, Marc Gerspacher, and Klaus Seuwen. "The 7 TM G-Protein-Coupled Receptor Target Family." *ChemMedChem* 1, no. 8 (August 2006): 761–82. doi:10.1002/cmdc.200600134.

Kolkova, Z., Casslén, V., Henic, E., Ahmadi, S., Ehinger, A., Jirström, K., Casslén, B., 2012. The G protein-coupled estrogen receptor 1 (GPER/GPR30) does not predict survival in patients with ovarian cancer. J Ovarian Res 5, 9. doi:10.1186/1757-2215-5-9

Kvingedal, A.M., Smeland, E.B., 1997. A novel putative G-protein-coupled receptor expressed in lung, heart and lymphoid tissue. FEBS Lett. 407, 59–62.

Langer, Gernot, Benjamin Bader, Luca Meoli, Jörg Isensee, Martina Delbeck, Patricia Ruiz Noppinger, and Christiane Otto. "A Critical Review of Fundamental Controversies in the Field of GPR30 Research." *Steroids* 75, no. 8–9 (September 2010): 603–10. doi:10.1016/j.steroids.2009.12.006.

Leeb-Lundberg, L. M. Fredrik, Francois Marceau, Werner Müller-Esterl, Douglas J. Pettibone, and Bruce L. Zuraw. "International Union of Pharmacology. XLV. Classification of the Kinin Receptor Family: From Molecular Mechanisms to Pathophysiological Consequences." *Pharmacological Reviews* 57, no. 1 (March 2005): 27–77. doi:10.1124/pr.57.1.2.

Lee, Ho-Jin, and Jie J Zheng. "PDZ Domains and Their Binding Partners: Structure, Specificity, and Modification." *Cell Communication and Signaling* 8, no. 1 (2010): 8. doi:10.1186/1478-811X-8-8.

Luttrell, L.M., Lefkowitz, R.J., 2002. The role of beta-arrestins in the termination and transduction of G-protein-coupled receptor signals. J. Cell. Sci. 115, 455–465.

Maggiolini, Marcello, Adele Vivacqua, Giovanna Fasanella, Anna Grazia Recchia, Diego Sisci, Vincenzo Pezzi, Daniela Montanaro, Anna Maria Musti, Didier Picard, and Sebastiano Andò. "The G Protein-Coupled Receptor GPR30 Mediates c-Fos up-Regulation by 17beta-Estradiol and Phytoestrogens in Breast Cancer Cells." *The Journal of Biological Chemistry* 279, no. 26 (June 25, 2004): 27008–16. doi:10.1074/jbc.M403588200.

Michel, Martin C., Thomas Wieland, and Gozoh Tsujimoto. "How Reliable Are G-Protein-Coupled Receptor Antibodies?" *Naunyn-Schmiedeberg's Archives of Pharmacology* 379, no. 4 (April 2009): 385–88. doi:10.1007/s00210-009-0395-y.

Milligan, G., 2007. G protein-coupled receptor dimerisation: Molecular basis and relevance to function. Biochimica et Biophysica Acta (BBA) - Biomembranes 1768, 825–835. doi:10.1016/j.bbamem.2006.09.021

Milligan, G. "A Day in the Life of a G Protein-Coupled Receptor: The Contribution to Function of G Protein-Coupled Receptor Dimerization." *British Journal of Pharmacology* 153 Suppl 1 (March 2008): S216–29. doi:10.1038/sj.bjp.0707490.

Morley, P., Whitfield, J.F., 1994. Effect of tamoxifen on carbachol-triggered intracellular calcium responses in chicken granulosa cells. Cancer Res. 54, 69–74.

O'Dowd, B. F., T. Nguyen, A. Marchese, R. Cheng, K. R. Lynch, H. H. Heng, L. F. Kolakowski, and S. R. George. "Discovery of Three Novel G-Protein-Coupled Receptor Genes." *Genomics* 47, no. 2 (January 15, 1998): 310–13. doi:10.1006/geno.1998.5095.

Olalla, L., Aledo, J.C., Bannenberg, G., Márquez, J., 2001. The C-terminus of human glutaminase L mediates association with PDZ domain-containing proteins. FEBS Lett. 488, 116–122.

Owman, C., P. Blay, C. Nilsson, and S. J. Lolait. "Cloning of Human cDNA Encoding a Novel Heptahelix Receptor Expressed in Burkitt's Lymphoma and Widely Distributed in Brain and Peripheral Tissues." *Biochemical and Biophysical Research Communications* 228, no. 2 (November 12, 1996): 285–92. doi:10.1006/bbrc.1996.1654.

Pandey, Deo Prakash, Rosamaria Lappano, Lidia Albanito, Antonio Madeo, Marcello Maggiolini, and Didier Picard. "Estrogenic GPR30 Signalling Induces Proliferation and Migration of Breast Cancer Cells through CTGF." *The EMBO Journal* 28, no. 5 (March 4, 2009): 523–32. doi:10.1038/emboj.2008.304.

Prinster, S.C., 2005. Heterodimerization of G Protein-Coupled Receptors: Specificity and Functional Significance. Pharmacological Reviews 57, 289–298. doi:10.1124/pr.57.3.1

Rasmussen, S.G.F., Choi, H.-J., Rosenbaum, D.M., Kobilka, T.S., Thian, F.S., Edwards, P.C., Burghammer, M., Ratnala, V.R.P., Sanishvili, R., Fischetti, R.F., Schertler, G.F.X., Weis, W.I., Kobilka, B.K., 2007. Crystal structure of the human beta2 adrenergic G-protein-coupled receptor. Nature 450, 383–387. doi:10.1038/nature06325

Revankar, Chetana M., Daniel F. Cimino, Larry A. Sklar, Jeffrey B. Arterburn, and Eric R. Prossnitz. "A Transmembrane Intracellular Estrogen Receptor Mediates Rapid Cell Signaling." *Science (New York, N.Y.)* 307, no. 5715 (March 11, 2005): 1625–30. doi:10.1126/science.1106943.

Schiöth, H.B., Fredriksson, R., 2005. The GRAFS classification system of G-protein coupled receptors in comparative perspective. Gen. Comp. Endocrinol. 142, 94–101. doi:10.1016/j.ygcen.2004.12.018

Sjöström, M., Hartman, L., Grabau, D., Fornander, T., Malmström, P., Nordenskjöld, B., Sgroi, D.C., Skoog, L., Stål, O., Leeb-Lundberg, L.M.F., Fernö, M., 2014. Lack of G protein-coupled estrogen receptor (GPER) in the plasma membrane is associated with excellent long-term prognosis in breast cancer. Breast Cancer Res. Treat. 145, 61–71. doi:10.1007/s10549-014-2936-4

Somvanshi, R.K., Chaudhari, N., Qiu, X., Kumar, U., 2011. Heterodimerization of β2 adrenergic receptor and somatostatin receptor 5: Implications in modulation of signaling pathway. J Mol Signal 6, 9. doi:10.1186/1750-2187-6-9

Takada, Y., C. Kato, S. Kondo, R. Korenaga, and J. Ando. "Cloning of cDNAs Encoding G Protein-Coupled Receptor Expressed in Human Endothelial Cells Exposed to Fluid Shear Stress." *Biochemical and Biophysical Research Communications* 240, no. 3 (November 26, 1997): 737–41. doi:10.1006/bbrc.1997.7734.

Thomas, P., Y. Pang, E. J. Filardo, and J. Dong. "Identity of an Estrogen Membrane Receptor Coupled to a G Protein in Human Breast Cancer Cells." *Endocrinology* 146, no. 2 (February 2005): 624–32. doi:10.1210/en.2004-1064.

Wang, C., Lv, X., Jiang, C., Davis, J.S., 2012. The putative G-protein coupled estrogen receptor agonist G-1 suppresses proliferation of ovarian and breast cancer cells in a GPER-independent manner. Am J Transl Res 4, 390–402.

Wittliff, J.L., 1984. Steroid-hormone receptors in breast cancer. Cancer 53, 630–643.

Aims

1. To identify/develop immunological tools and cell–based reporter assays to monitor and explore GPER1 expression, maturation, trafficking, and signaling in cellular model systems and breast cancer cells.

Paper I,III and IV

2. To screen natural and synthetic chemical libraries in cell–based reporter systems for substances that can modulate receptor function by acting as receptor agonists/antagonists and/or by perturbing receptor maturation and trafficking.

Paper I, III, IV

3. To probe human breast cancer cells and specimens with GPER1–specific immunological, natural, and natural/synthetic GPER1 ligands for identification of novel prognostic and therapeutic tools in breast cancer.

Paper II

Paper summaries

Paper I

This study was undertaken to develop tools and identify cellular models, both native and recombinant, to study the cellular localization, function and regulation of GPR30.

In this article, I present studies of GPR30 expression in both overexpressing recombinant cell lines (HeLa, HEK293, T47-D) and in natively expressing cell lines (MDCK, T47-D). To do this, multiple plasmids coding for human and murine epitope-tagged GPR30 were created and used and to generate stable cell lines HeLa(GPR30) and HEK(GPR30). The plasmids were also used as crucial tools in transient transfection-based assays. Another aim was to identify a reliable antibody specifically recognizing GPR30. No thoroughly validated antibody against murine GPR30 has to my knowledge been identified, hampering important in-vivo studies in mouse models.

After a lengthy searching process, we acquired and extensively validated an anti-human GPR30 antibody. The antibody detected no receptors in naïve HeLa cells but specific detection in stable HeLa(GPR30) cells, both by western blotting of cell lysates and by confocal immunofluorescence microscopy analysis. The same results were obtained when the experiments were repeated in stable HEK(GPR30) cells as well in transiently transfected HEK cells. Over-expressed FLAG-GPR30 and HA-GPR30 were also confirmed to colocalize with endogenous GPR30 in T47-D cells, validating that the epitope-tags had no influence on subcellular localization of the receptor.

The immunoblotting profile of the receptor (both overexpressed and endogenous) showed multiple bands of varying sizes, as can be expected of a GPCR, which are commonly subjected to prominent post-translational modifications such as glycosylation, phosphorylation and palmitoylation. A band of the predicted monomeric size of the receptor (~40 kDa) was identified. In addition, immunoreactive bands of larger sizes were also present, suggesting larger multimeric complexes. Deglycoslyation of the receptor with PNGase F reduced the monomeric band slightly as can be expected. Counter-intuitively, the deglycosylation also yielded a band of a larger molecular weight (100 kDa). These results strongly suggest that the receptor is indeed N-glycosylated and that N-deglycosylation results in structural changes in the receptor.

GPR30-dependent cAMP signaling was also investigated in ectopically overexpressed cells and in native cells. GPR30-overexpressing C2C12 cells and MDCK cells showed a very weak cAMP signal in response to 17β-estradiol (E2), even at extremely high concentrations (>10^{-4}M). On the other hand, G1 caused a more reliable dose-dependent cAMP signal. GPR30 antisense constructs against murine GPR30 and canine GPR30 were used to establish that the signals appeared to be receptor-dependent. In both C2C12 cells and in MDCK cells, the cAMP levels in response to both E2 and G1 were blunted by expression of antisense constructs. A third cell line, T47D, also responded to G1 in a dose-dependent manner, although this response was not validated as GPR30-specific.

Of note, the amplitude of the cAMP response was significantly higher from G1 stimulation compared to E2 stimulation, indicating that E2 may not be the cognate ligand for GPR30, since cognate ligands most often are full agonists.

As G1 was shown to produce receptor-specific responses, I also evaluated if G1 also relocated β-arrestin to the receptor, an early event of agonist-promoted internalization. β-Arr2-GFP translocated to the cell membrane of MDCK cells in response to G1 and E2 and isoproterenol, a β2-adrenergic receptor (β2AR) agonist, known to recruit β-Arr2 to in HEK293 cells and therefore used as positive controls. However, whether these responses are truly GPR30-dependent remains to be determined.

Examining GPR30 subcellular localization by confocal immunofluorescence microscopy in different cell lines using our validated antibody yielded intriguing results. I fixed MDCK cells grown on glass with 4% paraformaldehyde for fifteen minutes. This followed some gentle washing of the cells and then some incubation with a blocking agent including 0.1% Triton-x-100, a detergent and gentle cell membrane perforator. It will allow antibodies to enter inside of the cell and label the entirety of the revealed intracellular landscape. Describing the GPR30 staining in these cells by words is challenging but is best described as web-like or cytoskeletal in nature with the majority of receptors residing internally, with only a fraction at the cell surface. Co-staining with known markers against ER, golgi, and tubulin showed no apparent colocalization with those structures. In addition, the filaments did not look as organized as actin filaments. The most similar structures I could find when researching filamentous or cytoskeletal proteins *in silico* were cytokeratins, members of the cytoskeletal intermediate filaments. GPR30 association was confirmed by reciprocal co-immunoprecipitation, as well as colocalization imaged by confocal immunofluorescence microscopy, using an antibody against pan-cytokeratin in combination with our validated GPR30 antibody. HPLC-MSMS analysis of GPR30-immunoprecipitations also found several cytoskeletal cytokeratins (unpublished data).

The final part of this study was to investigate the membrane trafficking of the receptor. Cell surface receptors were labeled with antibodies directed against an extracellular epitope of GPR30, by adding antibodies to the cell growth medium, and incubating the cells at 37°C for 30 minutes. Following fixation and the addition of a secondary fluorescent antibody, the membrane trafficking of receptors originating at the cell surface were monitored.

These two different techniques, I have learnt to call "fed" and "dead", because one technique involves feeding antibodies to live cells, hence "fed". "Dead", because we fix (kill) and gently perforate them to give the antibodies access to the whole of the cell, before staining them with our antibodies.

Extensive constitutive internalization of the receptor occurred, with the internalized receptors forming a web-like intracellular structure. Neither E2 nor G1 treatment had any effect on internalization rate (data not shown). Surface labeling in presence of sucrose to block clathrin-mediated endocytosis also confirmed the existence of a pool of receptors residing in the plasma membrane.

To summarize, this paper shows that GPR30 localizes differently in different cell lines and that there is a novel association of the receptor with cytokeratin filaments. The paper also present novel results regarding high constitutive agonist-independent GPR30 endocytosis as well as some data that G1 elicits responses that are in part dependent on this receptor.

Paper II

The purpose of this study was to examine whether GPR30 expression plays a role in breast cancer. This was done correlating GPR30 expression with clinicopathological variables and distant disease-free survival (DDFS) in breast cancer biopsies gathered from women with different stages and types of breast cancer.

Two cohorts were analyzed by immunohistochemistry (IHC), one patient group with tamoxifen-treated stage II carcinoma, and one with a lymph node-negative and mainly untreated patient group. IHC was done using the GPR30 antibody previously confirmed by me to be receptor specific. I contributed minimally to sample preparation, analysis of the tissue micro-arrays or the statistical analysis of the patient data.

The clinical results revealed that GPR30 positively correlates with ER and PGR and that GPR30 is an independent prognostic marker of increased 10-year DDFS in the ER^+ subgroup of patients, i.e. ER^+ cancer patients may benefit from GPR30 expression.

Based on the clinical data, as well as observations that GPR30 expression tends to decrease cell growth, I hypothesized that GPR30 expression might confer apoptotic signaling. To test this, HEK293 cells stably expressing murine GPR30 (HEK-R) and naïve HEK293 cells (HEK) as controls were assayed for viability using the standardized MTT assay. A significant decrease in viability was observed in HEK-R cells compared to HEK cells. This led me to propose that GPR30 may be pro-apoptotic.

Recent research suggests that GPR30 is degraded through the proteosomal pathway. Therefore, I used the specific proteasomal inhibitor epoxomicin to try to increase the total amount of GPR30 on the cell surface. Indeed, epoxomicin treatment led to ~100% increase in the amounts of surface GPR30 as quantified by FACS analysis (not performed by me) and confocal immunofluorescence microscopy. Epoxomicin is also a known proapoptotic stimulus, as observed by increased cytochrome C release and cleavage of PARP (a caspase substrate) in both HEK and HEK-R cells. However, HEK-R cells were much more sensitive to epoxomicin, as all pro-apoptotic signals were amplified. The most prominent effect in HEK-R cells was the increased caspase 3 cleavage, whereas the HEK cells show only trace amounts in response to epoximicin treatment. Thus, GPR30 constitutively sensitizes cells to apoptotic stimulation.

Next, I proceeded to investigate GPR30-mediated effects in an ER^+ breast cancer cell line, MCF7 cells. As MCF7 cells express endogenous GPR30, we created an MCF7 subclone stably expressing a GPR30-silencing vector MCF7(shGPR30) as a tool to study the function of GPR30. As expected, the GPR30 protein level in MCF7(shGPR30) cells is significantly lower than in MCF7 cells.

The effects of G1 and 4-OHT on pro-apoptotic signaling were also evaluated in MCF7 cells and MCF7(shGPR30) cells. MCF7(shGPR30) cells showed a lower basal and agonist-induced apoptotic signaling as compared to MCF7 cells, indicating that GPR30 has some intrinsic constitutive apoptotic signaling that can be enhanced by G1 in a GPR30-dependent way. In addition, G1 seems to inhibit cell cycle progression in a GPR30-dependent manner, yet another sign of apoptotic signaling somehow involving GPR30.

To summarize, this is a translational study showing that GPR30 is pro-apoptotic in ER^+ breast cancer cells, which may translate into improved prognosis for patients with certain ER^+ breast tumors.

Paper III

Paper III describes the novel finding that Receptor Activity Modifying Protein 3 (RAMP3) directly interacts with GPR30 both in-vitro and in-vivo. This is the first report of a RAMP protein interacting with a type I GPCR.

Considering that GPR30 has an unusually high ligand-independent internalization, I began investigating potential GIPs that could be involved in this process. During this time, I was given some preliminary data that GPR30 associates with RAMP3, the most estrogen-induced gene found in the human genome. Compelling BRET results from Dr. Caron *et al.* led to the establishment of a research partnership where I would confirm the BRET data through other means to strengthen the manuscript.

Transient transfection of HEK293 cells with a liposome-DNA mix consisting of ha-RAMP3 and flag-GPR30 yields cells that express flag-GPR30 OR ha-RAMP3 OR a combination of both OR none of them, since there will always be some untransfected cells. Both ”fed” and ”dead” staining of flagGPR30 and haRAMP3 was performed as described in detail in *Paper I*. The confocal image chosen for the article has all of the advantages of transient transfection, namely we can see cells that express GPR30, RAMP3, both or none. “Dead”-staining revealed that RAMP3 expressed by itself is expressed diffusely throughout the cytoplasm, but when expressed in a cell also expressing GPR30, RAMP3 is found at the site of GPR30, thus colocalization is observed. “Fed”-staining revealed that RAMP3 when expressed by itself is primarily seen in intracellular punctae far from the cell membrane, whereas when co-expressed with GPR30, RAMP3 seems to be retained at the cell surface at the same site as GPR30.

Next, the implications of this interaction were investigated in-vivo in $RAMP3^{-/-}$ and $RAMP^{+/+}$ mice. There was a marked sex difference in the subcellular localization of GPR30 in murine hearts where female hearts had more plasma membrane GPR30 than male hearts. In addition, loss of RAMP3 further reduced the amount of GPR30 found in the membrane fraction of both male and female hearts. Since female mice produce more estrogen than male mice and RAMP3 is the most estrogen-induced gene found, the sex differences in GPR30 localization in the murine heart could be explained by the different concentrations of estrogen in male and female mice.

Finally, $RAMP3^{+/+}$ and $RAMP3^{-/-}$ mice bred on a heart disease-prone background were treated with G1 to examine any cardiovascular effects of GPR30 activation with and without RAMP3. Activation of GPR30 by G1 resulted in significant reductions

in cardiac hypertrophy and perivascular fibrosis only in hearts from $RAMP^{+/+}$ mice. The results of this study demonstrate that GPR30-RAMP3 physically interacts and that the interaction has functional consequences on the localization of these proteins both in-vitro and in-vivo. Additionally, our results suggest that RAMP3 is required for GPR30-mediated cardioprotection.

Paper IV

Because of the current controversy regarding the pharmacological profile and effector coupling of GPR30, I took a completely unbiased approach in this study. Based in part of the constitutive internalization of GPR30, I hypothesized investigating that there could be constitutive receptor signaling that I was not aware of, because internalization is often a response to activation.

Reports have occurred that GPR30 may be linked to cAMP signaling and that this pathway is capable of regulating both apoptotic and proliferative signaling, depending on cell type and/or tissues, we started out to investigate this pathway. We chose HEK293 cells as it is one of the most well described model cell lines and contains all the required effector molecules.

E2 and G1, two reported agonists for GPR30, did not change cAMP signal, however, as I included mock-transfected cells in my assay, I noted that GPR30-transfected cells inhibited the response to heterologous GPCR agonists, such as isoproterenol or PGE2 and even the diterpene forskolin, a direct activator of adenylate cyclases, as compared to the mock-transfected cells. This was repeated in three different cell lines with three different cAMP assays in two different labs. Thus, GPR30 inhibits the response of adenylate cyclase.

Because GPR30 inhibition of cAMP production was insensitive to pertussis toxin, and therefore not mediated by G_i-proteins, I addressed the coupling mechanism by truncating the receptor C-terminus. This approach also removed a PDZ motif, which often are important for receptor coupling and membrane trafficking. The truncated receptor mutant lacks S-S-A-V in its intracellular tail but is in all other regards identical to GPR30.

Investigating GPR30ΔSSAV, I found that receptor inhibition of cAMP production was completely dependent on this motif. In addition, GPR30ΔSSAV internalized to a much greater degree than GPR30 receptors, as determined by both confocal microscopy and FACS analysis.

Therefore, the PDZ ligand recognition motif in the extreme C-terminus of GPR30 is responsible for a blunting of adenylate cyclase activity, as well as involved in retaining the receptor in the cell membrane.

Type I PDZ motifs are known to interact with Membrane Associated Guanylate kinases (MAGUKs). Co-immunoprecipitation and confocal immunofluorescence microscopy in transiently transfected HEK293 cells using a pan-MAGUK antibody which recognizes four related MAGUK proteins, PSD-95, Chapsyn-110, SAP97 and SAP102 showed that GPR30 forms a complex with one or more MAGUKs and co-localize with these proteins in the plasma membrane.

An epitope-tagged PSD-95 plasmid was used to show that PSD-95 is one of the MAGUKs that GPR30 interacts with. Since HEK293 cells do not express PSD-95 endogenously, we hypothesized that another MAGUK interacts with GPR30 in HEK293 cells. The pan-MAGUK antibody recognized proteins around ~120 kDa in GPR30-immunprecipitates from HEK293 cells, consistent with the size of SAP97. A specific SAP97 antibody was used to immunoblot GPR30-immunoprecipitates. The results showed that SAP97 is indeed the endogenous MAGUK that GPR30 interacts with in HEK293 cells through its PDZ ligand recognition motif, and that this constitutive interaction may confer attenuation in cAMP production in these cells.

A well-known binding partner of the MAGUK proteins is AKAP5/AKAP79, a docking protein with multiple binding sites for many important enzymes and effectors, including PKA, PKC, CaM, PP2B/Calcineurin, PDE4 and certain adenylate cyclase isoforms. By co-immunoprecipitation and confocal immunofluorescence microscopy colocalization studies, I showed that AKAP5 can be co-immunoprecipitated from HEK(GPR30) lysates but not from HEK(GPR30ΔSSAV) lysates and that only GPR30 and not GPR30ΔSSAV colocalizes with GPR30 in the plasma membrane.

Similar studies were done in MDCK cells where endogenous GPR30 was pulled down through immunoprecipitation. Immunoreactive bands to both endogenous MAGUKs and AKAP5 were observed, arguing strongly that this occur in more natural cell lines with native proteins.

To examine the role of AKAP5 in GPR30-mediated cAMP inhibition, we inhibited enzymes known to be associated with AKAP5. A short peptide, st-HT31, known to disrupt PKA-RII-AKAP interactions was acquired as a means to dissociate PKA from AKAP5. A control peptide, identical by all means except for a functional disrupting proline at the end of the peptide, st-HT31P, was also acquired. When GPR30-transfected cells were pretreated with st-HT31 or st-HT31P prior to stimulation of the cells with forskolin or isoproterenol to elevate cAMP, the GPR30 inhibition was significantly attenuated in st-HT31-pretreated but not st-HT31P cells.

St-HT31 but not st-HT31P pretreatment also increased the already prominent constitutive receptor internalization even further.

Colocalization studies of GPR30/GPR30ΔSSAV and PKA-RII were also done to strengthen the results further. In line with previous results, PKA-RII specifically colocalizes with GPR30 but not GPR30ΔSSAV, additional evidence that GPR30 forms a complex with AKAP5-PKA-RII.

To summarize, the C-terminal motif of GPR30 binds to MAGUK proteins, which in turn binds to AKAP5. PKA-RII negatively regulates adenylate cyclase activity. Other AKAP5-docked proteins such as PDEs and protein phosphatases may allow for a very spatially and temporally regulated form of signaling. Even though the underlying mechanism for GPR30-regulated cAMP signaling now has been uncovered, there are still questions as to exactly what PKA phosphorylates and what functions the other proteins present in the signalosome has on GPR30-mediated effects.

Future perspectives

Through my research, I have uncovered a number of proteins that specifically interact with the receptor GPR30. I have also identified a GPR30-dependent signaling pathway, however there are still many unanswered questions regarding GPR30.

The discovery of the signalosome and all the associated effector molecules and enzymes in the vicinity of GPR30 of course leads to more questions that need to be answered. Do all these proteins have the ability to influence GPR30 in some way? Multiple GPCRs have similar type I PDZ-motifs and therefore interact with the same PDZ proteins. Is there ligand-specificity for different PDZ domains? What determines whether SAP97 binds to GPR30, β1AR, 5HT2A or 5HT2C since they can all bind to SAP97? Can many bind simultaneously? Do GPR30 and β1AR, since they bind the same MAGUKs, localize to the same signalosome or are they separate? Both MAGUKs and AKAP5 are known to oligomerize but how and to what extent? These are some interesting questions that I would like to work with in my future research.

Another transition I would like to make is to study GPR30 in the brain, which is the organ with the densest population of GPR30 receptors. The quintessential MAGUK protein, PSD-95, which I have confirmed interact with GPR30, is exclusively expressed in the brain. Naturally, neuronal cell lines would make for much better models to study the effects of the both proteins. Also, in the brain, there are no cytokeratins with which GPR30 can associate. Does it instead interact with neurofilaments?

GPR30, AKAP5, RAMP3 and PSD-95 are all proteins known to be induced by E2, but how is the receptor truly involved in estrogen signaling? More research is needed to finally elucidate this long-lasting question.

And lastly, the most important question to answer is still, what is the cognate ligand of GPR30, or does it even need one?

Populärvetenskaplig sammanfattning

Den här avhandlingen handlar om ett protein, en receptor, kallad GPR30. GPR30 tillhör proteinfamiljen G protein-kopplade receptorer vilka är nödvändiga för att celler ska kunna kommunicera med varandra och med sin omgivning. Förenklat sätt kan de ses sitta på ytan av en cell där de väntar på att någonting ska binda till dem, vilket aktiverar receptorerna och får dem att börja signalera. Vad för slags signal det blir i slutändan handlar om vad för slags cell det är, vilken typ av GPCR som aktiveras och av vad för stimuli. Ytterligare faktorer som spelar in är vilka varianter av G-proteiner som finns associerade med receptorerna. Beroende på vilka, så sätter de igång olika signalkaskader som kan få vitt olika konsekvenser.

Förutom att plötsligt aktiveras av att någonting binder till en GPCR så har det på senare år visat sig att de flesta GPCRer har en inneboende egenaktivitet, d.v.s. istället för att se på en receptor som en lampknapp så bör man se på den som en halvt påslagen dimmer. Hur pass uppvriden dimmern är, det beror på vilken GPCR man pratar om, men den går att vrida åt båda hållen. Detta är vad man utnyttjar när man utvecklar läkemedel som är riktade mot GPCRer, antingen vill man stänga av deras egenaktivitet, eller så vill man öka den.

I artikel 1 så visar jag att GPR30 har en omfattande konstitutiv internalisering av receptorn (d.v.s. ett ständigt flöde av GPR30 från ytan inåt i cellen) samt att den kan interagera med cytokeratiner, strukturella proteiner som bl.a. ger cellen stadga. Internalisering av GPCRer är generellt något som händer efter aktivering utav en receptor, så inflödet av receptorer kan tolkas som att GPR30 signalerar kontinuerligt (frågan är bara hur), utan krav på bindning av ligand.

I artikel 2 så tittar vi på mängden GPR30 i bröstcancervävnad och försöker hitta samband mellan uttrycksnivå och överlevnad. Vi fann att GPR30 är en oberoende prognostisk markör för god överlevnad hos patienter med bröstcancer som uttrycker den klassiska östrogen-receptorn ERα. Förutom den kliniska utvärderingen så undersökte jag även om GPR30 möjligen medför programmerad celldöd (apoptos), något som låter hemskt men är önskvärt vid cancer. En cancerforskares våta dröm är nämligen att cancerceller skall gå i apoptos medan normala celler inte skall påverkas. Vad jag såg var att celler som överuttryckte receptorn hade en lägre viabilitet, hade en

rundare morfologi samt visade tecken på proapoptotiska signaler. Samma slutsats kunde dras när jag upprepade försöken i mer kliniskt relevanta bröstcancer-cellinjer.

I artikel 3 så visar vi för första gången på en interaktion mellan en typ 1 GPCR (GPR30) och Receptor Activity Modifying Protein 3 (RAMP3). Det var en transnationell studie som vi genomförde med Dr Caron från University of North Carolina, Chapel Hill, USA. Med hjälp av diverse tekniker och djurstudier kunde vi påvisa att proteinerna interagerar direkt med varandra och att RAMP3 verkar styra membranlokaliseringen av GPR30 i hjärtat. Dessutom har detta en kardioprotektiv effekt.

I artikel 4 som gav oss de största och mest omfattande resultaten för den här avhandlingen presenterar jag en rad nyheter. Efter ytterligare letande efter konstitutiva signaler så hittade jag av en slump att celler som uttrycker GPR30 har ett dämpat svar i en av de stora signaleringsvägarna, cAMP, som används i alla celler hela tiden kontinuerligt. Aktiviteten av denna signalväg mäts oftast i mängden cykliskt adenosinmonofosfat (cAMP) inne i cellerna. Jag tillverkade en receptormutant som saknade de fyra sista aminosyrorna i svansen på receptorn då vi trodde att de utgjorde en protein-protein-interaktionsdomän, kallad PDZ-ligand, som skulle kunna vara inblandad i detta. Mycket riktigt så visade det sig att hela effekten var beroende på en intakt receptorsvans där andra proteiner kan binda in och förmedla effekten. MAGUK-proteiner är proteiner som känner igen receptorer med PDZ-ligander och är kända för att vara inblandade i membranlokalisering och signalering. Därför testade vi en antikropp mot MAGUK-proteiner och glädjande nog hittade vi de i samma proteinkomplex som GPR30. MAGUK-proteiner i sin tur är kända för att associera med en mängd olika proteiner men bl.a. AKAP5 (A Kinase Anchoring Protein 5). Med hjälp av en antikropp mot AKAP5 så kunde vi slå fast att även AKAP5 befanns i samma komplex. AKAP5 är ett slags dockningsprotein och med det menar jag att en massa olika enzymer och effektormolekyler kan binda in till AKAP5. Exempelvis kinaser (som fosforylerar) och fosforylaser (som defosforylerar). cAMP-beroende proteinkinas A (PKA) är ett kinas som sitter ihop med AKAP5. Med hjälp av en liten peptid som stör PKA från att binda AKAP5 kunde jag reversera hämningen av cAMP även när GPR30 fanns närvarande. Mekanismen sattes i sten när vi ”knockade ner” AKAP5 ifrån celler som normalt uttrycker både AKAP5 och GPR30. Försvann AKAP5 så försvann också hämningen av cAMP. En ytterligare effekt vi såg var att förbehandling med PKA-AKAP-dissocierande peptid även gjorde att den spontana internaliseringen ökade. Sammanfattningsvis så bildar GPR30 alltså ett komplex med bl.a. MAGUK-proteiner och AKAP5 som förankrar receptorn i cellmembranet och samtidigt dämpar cAMP-signalering.

Acknowledgements

A big thanks to everyone that has supported me throughout this venture we call a Ph.D. education. I did it!

Mom and dad, thank you for always encouraging me to do hard work and for never cutting corners. In addition, thank you for having me and shaping me into the 'full fledged' scientist I am today!

Fredrik, thank you for taking me on as a Ph.D. student and teaching me the proper way to do science. You are always welcoming, resourceful and enthusiastic about our work and have been an excellent supervisor. I hope we will continue to work together in the future, either directly or through a collaboration of sorts.

Björn, thank you for your impressive insights and immense practical knowledge and also your never-ending rants about bureaucracy or stupid online-courses. Your non-consolidating uprightness is something that I respect and have learnt to like!

Joanna, thank you for letting me have the opportunity to work with you. It is impossible to be in a bad mood when in your presence. Your spirituality and philosophy are great parts of your personality. Also thanks for pep-talking me when I have been feeling blue, it always feel better when I have listened to your advice!

Snobben, Emmy, Meg and Hannes thank you for your awesomeness and all the fun HHA has had together.

Daniel, thanks for always being a step ahead of me so that I can see which tracks to follow. Also for being the ignorant schmuck you are, I wouldn't want no other as a friend.

Martin, thank you for your hard work and dedication in the lab and all the table-tennis games we've enjoyed! I'd like to have you as my GP when you eventually become an MD.

Krister, thanks for all the hard work you have done in the lab and for being a good friend. Your stories from your Ph.D. studies in Oslo are always interesting and put a smile on my face,

Johanna, thanks for taking care of me when I've been too tired to sleep or felt unwell, you are the cure for most! Love you!

Blekingska nationen, thank you for existing and for all the wonderful people and friends I have made while staying and working at the nation. Too many names to put on the list so unfortunately you get a shared acknowledgement.

Co-workers at A12, thank you for giving me a nice environment to work in and for the competence.

Paper I

0026-895X/11/7903-400–410$20.00
MOLECULAR PHARMACOLOGY
Copyright © 2011 The American Society for Pharmacology and Experimental Therapeutics
Mol Pharmacol 79:400–410, 2011

Vol. 79, No. 3
69500/3669528
Printed in U.S.A.

G Protein-Coupled Estrogen Receptor 1/G Protein-Coupled Receptor 30 Localizes in the Plasma Membrane and Traffics Intracellularly on Cytokeratin Intermediate Filaments[S]

Caroline Sandén, Stefan Broselid, Louise Cornmark, Krister Andersson, Joanna Daszkiewicz-Nilsson, Ulrika E. A. Mårtensson, Björn Olde, and L. M. Fredrik Leeb-Lundberg

Department of Experimental Medical Science, Lund University, Lund, Sweden

Received October 19, 2010; accepted December 13, 2010

ABSTRACT

G protein-coupled receptor 30 [G protein-coupled estrogen receptor 1 (GPER1)], has been introduced as a membrane estrogen receptor and a candidate cancer biomarker and therapeutic target. However, several questions surround the subcellular localization and signaling of this receptor. In native cells, including mouse myoblast C_2C_{12} cells, Madin-Darby canine kidney epithelial cells, and human ductal breast epithelial tumor T47-D cells, G-1, a GPER1 agonist, and 17β-estradiol stimulated GPER1-dependent cAMP production, a defined plasma membrane (PM) event, and recruitment of β-arrestin2 to the PM. Staining of fixed and live cells showed that GPER1 was localized both in the PM and on intracellular structures. One such intracellular structure was identified as cytokeratin (CK) intermediate filaments, including those composed of CK7 and CK8, but apparently not endoplasmic reticulum, Golgi, or microtubules. Reciprocal coimmunoprecipitation of GPER1 and CKs confirmed an association of these proteins. Live staining also showed that the PM receptors constitutively internalize apparently to reach CK filaments. Receptor localization was supported using FLAG- and hemagglutinin-tagged GPER1. We conclude that GPER1-mediated stimulation of cAMP production and β-arrestin2 recruitment occur in the PM. Furthermore, the PM receptors constitutively internalize and localize intracellularly on CK. This is the first observation that a G protein-coupled receptor is capable of associating with intermediate filaments, which may be important for GPER1 regulation in epithelial cells and the relationship of this receptor to cancer.

Introduction

G protein-coupled receptor 30 (GPER1) is a GPCR that has been proposed to be an estrogen receptor responsible for at least some nongenomic estrogen signaling (Filardo and Thomas, 2005; Prossnitz et al., 2008). Estrogens are important sex hormones in both genders that have long been recognized to act through both genomic and nongenomic mechanisms. The genomic mechanisms are the best described and involve the binding of estrogens to two nuclear estrogen receptors, ERα and ERβ, which function as nuclear transcription factors regulating gene expression (Heldring et al., 2007). Membrane-associated full-length ERα also exists that is at least in part responsible for nongenomic estrogen signaling (Razandi et al., 2004).

GPER1 is ubiquitously expressed in both human and rodents, and GPER1-deficient mice show that this receptor may participate in metabolic, cardiovascular, bone, and immune regulation, at least in part, in an estrogen-dependent manner (Mårtensson et al., 2009; Olde and Leeb-Lundberg, 2009; Windahl et al., 2009). In addition, GPER1 was found to be associated with the growth of both breast and endometrial

This work was supported in part by funds from European Foundation for the Study of Diabetes/Servier, Swedish Research Council, Alfred Österlund Foundation, The Swedish Diabetes Association, Konsul Thure Carlssons Minne Foundation, Magnus Bergvalls Foundation, Diabetes Association in Malmö, Syskonen Svenssons Foundation, Anders Otto Swärds Foundation, Royal Physiographic Society in Lund, and the Faculty of Medicine at Lund University through the Vascular Wall prioritized program.

C.S. and S.B. contributed equally to this work.

Article, publication date, and citation information can be found at http://molpharm.aspetjournals.org.

doi:10.1124/mol.110.069500.

[S] The online version of this article (available at http://molpharm.aspetjournals.org) contains supplemental material.

ABBREVIATIONS: GPER1, G protein-coupled estrogen receptor 1; B2R, B2 bradykinin receptor; ERα, estrogen receptor α; ERβ, estrogen receptor β; CK, cytokeratin; E2, 17β-estradiol; ER, endoplasmic reticulum; PM, plasma membrane; HEK, human embryonic kidney; MDCK, Madin-Darby canine kidney; GPCR, G protein-coupled receptor; FBS, fetal bovine serum; PCR, polymerase chain reaction; PBS, phosphate-buffered saline; PNGase F, peptide:*N*-glycanase; HA, hemagglutinin; ATCC, American Type Culture Collection; GFP, green fluorescent protein; siRNA, short interfering RNA.

cancers (Filardo et al., 2006; Smith et al., 2007). An agonist, G-1, with selectivity for GPER1 over ERα and ERβ, was reported (Bologa et al., 2006) and is now being used extensively to study this receptor. Furthermore, some antiestrogens (e.g., hydroxytamoxifen) act as agonists at this receptor (Maggiolini et al., 2004; Thomas et al., 2005).

At the cellular level, GPER1 was reported to bind E2 with high affinity (Revankar et al., 2005; Thomas et al., 2005) to influence growth factor signaling pathways, including transactivation of the epidermal growth factor receptor, intracellular Ca^{2+} mobilization, phosphatidylinositol 3-kinase translocation, Src activation, extracellular signal-regulated kinase activation, and cAMP production (Filardo and Thomas, 2005; Prossnitz et al., 2008) and to modulate downstream transcription factor networks (Pandey et al., 2009). GPER1 was antiproliferative in ERα- and ERβ-positive MCF-7 breast cancer cells but proliferative in ERα- and ERβ-negative SkBr3 breast cancer cells (Ariazi et al., 2010), suggesting that GPER1 function depends on the genetic environment of the cell.

Limited detailed studies have been done on the subcellular localization and membrane trafficking of GPER1, and then mostly in recombinant cells. Based on available studies, the localization of the receptor and receptor signaling is in debate, with some groups stating that the receptor is present and functions exclusively intracellularly in the ER either with (Revankar et al., 2005) or without estrogen receptor functions (Otto et al., 2008), whereas others state that GPER1 is present and acts as an estrogen receptor in the PM (Funakoshi et al., 2006; Filardo et al., 2007), as would be expected of a typical GPCR.

Here, we used several native cell lines to show that GPER1 is functional and localizes in the PM and intracellularly on CK intermediate filaments. CKs are proteins important for the structural integrity primarily of epithelial cells. The human genome contains a total of 54 functional CK genes, of which 37 are epithelial (Schweizer et al., 2006; Moll et al., 2008). Filamentous CK structures form by heteromeric pairing of acidic type I and basic or neutral type II CKs. Little is still known about CK beyond structural roles, but evidence is accumulating that CK may also serve additional roles as signaling platforms in cell adhesion, apoptosis/survival, and proliferation (Eriksson et al., 2009).

Materials and Methods

Cell Culture and DNA Constructs. C_2C_{12} cells, MDCK cells, and HeLa cells (ATCC, Manassas, VA) were grown in phenol-free Dulbecco's modified Eagle's medium (Invitrogen, Carlsbad, CA) supplemented with 10% fetal bovine serum (FBS) (HyClone Laboratories, Logan, UT) in 5% CO_2 at 37°C. T47-D cells (ATCC) were grown in RPMI 1640 media supplemented with 10% FBS and 10 μg/ml insulin in 5% CO_2 at 37°C. HEK293 cells (ATCC) were grown in Dulbecco's modified Eagle's medium supplemented with 10% FBS in 10% CO_2 at 37°C. The human GPER1 cDNA was subcloned into the pIRESpuro vector (Clontech, Mountain View, CA) containing a puromycin selection marker. The mouse GPER1 cDNA and human B2 bradykinin receptor (B2R) were subcloned into a pcDNA3.1 vector containing a zeosin selection marker. An N-terminal artificial signal sequence, as described previously (Whistler et al., 2002; Enquist et al., 2007), and the FLAG sequence tag were added in series to make the GPER1 construct FGPER1 and B2R construct FB2R. To make mouse GPER1 antisense cDNA, the mouse GPER1 sequence was amplified from a plasmid by PCR using the following primers: upper, 5′-CAAGCGGCCGCTATGGATGCGACTACTCCAGC-3′, and lower, 5′-CAGAAGCTTAGCACTGCTGAACCTGACCT-3′ containing a NotI and a HindIII site, respectively. The insert was then cloned in reverse orientation into the NotI/HindIII site of the pEAK12 vector. Clones containing mouse GPER1, in reverse orientation, were identified by HindIII/NotI digestion and sequencing using the BigDye terminator sequencing kit (PerkinElmer Life and Analytical Sciences, Waltham, MA). A cDNA construct of GPER1 tagged in the N terminus with three HA epitopes in series (HGPER1) was obtained from Missouri S&T cDNA Resource Center (Rolla, MO). A β-arrestin2-GFP cDNA construct was kindly provided by Dr. Marc Caron (Duke University Medical Center, Durham, NC) (Barak et al., 1997).

HEK293 cells were transfected with FGPER1 and FB2R cDNA using the calcium phosphate precipitate method and HeLa cells with human GPER1 by electroporation as described previously (Kotarsky et al., 2001). Single colonies were then chosen and propagated in the presence of selection-containing media to generate clonal stable cell lines. C_2C_{12} cells, MDCK cells, and/or T47-D cells were transiently transfected with antisense GPER1 cDNA, β-arrestin2-GFP cDNA, FGPER1 cDNA, HGPER1 cDNA, and/or GPER1 siRNA using Lipofectamine and Lipofectamine PLUS (Invitrogen) or FuGENE-6 (Roche Diagnostics, Indianapolis, IN) according to the manufacturer's instructions.

RNA Isolation and PCR. Isolation of RNA was performed using a method described previously (Chomczynski and Sacchi, 1987). cDNA synthesis was performed using the SuperScript III First-Strand Synthesis System for PCR (Invitrogen). The GPER1 cDNA was amplified using PCR with the following GPER1 primers: upper, 5′-TGGCTTTGTGGGCAACATCC-3′, and lower, 5′-GGTGCTTGGTGCGGAAGAGGC-3′ (mouse); upper, 5′-TCTACACCATCTTCCTCTTCC-3′, and lower, 5′-GTAGCGATCAAAGCTCATCC-3′ (canine and human); the products were visualized on a 0.8% agarose gel.

Immunoprecipitation and Immunoblotting. Confluent cells grown on 10-cm dishes were washed twice with ice-cold PBS and lysed in 0.5 to 1 ml of lysis buffer (0.1% Triton X-100, 10 mM Tris-HCl, pH 7.4, 150 mM NaCl, and 25 mM KCl) with complete protease inhibitor cocktail (Roche Diagnostics). Lysates were cleared by centrifugation at 10,000*g* for 10 min at 4°C. Receptors were immunoprecipitated by incubating the cleared lysates overnight at 4°C with goat anti-GPER1 antibody (R&D Systems, Minneapolis, MN) coupled to protein G-Sepharose (GE Healthcare, Chalfont St. Giles, Buckinghamshire, UK) or mouse anti-M2 FLAG agarose (Sigma-Aldrich, St. Louis, MO) overnight at 4°C, and CKs were immunoprecipitated with mouse anti-pan CK (clone C-11), mouse anti-CK7, or mouse anti-CK8 antibody coupled to protein G-Sepharose (all from Sigma-Aldrich). The precipitate was washed extensively and sequentially in the lysis buffer and in 10 mM Tris-HCl, pH 7.4. For immunoblotting, proteins were denatured in SDS-polyacrylamide gel electrophoresis sample buffer including 6% β-mercaptoethanol for 30 min at 37°C, fractionated by SDS-polyacrylamide gel electrophoresis, transferred to a nitrocellulose membrane, and the membrane was blocked for at least 45 min in Tris-buffered saline and 10% nonfat milk. The proteins were stained by incubating with goat anti-GPER1 antibody (1:200), mouse anti-M2 FLAG antibody (1:1000; Sigma-Aldrich), mouse HA.11 antibody (1:1000; Biosite Inc., San Diego, CA), mouse anti-pan CK antibody (1:1000), mouse anti-CK7 antibody (1:200), or mouse anti-CK8 antibody (1:200) for 1 h at 22°C. Immunoreactive bands were visualized with a chemiluminescence immunodetection kit using peroxidase-labeled secondary antibody (Invitrogen, Carlsbad, CA) according to the procedure described by the supplier (PerkinElmer Life and Analytical Sciences).

Enzymatic Deglycosylation. To determine the presence of N-glycosylation in FGPER1, immunoprecipitates were treated with 500 units of PNGase F (New England Biolabs, Ipswich, MA) in 10 mM Tris-HCl, pH 7.4, for 2 h at 37°C.

Immunofluorescence Microscopy. Cells were propagated to approximately 50% confluence in growth media on glass coverslips, coated with poly(D-lysine) or 0.1% gelatin (both from Sigma-Aldrich), and then incubated in serum- and phenol-free media for at least 1 h at 37°C before treatment. For live cell staining, live cells were incubated in serum- and phenol-free media containing goat anti-GPER1 antibody (1:100) or mouse anti-M1 FLAG antibody (1:500; Sigma-Aldrich) for 30 min at 37°C. In some experiments, live cells were treated with 0.4 M sucrose for 60 min at 37°C before incubation with antibody to disrupt clathrin-mediated endocytosis (Heuser and Anderson, 1989). Cells were then fixed with 3.7% formaldehyde in PBS and permeabilized with blotto (3% dry milk, 0.1% Triton X-100, 1 mM $CaCl_2$, and 50 mM Tris-HCl, pH 7.4). For fixed cell staining, cells were incubated in serum- and phenol-free medium and then fixed and permeabilized. The cells were then incubated in blotto containing goat anti-GPER1 antibody (1:100), mouse anti-M1 FLAG antibody (1:500), and/or mouse HA.11 antibody (1:1000) for 1 h at 22°C. In all experiments, cells were then washed with PBS and receptors visualized by incubation with secondary Alexa488-labeled anti-goat antibody, anti-mouse IgG2b antibody (Invitrogen), or anti-mouse IgG1 antibody (Invitrogen). For colocalization studies, fixed and permeabilized cells were also incubated for 1 h at 22°C with rabbit anti-calnexin antibody (1:200; Sigma-Aldrich), mouse anti-GM130 antibody (1:250; BD Biosciences, San Jose, CA), mouse anti-α-tubulin antibody (1:4000; Sigma-Aldrich), mouse pan-CK antibody (1:1000), or mouse anti-CK7 antibody (1:200). Alexa568-labeled anti-mouse IgG1 or anti-rabbit antibody (Invitrogen) were then used as secondary antibodies. For β-arrestin2-GFP imaging, cells were incubated in serum- and phenol-free with or without 1 μM E2 (Sigma-Aldrich), 1 μM G-1 (Calbiochem, San Diego, CA), 1 μM isoproterenol (Sigma-Aldrich), or DMSO vehicle for 30 min at 37°C and then fixed with 3.7% formaldehyde in PBS and washed with PBS. Images were collected using a Nikon Eclipse confocal fluorescence microscope (Nikon, Tokyo, Japan). Some fluorescence images were analyzed using NIS Elements software (Nikon) and then graphed.

cAMP Production. Cells were grown to near confluence in six-well plates (Sarstedt, Nümbrecht, Germany). The cells were washed one time with serum- and phenol-free medium followed by incubation in the same medium for 1 h at 37°C. This was followed by 20 min of incubation at 37°C in medium containing 25 μM rolipram (Sigma-Aldrich). Different concentrations of E2 and G-1 were added, and the cells were further incubated for 30 min, after which the cells were lysed in 0.20 ml of ice-cold 0.1 M HCl for 30 min at 4°C, scraped, and centrifuged at 13,000*g* for 10 min. The amount of cAMP in the supernatant was assayed using an EIA kit (Cayman Chemical, Ann Arbor, MI) according to the manufacturer's instructions.

Data Analysis. Data are presented as means ± S.E.M. Student's two-tailed *t* test for unpaired data were performed to evaluate statistical significance. *P* values less than 0.05 were regarded as statis-

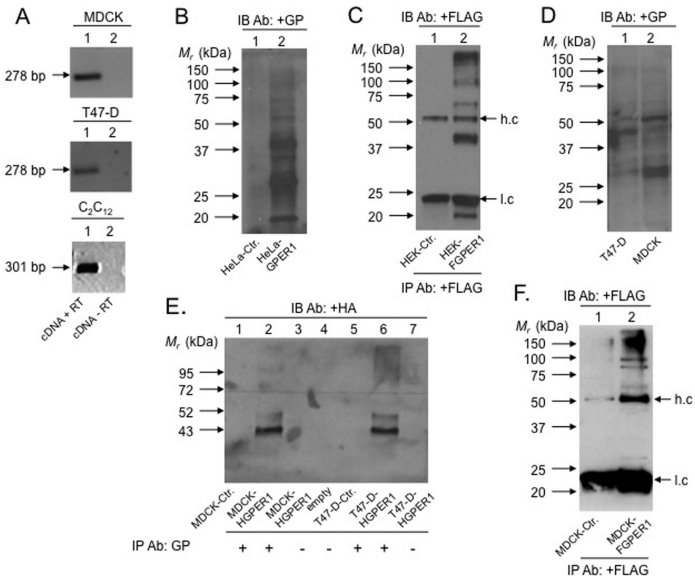

Fig. 1. GPER1 expression. A, RNA from MDCK cells, T47-D cells, and C_2C_{12} cells was isolated and cDNA synthesized and analyzed with (cDNA+RT, lane 1) and without reverse transcriptase (cDNA-RT, lane 2). B, HeLa cells without (HeLa-Ctr., lane 1) and with stable expression of human GPER1 (HeLa-GPER1, lane 2) were lysed and immunoblotted with goat GPER1 antibody (GP). C, HEK293 cells without (HEK-Ctr., lane 1) and with stable expression of mouse FGPER1 (HEK-FGPER1, lane 2) were lysed, immunoprecipitated with mouse M2 FLAG antibody-agarose, and immunoblotted with M2 FLAG antibody (FLAG). D, T47-D cells (T47-D, lane 1) and MDCK cells (MDCK, lane 2) were lysed and immunoblotted with GPER1 antibody (GP). E, mock-transfected MDCK cells (MDCK-Ctr., lane 1) and T47-D cells (T47-D-Ctr., lane 5) and MDCK cells (MDCK-HGPER1, lanes 2 and 3) and T47-D cells (T47-D-HGPER1, lanes 6 and 7) transiently transfected with HGPER1 cDNA were lysed, immunoprecipitated with protein G-Sepharose without (−, lanes 3 and 7) and with GPER1 antibody (GP) (+, lanes 2 and 3), and immunoblotted with HA antibody. F, mock-transfected MDCK cells (MDCK-Ctr., lane 1) and MDCK cells transiently transfected with FGPER1 cDNA (MDCK-FGPER1, lane 2) were lysed, immunoprecipitated with M2 FLAG antibody beads, and immunoblotted with M2 FLAG antibody. Molecular mass (M_r) standards (in kilodaltons), or base pairs (bp) (left side arrows), and position of IgG heavy chain (h.c.) and light chain (l.c.) (right side arrows) are indicated. The results are representative of experiments performed at least three times.

tically significant. Data analysis was performed using the Prism program (GraphPad Software Inc., San Diego, CA).

Results

GPER1 Expression. Several native cell systems relevant to GPER1 physiology from several species were used to study GPER1, including canine kidney epithelial MDCK cells, mouse myoblast C_2C_{12} cells, and human ductal breast epithelial tumor T47-D cells. All of the cells expressed GPER1 as determined at the mRNA level (Fig. 1A). Receptor expression at the protein level was monitored with a goat anti-GPER1 antibody raised against the human receptor N-terminal domain, which was used previously to detect GPER1 (Kolkova et al., 2010). To verify that this antibody reacts specifically with GPER1, we immunoblotted control HeLa cells (HeLa-Ctr.) (Fig. 1B, lane 1) and cells stably expressing human GPER1 (HeLa-GPER1) (lane 2). No bands were observed in HeLa-Ctr. cells, whereas major bands were observed in HeLa-GPER1 cells. The 40- to 45-kDa band corresponds most closely with the theoretical mass of the receptor, whereas the lower bands (20 and 30 kDa) are probably degradation products thereof. To further evaluate receptor expression, control HEK293 cells (HEK-Ctr.) (Fig. 1C, lane 1) and cells stably expressing mouse GPER1 with the FLAG epitope inserted at the N-terminal end (FGPER1) (HEK-FGPER1) (lane 2) were immunoprecipitated with M2 FLAG antibody covalently coupled to agarose and immunoblotted with FLAG antibody. A receptor band at 40 to 45 kDa was present also in HEK-FGPER1 cells as well as a band at 20 kDa. In addition, these cells contained receptor bands at 65 and 100 kDa and greater that may be receptor complexes.

Immunoblotting of T47-D cell (Fig. 1D, lane 1) and MDCK cell lysates (lane 2) with GPER1 antibody revealed bands common to these cells at approximately 40 to 45 kDa as well as at 30 and 50 to 55 kDa, albeit with slightly different relative intensities. The GPER1 antibody did not recognize the mouse receptor as determined with both mouse C_2C_{12} cells and HEK-FGPER1 cells. Thus, to further evaluate the GPER1 antibody specificity, T47-D cells and MDCK cells were transfected with or without a cDNA of human GPER1 containing the HA epitope at the N-terminal end (HGPER1) and then immunoprecipitated with protein G-Sepharose with and without precoupled GPER1 antibody. As shown in Fig. 1E (lanes 2 and 6), the GPER1 antibody recognized HGPER1 bands at 40 to 45 and 50 to 55 kDa as well as a weak band at approximately 100 kDa in both T47-D-HGPER1 cells and MDCK-HGPER1 cells that were absent in mock-transfected T47-D-Ctr. and MDCK-Ctr. cells (lanes 1 and 5) and immunoprecipitates with only protein G-Sepharose (lanes 3 and 7). In MDCK cells transfected with FGPER1 cDNA (MDCK-FGPER1), FGPER1-specific bands were present at 50 to 55 kDa, in part overlapping with the IgG heavy chain, and at approximately 65 and 90 to 100 kDa (Fig. 1F, lane 2) that were absent in mock-transfected MDCK- Ctr. cells (Fig. 1F, lane 1). Thus, FGPER1 migrates in part differently in MDCK and HEK293 cells with a band at 40 to 45 kDa in the former cells and a band at 50- to 55-kDa band in the latter cells. However, the presence of a 50- to 55-kDa band also in HEK293 cells was indicated after PNGase deglycosylation (see below). On the other hand, HGPER1 clearly migrates at both masses. Thus, GPER1 seems to reside on proteins of 40 to 45 and 50 to 55 kDa as determined with GPER1 antibody, which reacts with the native receptor, FLAG antibody, which reacts with FGPER1, and HA antibody, which reacts with HGPER1. Receptor immunoprecipitates also enriched for a higher mass receptor form(s) at approximately 100 kDa, which may be a detergent-resistant receptor complex(es). Together, these results show that the GPER1 antibody is specific for GPER1.

GPER1 N-Glycosylation. The presence of multiple immunoreactive GPCR species is typical and often caused by variations in receptor N-glycosylation. To address this modification as a basis for GPER1 heterogeneity, FLAG immunoprecipitates from HEK-FGPER1 cell lysates were N-deglycosylated with PNGase F and then immunoblotted with FLAG antibodies. Surprisingly, PNGase F treatment resulted in a dramatic decrease in the intensities of the 20-, 40- to 45-, and 65-kDa bands and an increase in the intensity of the 100-kDa band (Fig. 2A), which is contrary to the typical decrease in apparent receptor mass that occurs upon deglycosylation. A decrease did occur in the mass of a FLAG-specific protein corresponding to that of the IgG heavy chain (50–55 kDa) supporting the presence of a receptor band here also in these cells. Similar changes occurred upon PNGase F treatment of FGPER1 immunoprecipitates from lysates of MDCK-FGPER1 cells and T47-D-FGPER1 cells (Fig. 2B), again with the notable decrease in mass at 50 to 55 kDa. These results show that the receptor is N-glycosylated and that this modification has additional effects on the physical properties of the receptor, at least FGPER1.

GPER1-Mediated cAMP Production. G-1, a substance reported previously to be an agonist on GPER1-mediated intracellular Ca^{2+} signaling (Bologa et al., 2006), dose-dependently increased cAMP production in a saturable manner in

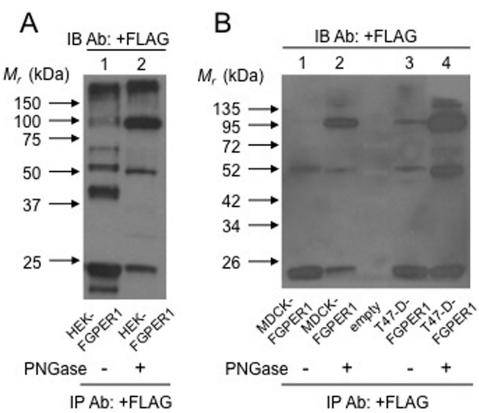

Fig. 2. GPER1 N-glycosylation. A, HEK293 cells stably expressing mouse FGPER1 (HEK-FGPER1) were lysed, immunoprecipitated with mouse M2 FLAG antibody-agarose, treated without (lane 1) and with PNGase F (lane 2), and immunoblotted with M2 FLAG antibody. B, MDCK cells (MDCK-FGPER1, lanes 1 and 2) and T47-D cells (T47-D-FGPER1, lanes 3 and 4) transiently transfected with FGPER1 cDNA were lysed, immunoprecipitated with M2 FLAG antibody beads, treated without (lanes 1 and 3) and with PNGase F (lanes 2 and 4), and immunoblotted with M2 FLAG antibody. Molecular mass standards (in kilodaltons) (left side arrows) are indicated. The results are representative of experiments performed at least three times.

mouse C_2C_{12} cells with an EC_{50} value of 282 ± 52 nM (Fig. 3A). E2 also potently stimulated cAMP production in these cells with an EC_{50} value of 1.8 ± 0.3 nM (Fig. 3A). However, the maximal response, or efficacy, of E2 was only approximately 10% of that of G-1. To address the dependence of these responses on GPER1, we transiently transfected C_2C_{12} cells with a mouse antisense GPER1 cDNA construct used previously and validated in detail (Ahola et al., 2002; Revankar et al., 2005). The G-1- (Fig. 3B) and E2-promoted responses (Fig. 3C) were both inhibited by this antisense construct. G-1 and E2 also stimulated cAMP production in MDCK cells with relative efficacies and potencies similar to those in C_2C_{12} cells (Fig. 3D). A canine GPER1-specific siRNA, but not a scrambled nonspecific siRNA, inhibited the G-1 response in MDCK cells (Fig. 3E), indicating that this response was also dependent on GPER1. G-1 also stimulated cAMP production in human T47-D cells (Fig. 3F), which express GPER1 (Fig. 1A). Thus, G-1- and E2-stimulated cAMP production in these native cells is mediated at least in part by GPER1.

GPER1-Mediated β-Arrestin2 Recruitment. Receptor-mediated cAMP production is a PM-dependent event. To further address the subcellular localization of GPER1 signaling, we analyzed the distribution of β-arrestin2, a regulatory and signaling effector protein that physically associates with many GPCRs at their site of function. Consistent with cAMP signaling, G-1 and E2 increased β-arrestin2-GFP in the PM in MDCK cells (Fig. 4). Isoproterenol was used as a positive control presumably by acting through a small but significant number of β_2-adrenergic receptors expressed on these cells (Meier et al., 1983). PM recruitment of β-arrestin2-GFP by these agents was also observed in T47-D cells (data not shown). These results provide additional evidence that GPER1 functions at least in part in the PM. Even though only semiquantitative, this assay further suggests that G-1 and E2 exhibit similar efficacies on this response.

Subcellular GPER1 Trafficking. Limited detailed studies have been done to localize GPER1 subcellularly in native cells. To do so, we performed confocal immunofluorescence microscopy using the GPER1 antibody. The dependence of antibody reactivity on GPER1 expression was again confirmed by positive staining in HeLa-GPER1 cells but not in HeLa-Control cells (Fig. 5A). A calnexin antibody was used as a control to show ER staining in both cells types. Some overlap in receptor and ER staining occurred, which is common in overexpressed recombinant GPCR cell systems and is often due to saturation of maturation mechanisms (Fig. 5A).

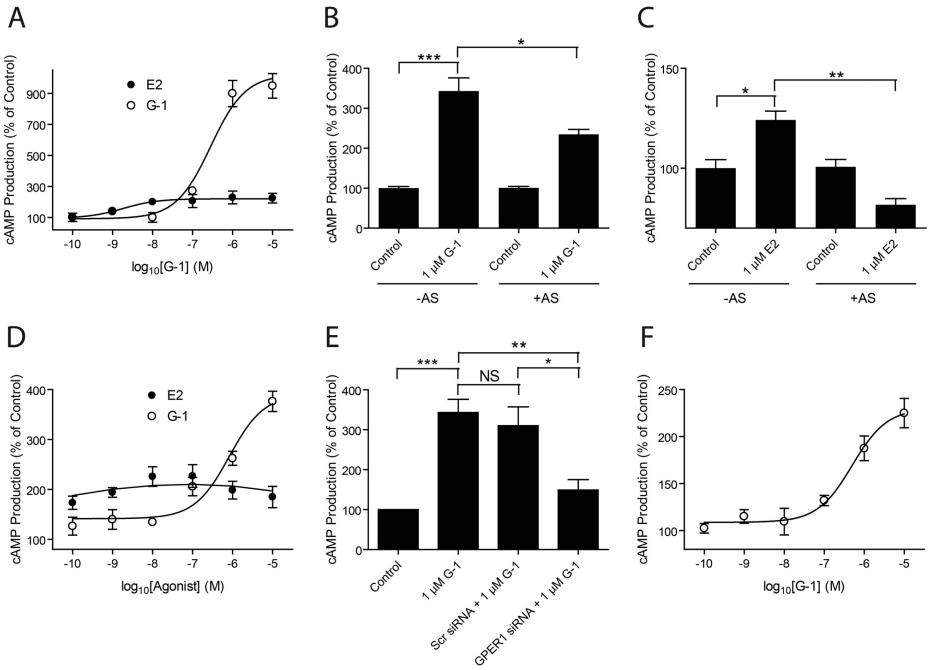

Fig. 3. GPER1-mediated cAMP production. A, C_2C_{12} cells were stimulated with increasing concentrations of G-1 (○) or E2 (●) for 30 min at 37°C and then assayed for cAMP production. B and C, C_2C_{12} cells were transfected with a mouse GPER1 antisense construct (+AS) or empty vector (−AS), stimulated without (Control) or with 1 μM G-1 (B) or 1 μM E2 (C) for 30 min at 37°C and then assayed for cAMP production. D, MDCK cells were stimulated with increasing concentrations of G-1 or E2 for 30 min at 37°C and then assayed for cAMP production. E, MDCK cells were transfected with a canine GPER1 siRNA (GPER1 siRNA) or scrambled siRNA (Scr siRNA) construct, stimulated without (Control) or with 1 μM G-1 for 30 min at 37°C, and then assayed for cAMP production. F, T47-D cells were stimulated with increasing concentrations of G-1 and then assayed for cAMP production. Data are presented as a percentage of control where control corresponds to 15 to 20 pmol cAMP/well. Values are means ± S.E.M. with each data point performed in quadruplicate. NS, not significant; *, $P < 0.05$; **, $P < 0.01$; ***, $P < 0.001$.

The specificity of the antibody for GPER1 was further underlined by colocalization of GPER1 antibody and FLAG antibody staining in T47-D cells transfected with human GPER1 and FGPER1 (Fig. 5B). Furthermore, FLAG antibody and HA antibody staining colocalized in cells transfected with FGPER1 and HGPER1 (Fig. 5B). Costaining of GPER1 and HGPER1 with the GPER1 antibody could not be done because both receptor constructs are of human origin and are thus recognized by this antibody. It is noteworthy that the intracellular costaining had a web-like appearance in all cells, suggesting receptor localization on a cytoskeletal structure.

Staining of endogenous GPER1 with the GPER1 antibody in fixed MDCK cells was observed both at the cell periphery and intracellularly, the latter also exhibiting a web-like cytoskeletal appearance (Fig. 5B; Supplemental Fig. 1). Staining also occurred under live conditions at 37°C, providing direct evidence for PM receptors because the antibody is directed against the extracellular N-terminal receptor domain (Fig. 5C). A significant amount of the live staining was intracellular, showing that the PM receptors undergo constitutive endocytosis (Fig. 5C). The live intracellular staining exhibited the same web-like pattern as the fixed intracellular staining (Fig. 5C), suggesting that this pattern is at least in part caused by constitutive receptor internalization.

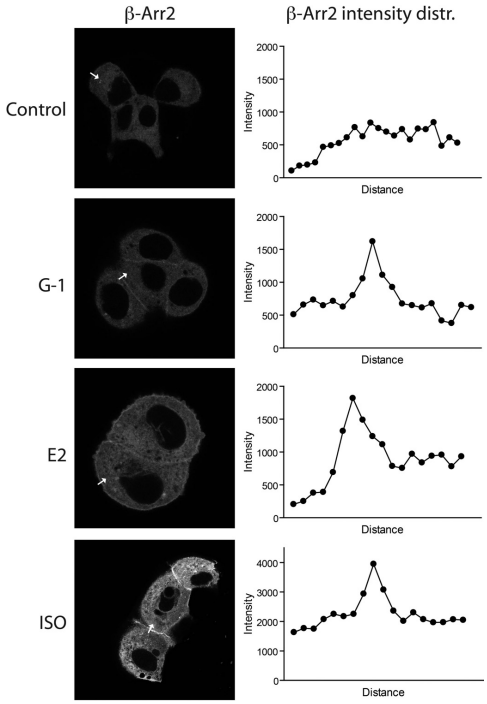

Fig. 4. GPER1-mediated β-arrestin2 recruitment. MDCK cells transiently transfected with β-arrestin2-GFP cDNA were stimulated without (Control) or with 1 μM G-1, 1 μM E2, or 1 μM isoproterenol (ISO) for 30 min at 37°C. Images of fixed cells were collected using a Nikon Eclipse confocal microscope with 60× objective and 50 μm zoom. Arrows indicate cellular distance that was analyzed for changes in β-arrestin2-GFP fluorescence intensity upon agonist stimulation using the NIS Elements software program (Nikon), and the results are graphed. Distance (arrow) is 2 μm. The results are representative of experiments performed at least three times.

To confirm constitutive GPER1 endocytosis, we used HEK-FGPER1 cells. Fixed staining with M1 FLAG antibody showed that FGPER1 was present primarily intracellularly (Fig. 5C), similar to HeLa-GPER1 cells (Fig. 5A). Live staining was again observed, indicating the presence of PM receptors also in these cells. Similar to MDCK cells, the live staining was almost exclusively intracellular, again showing constitutive receptor internalization (Fig. 5D). The live staining in HEK-FGPER1 cells was punctate rather than web-like, which again may be due to the heterologous nature of this overexpressed recombinant cell system. Incubating cells in the absence of serum for 24 h did not change the live staining pattern, showing that it was not caused by a serum-derived factor. The relative amount of cell surface receptor staining increased dramatically by treating the cells before antibody incubation with hyperosmotic sucrose for 30 min, which blocks endocytosis by yielding abnormal clathrin polymerization, resulting in empty microcages in the membrane (Heuser and Anderson, 1989) (Fig. 5D). The live intracellular staining was not caused by nonspecific uptake of the antibody or antibody-promoted receptor internalization because GPCRs vary in their ability to generate such staining as described previously by us (Enquist et al., 2007). Indeed, FLAG-tagged B2 bradykinin receptors (FB2Rs) stably expressed in HEK293 (HEK-FB2R) remained in the PM during live staining until exposed to the agonist bradykinin, upon which the receptor-antibody complex internalized (Fig. 5D). Thus, two different cell systems (MDCK cells and HEK-FGPER1) using two different receptor-specific antibodies (GPER1 antibody and M1 FLAG antibody) show that at least a fraction of the cellular GPER1 is localized in the PM and undergoes constitutive endocytosis to populate intracellular structures.

Subcellular GPER1 Localization. Antibodies against various subcellular marker proteins were then used to determine the intracellular localization of GPER1 in native cells. Intracellular GPER1 staining in MDCK cells was not associated with ER, as determined by the lack of overlap with calnexin staining (Fig. 6A). In addition, no overlap occurred with GM130 staining of Golgi (data not shown). The web-like intracellular staining pattern suggested receptor association with a cytoskeletal structure. Lack of costaining with α-tubulin staining showed that this structure is not microtubules (Fig. 6B). In addition, receptor staining seemed too disorganized to be associated directly with actin filaments. On the other hand, a significant overlap occurred in receptor and CK staining (Fig. 6C). The same overlap was observed in T47-D cells (Fig. 6C). The pan-CK antibody that was used recognizes several CKs including the simple epithelial CK8, but not CK7. Using a specific CK7 antibody, overlap was also found with this CK subtype (Fig. 6D). Thus, in MDCK cells and T47-D cells, GPER1 is localized in the PM and intracellularly at least in part on CK intermediate filaments but not in the ER, Golgi, or on microtubules.

GPER1-CK Association. GPER1-CK association was further addressed by coimmunoprecipitation. Immunoblotting of MDCK and T47-D cells with anti-pan-CK antibody re-

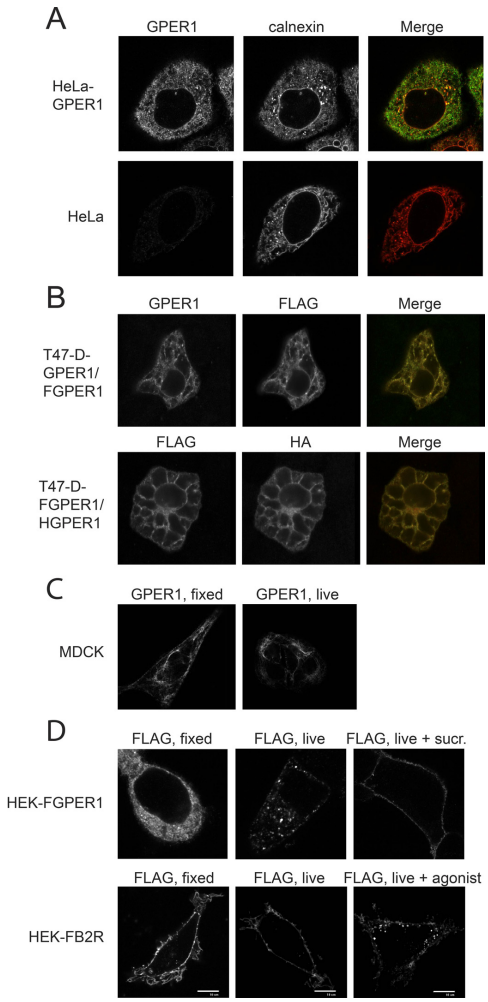

Fig. 5. Subcellular GPER1 trafficking. A, HeLa cells without (HeLa-Control) and with stable expression of human GPER1 (HeLa-GPER1) were fixed and permeabilized before incubation with goat GPER1 antibody (GPER1) and rabbit calnexin antibody (calnexin). B, T47-D cells transfected with human GPER1 and FGPER1 (T47-D-GPER1/FGPER1) or FGPER1 and HGPER1 (T47-D-FGPER1/HGPER1) were fixed and permeabilized before incubation with goat GPER1 antibody (GPER1), mouse FLAG antibody (FLAG), and/or mouse HA antibody (HA). C, MDCK cells (MDCK) were fixed and permeabilized before incubation with GPER1 antibody (GPER1, fixed) or preincubated live with GPER1 antibody for 30 min at 37°C before fixation and permeabilization (GPER1, live). D, HEK293 cells stably expressing mouse FGPER1 (HEK-FGPER1) and human FB2R (HEK-FB2R) were fixed and permeabilized before incubation with mouse M1 FLAG antibody (FGPER1, fixed; FB2R, fixed) or preincubated live without (FGPER1, live; FB2R, live) or with 0.4 M sucrose for 60 min (FGPER1, live + sucr) or 1 μM bradykinin for 30 min (FB2R, live + agonist) at 37°C before incubation with M1 FLAG antibody for an additional 30 min at 37°C. The cells were then fixed and permeabilized. In A to D, cells were subsequently incubated with secondary donkey anti-goat, rabbit anti-mouse, or mouse anti-rabbit ALEXA488- or ALEXA568-labeled antibody. The individual and merged (Merge) images were collected using a Nikon Eclipse confocal microscope, 60× objective, 50 μm zoom. The results are representative of experiments performed at least three times.

vealed that both cells express CKs at masses of 50 to 55 kDa, which is typical of epithelial CKs (Fig. 7A, lanes 1 and 2). The T47-D cell line was the richest source of CK, which is expected of a breast cancer epithelial cell line. Typical of a simple epithelial cell, T47-D cells expressed the basic type-II CKs CK8 (Fig. 7A, lane 3) and CK7 (lane 4), often as doublets, and as reported previously (Ferrero et al., 1989). Even though MDCK cells have been reported to express CK8 (Pollack et al., 1997), we were unable to effectively detect CK7 or CK8 in MDCK cell lysates, which is probably due to the relatively low CK expression in this cell line (Fig. 7A, lane 1).

Consistent with GPER1-CK association, GPER1 immunoprecipitates from both MDCK and T47-D cells contained CK (Fig. 7B, lanes 1 and 2) including both CK7 (lanes 3 and 4) and CK8 (lanes 5 and 6). CKs detected by the pan-CK antibody in both cells (Fig. 7B, lanes 1 and 2) and CK7 antibody in MDCK cells (lane 3) migrated as monomers, whereas higher mass forms were detected of CK7 in T47-D cells (lane 4) and CK8 in both cells (lanes 5 and 6). The reason for this is unknown but may be due in part to detergent-resistant CK complexes with, for example, GPER1. Indeed, pan-CK immunoprecipitates from T47-D cells contained a GPER1 antibody-reactive band at approximately 100 kDa (Fig. 7C, lane 2) that was not present in protein G-Sepharose precipitates (lane 1). The same specific band was present in CK8 and/or CK7 immunoprecipitates of MDCK cells (Fig. 7D, lanes 2 and 3) and T47-D cells (lane 4). Weaker bands at approximately 50 kDa occasionally appeared in protein G-Sepharose precipitates (Fig. 7D, lane 1). PNGase F treatment of the pan-CK immunoprecipitate from T47-D cells resulted in a small downward shift in the 100-kDa GPER1 band (Fig. 7E, lanes 1 and 2), whereas this treatment did not influence the CK band in the GPER1 immunoprecipitate (Fig. 7E, lanes 3 and 4).

FLAG immunoprecipitates of MDCK-FGPER1 cells also contained pan-CK and CK8 immunoreactivities of higher masses (Fig. 8, lanes 2 and 4) that were not present in mock-transfected MDCK-Ctr. cells (lane 1). Consistent with native cells, pan-CK immunoprecipitates from MDCK-FGPER1 cells contained a 100-kDa FLAG-receptor-specific band (Fig. 8, lane 5). Thus, the 100-kDa receptor species observed in both FGPER1 and HGPER1 immunoprecipitates seems to be a major CK-interacting partner as determined by immunoblotting with both GPER1 antibody for the native receptor (Fig. 7, C–E) and FLAG antibody for FGPER1 (Fig. 8, lane 5). In all, these results confirm those obtained by immunofluorescence microscopy that at least some GPER1 in MDCK cells and T47-D cells associate with CK intermediate filaments.

Discussion

Here, we investigated the subcellular distribution and signaling of GPER1 expressed endogenously in a series of pathophysiologically relevant cell lines from various species, including MDCK cells, T47-D cells, and C_2C_{12} cells. GPER1 was localized both in the PM and on intracellular cytoskeletal structures. The PM receptors were subject to relatively

rapid constitutive endocytosis to reach such structures. These structures were identified at least in part as CK intermediate filaments, including those composed of CK7 and CK8, but not ER, Golgi, or microtubules. The GPER1 agonist G-1 and E2 stimulated GPER1-dependent cAMP production and β-arrestin2 recruitment to the PM. We conclude from this study that GPER1 couples to cAMP and β-arrestin2 signaling in the PM and associates intracellularly with CK, the latter of which may be a mechanism for subcellular redistribution of the receptor after endocytosis.

The subcellular localization of GPER1 has been a point of debate ever since this receptor was introduced as a putative estrogen receptor in 2005. Four studies were published early that addressed this issue using epitope-tagged receptors expressed in recombinant cell systems. Three of these studies used receptors tagged at the N terminus with either the HA epitope (Thomas et al., 2005; Filardo et al., 2007) or the FLAG epitope (Funakoshi et al., 2006) to claim that the receptor localized in the PM but reached intracellular compartments via E2-promoted endocytosis. Two other studies used receptors tagged in the C terminus with GFP, in the N terminus with the FLAG epitope, or nontagged receptor to claim that the receptor is more or less exclusively localized intracellularly in the ER (Revankar et al., 2005; Otto et al., 2008). Another study found that when GPER1 was tagged at the N terminus with the FLAG epitope it localized in the PM, whereas when tagged at the C terminus with GFP, it localized in the ER (Funakoshi et al., 2006), which agrees with some other epitope-tagged GPCR (Brothers et al., 2003) and indicates that tagging can influence GPCR trafficking. Since then, several studies have addressed endogenous receptor localization using various receptor antibodies and reported immunoreactivity at the cell periphery and/or intracellularly in the ER and/or Golgi (Funakoshi et al., 2006; Brailoiu et al., 2007; Sakamoto et al., 2007; Matsuda et al., 2008; Otto et al., 2008; Lin et al., 2009). Even though not emphasized, many of these reports, however, also show significant intracellular immunoreactivity not associated with either of these structures. Only in one study was PM localization of endogenous GPER1 directly addressed. In this case, specific radiolabeled E2 binding to a PM fraction from SkBr3 breast cancer cells was detected that was sensitive to prior treatment of the cells with a GPER1 siRNA (Thomas et al., 2005).

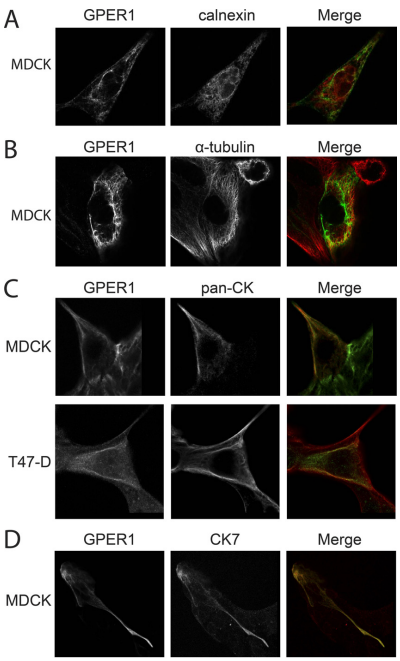

Fig. 6. Subcellular GPER1 localization. A to D, MDCK cells (MDCK) or T47-D cells (T47-D) were fixed and permeabilized before incubation with goat GPER1 antibody (GPER1), rabbit calnexin antibody (calnexin), mouse α-tubulin antibody (α-tubulin), mouse pan-CK antibody (pan-CK), or mouse CK7 antibody (CK7). Cells were subsequently incubated with secondary mouse anti-rabbit, rabbit anti-mouse, or donkey anti-goat ALEXA488- or ALEXA568-labeled antibody. The individual and merged (Merge) images were collected using a Nikon Eclipse confocal microscope, 60× objective, 50 μm zoom. The results are representative of experiments performed at least three times.

In this study, using an antibody that we confirmed to be specific for GPER1, immunostaining of fixed cells showed that endogenous GPER1 is localized both at the cell periphery and intracellularly in MDCK cells and T47-D cells. Furthermore, human GPER1, mouse FGPER1, and human HGPER1 colocalized on the same cytoskeleton-like cellular structures. MDCK cells stained positive under live nonfixed conditions, indicating that GPER1 is also present at the PM in these cells. No significant overlap occurred between receptor staining and either ER or Golgi staining, which suggests that the receptor matures normally in these cells. The ability of GPER1 to reach the PM was confirmed by live staining of HEK-FGPER1 cells with FLAG antibody. Live staining of MDCK cells and HEK-FGPER1 cells also showed that the PM receptors can reach intracellular structures via constitutive endocytosis. In MDCK cells, live and fixed staining had the same cytoskeleton-like patterns, suggesting, at least in part, that the constitutively internalized receptors give rise to such staining.

Three experimental observations led us to conclude that at least a portion of the cytoskeleton-like receptor staining represents receptors associated with CK intermediate filaments, including 1) colocalization of GPER1 and CK staining as determined by confocal immunofluorescence microscopy, 2) identification GPER1 staining on filamentous structures projecting between the nuclear membrane and the PM, and 3) reciprocal coimmunoprecipitation of GPER1 and CK, including CK7 and CK8. To our knowledge, this is the first observation that a GPCR is capable of reaching and interacting with intermediate filaments. CK7 and CK8 are simple-epithelial ductal-type CKs that are widely distributed and often coexpressed. Little is known about CK7, which usually pairs with CK19, but the related CK8, which pairs with CK18, has been shown to associate with the external leaflet of the PM in cancer cells (Gires et al., 2005). In addition, CKs are necessary for membrane incorporation of glucose transporters 1 and 3 (Vijayaraj et al., 2009). One suggestion is that endocytic vesicles use CK filaments to redistribute GPER1 to unique functional locations in the cell such as cell-cell or cell-

basement membrane contacts (Toivola et al., 2005) via interaction with the adapter complex AP3 involved in clathrin-mediated endocytosis in a way similar to the CK-related proteins vimentin, peripherin, and α-internexin (Styers et al., 2004).

GPER1 expression at the protein level is heterogeneous both in native and recombinant cells, with products observed both below and above the theoretical receptor mass, which may be consequences of detergent-resistant protein complexes, glycosylation, and degradation. The receptor monomer appears to be a 40- to 45-kDa protein as observed in both native and recombinant cells. The relationship of this protein to the 50- to 55-kDa receptor protein is not clear, but the latter may in part be a glycosylated form of the former because it decreased in mass upon PNGase F treatment. The 100-kDa receptor band identified primarily in receptor immunoprecipitates may be a detergent-resistant receptor dimer or a monomer interacting with another protein. It is noteworthy that the 100-kDa band was the primary receptor band enriched in CK immunoprecipitates, suggesting that it is this receptor form that interacts with CK. On the other hand, CK may serve as a scaffold for receptor interactions with other proteins. Some evidence was obtained that N-glycosylation plays a role in receptor interactions, at least for FGPER1, because PNGase treatment increased the amount of the 100-kDa FGPER1 band apparently at the expense of the lower mass bands. One explanation is that N-deglycosylation makes the proteins in the immunoprecipitate more hydrophobic, thus promoting complex formation. On the other hand, N-deglycosylation of the two asparagines in the receptor N-terminal domain may influence the immunoreactivity of the nearby N-terminal FLAG epitope. Apparent receptor degradation products were also observed, which should be cellular because all preparations contained a complete protease inhibitor cocktail. It is interesting to note that CK intermediate filaments associate with proteasomes (Olink-Coux et al., 1994), and ERα is degraded via a ubiquitin-proteasome pathway involving receptor association with CK8 and CK18 (Long and Nephew, 2006).

The localization of GPER1 signaling is also a matter of debate. Using recombinant cell systems and membrane-permeable and -impermeable E2 analogs, GPER1 was proposed to function either in the PM or intracellularly in the ER. PM signaling was based on GPER1 localization in this compartment, stimulation of cAMP production by mem-

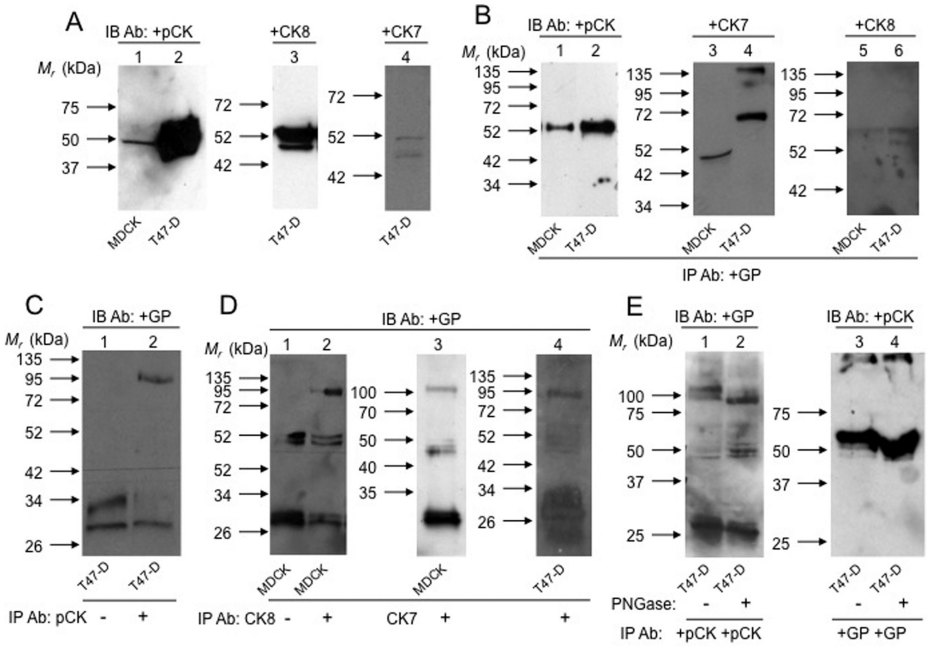

Fig. 7. Native GPER1-CK association. A, MDCK cells (MDCK, lane 1) and T47-D cells (T47-D, lanes 2–4) were lysed and immunoblotted with mouse pan-CK antibody (lanes 1 and 2), mouse CK8 antibody (lane 3), or mouse CK7 antibody (lane 4). B, MDCK cells (MDCK, lanes 1, 3, and 5) and T47-D cells (T47-D, lanes 2, 4, and 6) were lysed, immunoprecipitated with goat GPER1 antibody (GP) precoupled to protein G-Sepharose, and then immunoblotted with pan-CK antibody (lanes 1 and 2), CK7 antibody (lanes 3 and 4) or CK8 antibody (lanes 5 and 6). C, T47-D cells (T47-D) were lysed, immunoprecipitated with protein G-Sepharose without (−, lane) and with precoupled pan-CK antibody (+, lane), and then immunoblotted with GPER1 antibody (GP). D, MDCK cells (MDCK, lanes 1–3) and T47-D cells (T47-D, lane 4) were lysed, immunoprecipitated with CK8 antibody (lanes 1 and 2) or CK7 antibody (lane 3) precoupled to protein G-Sepharose, and then immunoblotted with GPER1 antibody. E, T47-D cells (T47-D) were lysed, immunoprecipitated with pan-CK antibody (lanes 1 and 2) or GPER1 antibody (lanes 3 and 4) precoupled to protein G-Sepharose, respectively, treated without (lanes 1 and 3) or with PNGase F (lanes 2 and 4) and then immunoblotted with GPER1 antibody. Molecular mass (M_r) standards (in kilodaltons) (left side arrows) are indicated. The results are representative of experiments performed at least three times.

brane-impermeable E2 analogs, E2-stimulated PM GTPγS binding, and GPER1-dependent PM E2 binding (Filardo et al., 2002, 2007; Thomas et al., 2005). On the other hand, ER-associated signaling was based on the identification of GPER1 in this compartment in some cells and stimulation of intracellular Ca^{2+} signaling and PI3-kinase translocation only by membrane-permeable E2 analogs (Revankar et al., 2005, 2007).

Here, we show that G-1 and E2 both stimulated GPER1-dependent cAMP production in several native cell lines from several species, which is a PM-defined event. G-1 and E2 also recruited β-arrestin2-GFP to the PM, which is consistent with the receptor for these agonists being localized in this compartment and also a possible mechanism of GPER1-mediated extracellular signal-regulated kinase signaling as shown previously for other receptors (Galandrin and Bouvier, 2006). Thus, we conclude that it is in the PM that GPER1 couples to G_s/adenylate cyclase and β-arrestin2 in native cells. Whether GPER1 is able to couple to other signals in other subcellular compartments such as intermediate filaments remains an open question. It is noteworthy that the efficacy of E2 on GPER1-mediated cAMP production in these cells was only a fraction of that of G-1, which suggests that E2 may act as a partial agonist or G-1 as a superagonist on this response. Although our assay of β-arrestin2 recruitment is only semiquantitative, the efficacies of G-1 and E2 on this response seemed to be approximately equal. Thus, E2 may exhibit biased signaling at GPER1 (i.e., full agonist on β-arrestin2 recruitment and partial agonist on cAMP production), a behavior described for agonists at several other GPCR (Kenakin, 2007), including receptors coupled to both cAMP and β-arrestin signaling (Galandrin and Bouvier, 2006).

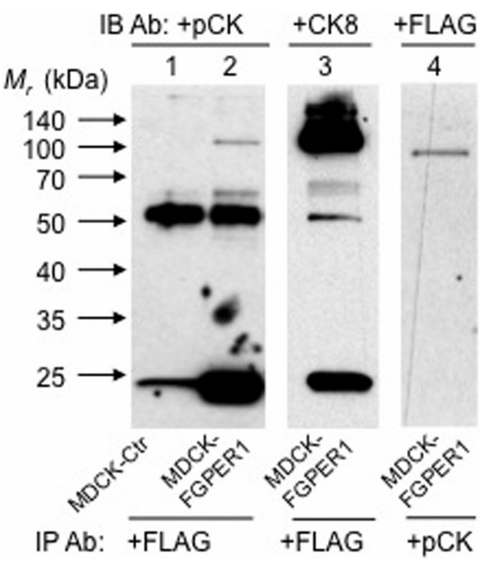

Fig. 8. Recombinant GPER1-CK association. MDCK cells without (MDCK-Ctr.) and with transient transfection of FGPER1 cDNA (MDCK-FGPER1) were lysed, immunoprecipitated with M2 FLAG antibody (lanes 1–3) or pan-CK antibody (lane 4), and immunoblotted with pan-CK antibody (lanes 1 and 2), CK8 antibody (lane 3), or M2 FLAG antibody (lane 4). Molecular mass (M_r) standards (in kilodaltons) (left side arrows) are indicated. The results are representative of experiments performed at least three times.

In summary, we show that GPER1 is localized and signals via cAMP production and β-arrestin2 recruitment in the PM. Receptors also reach CK intermediate filaments. CK is highly expressed in cancer epithelial cells and has long been used to classify cancer subtypes (Moll et al., 2008). Considering that GPER1 influences growth factor signaling pathways (Filardo and Thomas, 2005; Prossnitz et al., 2008) and cancer cell proliferation (Pandey et al., 2009; Ariazi et al., 2010) and that receptor expression is associated with cancer growth (Filardo et al., 2006; Smith et al., 2007), it is tempting to propose that GPER1-CK association in epithelial cells provides an important functional link in this disease.

Acknowledgments

We thank J. Enquist for assistance in constructing HEK293 cells stably expressing FGPER1 and FB2R, M. G. Caron for providing β-arrestin2-GFP, and M. Sjöström for experimental assistance.

Authorship Contributions

Participated in research design: Sandén, Broselid, Olde, and Leeb-Lundberg.

Conducted experiments: Sandén, Broselid, Cornmark, Andersson, Mårtensson, and Daszkiewicz-Nilsson.

Performed data analysis: Sandén, Broselid, Olde, and Leeb-Lundberg.

Wrote or contributed to the writing of the manuscript: Sandén, Broselid, and Leeb-Lundberg.

Other: Leeb-Lundberg acquired funding for the research.

References

Ahola TM, Manninen T, Alkio N, and Ylikomi T (2002) G protein-coupled receptor 30 is critical for a progestin-induced growth inhibition in MCF-7 breast cancer cells. *Endocrinology* **143:**3376–3384.

Ariazi EA, Brailoiu E, Yerrum S, Shupp HA, Slifker MJ, Cunliffe HE, Black MA, Donato AL, Arterburn JB, Oprea TI, et al. (2010) The G protein-coupled receptor GPR30 inhibits proliferation of estrogen receptor-positive breast cancer cells. *Cancer Res* **70:**1184–1194.

Barak LS, Ferguson SS, Zhang J, and Caron MG (1997) A beta-arrestin/green fluorescent protein biosensor for detecting G protein-coupled receptor activation. *J Biol Chem* **272:**27497–27500.

Bologa CG, Revankar CM, Young SM, Edwards BS, Arterburn JB, Kiselyov AS, Parker MA, Tkachenko SE, Savchuck NP, Sklar LA, et al. (2006) Virtual and biomolecular screening converge on a selective agonist for GPR30. *Nat Chem Biol* **2:**207–212.

Brailoiu E, Dun SL, Brailoiu GC, Mizuo K, Sklar LA, Oprea TI, Prossnitz ER, and Dun NJ (2007) Distribution and characterization of estrogen receptor G protein-coupled receptor 30 in the rat central nervous system. *J Endocrinol* **193:**311–321.

Brothers SP, Janovick JA, and Conn PM (2003) Unexpected effects of epitope and chimeric tags on gonadotropin-releasing hormone receptors: implications for understanding the molecular etiology of hypogonadotropic hypogonadism. *J Clin Endocrinol Metab* **88:**6107–6112.

Chomczynski P and Sacchi N (1987) Single-step method of RNA isolation by acid guanidinium thiocyanate-phenol-chloroform extraction. *Anal Biochem* **162:**156–159.

Enquist J, Skröder C, Whistler JL, and Leeb-Lundberg LM (2007) Kinins promote B_2 receptor endocytosis and delay constitutive B_1 receptor endocytosis. *Mol Pharmacol* **71:**494–507.

Eriksson JE, Dechat T, Grin B, Helfand B, Mendez M, Pallari HM, and Goldman RD (2009) Introducing intermediate filaments: from discovery to disease. *J Clin Invest* **119:**1763–1771.

Ferrero M, Spyratos F, Desplaces A, Andrieu C, Phillips E, and Rouëssé J (1989) Cytokeratin analysis of breast and leukemia tumor cell lines by flow cytometry. *Biol Cell* **65:**305–308.

Filardo E, Quinn J, Pang Y, Graeber C, Shaw S, Dong J, and Thomas P (2007) Activation of the novel estrogen receptor G protein-coupled receptor 30 (GPR30) at the plasma membrane. *Endocrinology* **148:**3236–3245.

Filardo EJ, Graeber CT, Quinn JA, Resnick MB, Giri D, DeLellis RA, Steinhoff MM, and Sabo E (2006) Distribution of GPR30, a seven membrane-spanning estrogen receptor, in primary breast cancer and its association with clinicopathologic determinants of tumor progression. *Clin Cancer Res* **12:**6359–6366.

Filardo EJ, Quinn JA, Frackelton AR Jr., and Bland KI (2002) Estrogen action via the G protein-coupled receptor, GPR30: stimulation of adenylyl cyclase and cAMP-mediated attenuation of the epidermal growth factor receptor-to-MAPK signaling axis. *Mol Endocrinol* **16:**70–84.

Filardo EJ and Thomas P (2005) GPR30: a seven-transmembrane-spanning estrogen receptor that triggers EGF release. *Trends Endocrinol Metab* **16:**362–367.

Funakoshi T, Yanai A, Shinoda K, Kawano MM, and Mizukami Y (2006) G protein-coupled receptor 30 is an estrogen receptor in the plasma membrane. *Biochem Biophys Res Commun* **346:**904–910.

Galandrin S and Bouvier M (2006) Distinct signaling profiles of beta1 and beta2 adrenergic receptor ligands toward adenylyl cyclase and mitogen-activated protein kinase reveals the pluridimensionality of efficacy. *Mol Pharmacol* **70:**1575–1584.

Gires O, Andratschke M, Schmitt B, Mack B, and Schaffrik M (2005) Cytokeratin 8 associates with the external leaflet of plasma membranes in tumour cells. *Biochem Biophys Res Commun* **328:**1154–1162.

Heldring N, Pike A, Andersson S, Matthews J, Cheng G, Hartman J, Tujague M, Ström A, Treuter E, Warner M, et al. (2007) Estrogen receptors: how do they signal and what are their targets. *Physiol Rev* **87:**905–931.

Heuser JE and Anderson RG (1989) Hypertonic media inhibit receptor-mediated endocytosis by blocking clathrin-coated pit formation. *J Cell Biol* **108:**389–400.

Kenakin T (2007) Functional selectivity through protean and biased agonism: who steers the ship? *Mol Pharmacol* **72:**1393–1401.

Kolkova Z, Noskova V, Ehinger A, Hansson S, and Casslén B (2010) G protein-coupled estrogen receptor 1 (GPER, GPR 30) in normal human endometrium and early pregnancy decidua. *Mol Hum Reprod* **16:**743–751.

Kotarsky K, Owman C, and Olde B (2001) A chimeric reporter gene allowing for clone selection and high-throughput screening of reporter cell lines expressing G-protein-coupled receptors. *Anal Biochem* **288:**209–215.

Lin BC, Suzawa M, Blind RD, Tobias SC, Bulun SE, Scanlan TS, and Ingraham HA (2009) Stimulating the GPR30 estrogen receptor with a novel tamoxifen analogue activates SF-1 and promotes endometrial cell proliferation. *Cancer Res* **69:**5415–5423.

Long X and Nephew KP (2006) Fulvestrant (ICI 182,780)-dependent interacting proteins mediate immobilization and degradation of estrogen receptor-alpha. *J Biol Chem* **281:**9607–9615.

Maggiolini M, Vivacqua A, Fasanella G, Recchia AG, Sisci D, Pezzi V, Montanaro D, Musti AM, Picard D, and Andò S (2004) The G protein-coupled receptor GPR30 mediates c-fos up-regulation by 17beta-estradiol and phytoestrogens in breast cancer cells. *J Biol Chem* **279:**27008–27016.

Mårtensson UE, Salehi SA, Windahl S, Gomez MF, Swärd K, Daszkiewicz-Nilsson J, Wendt A, Andersson N, Hellstrand P, Grände PO, et al. (2009) Deletion of the G protein-coupled receptor GPR30 impairs glucose tolerance, reduces bone growth, increases blood pressure, and eliminates estradiol-stimulated insulin release in female mice. *Endocrinology* **150:**687–698.

Matsuda K, Sakamoto H, Mori H, Hosokawa K, Kawamura A, Itose M, Nishi M, Prossnitz ER, and Kawata M (2008) Expression and intracellular distribution of the G protein-coupled receptor 30 in rat hippocampal formation. *Neurosci Lett* **441:**94–99.

Meier KE, Snavely MD, Brown SL, Brown JH, and Insel PA (1983) Alpha 1- and beta 2-adrenergic receptor expression in the Madin-Darby canine kidney epithelial cell line. *J Cell Biol* **97:**405–415.

Moll R, Divo M, and Langbein L (2008) The human keratins: biology and pathology. *Histochem Cell Biol* **129:**705–733.

Olde B and Leeb-Lundberg LM (2009) GPR30/GPER1: searching for a role in estrogen physiology. *Trends Endocrinol Metab* **20:**409–416.

Olink-Coux M, Arcangeletti C, Pinardi F, Minisini R, Huesca M, Chezzi C, and Scherrer K (1994) Cytolocation of prosome antigens on intermediate filament subnetworks of cytokeratin, vimentin and desmin type. *J Cell Sci* **107:**353–366.

Otto C, Rohde-Schulz B, Schwarz G, Fuchs I, Klewer M, Brittain D, Langer G, Bader B, Prelle K, Nubbemeyer R, et al. (2008) G protein-coupled receptor 30 localizes to the endoplasmic reticulum and is not activated by estradiol. *Endocrinology* **149:**4846–4856.

Pandey DP, Lappano R, Albanito L, Madeo A, Maggiolini M, and Picard D (2009) Estrogenic GPR30 signalling induces proliferation and migration of breast cancer cells through CTGF. *EMBO J* **28:**523–532.

Pollack V, Scheiber K, Pfaller W, and Schramek H (1997) Loss of cytokeratin expression and formation of actin stress fibers in dedifferentiated MDCK-C7 cell lines. *Biochem Biophys Res Commun* **241:**541–547.

Prossnitz ER, Arterburn JB, Smith HO, Oprea TI, Sklar LA, and Hathaway HJ (2008) Estrogen signaling through the transmembrane G protein-coupled receptor GPR30. *Annu Rev Physiol* **70:**165–190.

Razandi M, Pedram A, Merchenthaler I, Greene GL, and Levin ER (2004) Plasma membrane estrogen receptors exist and functions as dimers. *Mol Endocrinol* **18:**2854–2865.

Revankar CM, Cimino DF, Sklar LA, Arterburn JB, and Prossnitz ER (2005) A transmembrane intracellular estrogen receptor mediates rapid cell signaling. *Science* **307:**1625–1630.

Revankar CM, Mitchell HD, Field AS, Burai R, Corona C, Ramesh C, Sklar LA, Arterburn JB, and Prossnitz ER (2007) Synthetic estrogen derivatives demonstrate the functionality of intracellular GPR30. *ACS Chem Biol* **2:**536–544.

Sakamoto H, Matsuda K, Hosokawa K, Nishi M, Morris JF, Prossnitz ER, and Kawata M (2007) Expression of G protein-coupled receptor-30, a G protein-coupled membrane estrogen receptor, in oxytocin neurons of the rat paraventricular and supraoptic nuclei. *Endocrinology* **148:**5842–5850.

Schweizer J, Bowden PE, Coulombe PA, Langbein L, Lane EB, Magin TM, Maltais L, Omary MB, Parry DA, Rogers MA, et al. (2006) New consensus nomenclature for mammalian keratins. *J Cell Biol* **174:**169–174.

Smith HO, Leslie KK, Singh M, Qualls CR, Revankar CM, Joste NE, and Prossnitz ER (2007) GPR30: a novel indicator of poor survival for endometrial carcinoma. *Am J Obstet Gynecol* **196:**386.e1–e11.

Styers ML, Salazar G, Love R, Peden AA, Kowalczyk AP, and Faundez V (2004) The endo-lysosomal sorting machinery interacts with the intermediate filament cytoskeleton. *Mol Biol Cell* **15:**5369–5382.

Thomas P, Pang Y, Filardo EJ, and Dong J (2005) Identity of an estrogen membrane receptor coupled to a G protein in human breast cancer cells. *Endocrinology* **146:**624–632.

Toivola DM, Tao GZ, Habtezion A, Liao J, and Omary MB (2005) Cellular integrity plus: organelle-related and protein-targeting functions of intermediate filaments. *Trends Cell Biol* **15:**608–617.

Vijayaraj P, Kröger C, Reuter U, Windoffer R, Leube RE, and Magin TM (2009) Keratins regulate protein biosynthesis through localization of GLUT1 and -3 upstream of AMP kinase and Raptor. *J Cell Biol* **187:**175–184.

Whistler JL, Enquist J, Marley A, Fong J, Gladher F, Tsuruda P, Murray SR, and Von Zastrow M (2002) Modulation of postendocytic sorting of G protein-coupled receptors. *Science* **297:**615–620.

Windahl SH, Andersson N, Chagin AS, Mårtensson UE, Carlsten H, Olde B, Swanson C, Movérare-Skrtic S, Sävendahl L, Lagerquist MK, et al. (2009) The role of the G protein-coupled receptor GPR30 in the effects of estrogen in ovariectomized mice. *Am J Physiol Endocrinol Metab* **296:**E490–E496.

Address correspondence to: Dr. L. M. Fredrik Leeb-Lundberg, Department of Experimental Medical Science, Lund University, BMC A12, SE-22184 Lund, Sweden. E-mail: fredrik.leeb-lundberg@med.lu.se

Paper II

Human Cancer Biology

Clinical Cancer Research

G Protein–Coupled Estrogen Receptor Is Apoptotic and Correlates with Increased Distant Disease-Free Survival of Estrogen Receptor–Positive Breast Cancer Patients

Stefan Broselid[1], Benxu Cheng[5], Martin Sjöström[2], Kristina Lövgren[2], Heather L.P. Klug-De Santiago[5], Mattias Belting[2,4], Karin Jirström[3,4], Per Malmström[2,4], Björn Olde[1], Pär-Ola Bendahl[2], Linda Hartman[2], Mårten Fernö[2], and L.M. Fredrik Leeb-Lundberg[1,5]

Abstract

Purpose: G protein–coupled estrogen receptor 1 (GPER1), previously named GPR30, is a membrane receptor reported to mediate nongenomic estrogen responses. We investigated if GPER1 expression correlates with any clinicopathologic variables and distant disease-free survival (DDFS) in patients with breast cancer, if any prognostic impact of the receptor is dependent on estrogen receptor-α (ER-α) status, and if the receptor impacts apoptotic signaling in ER-positive breast cancer cells.

Experimental Design: GPER1 expression was analyzed by immunohistochemistry in breast tumors from 273 pre- and postmenopausal stage II patients, all treated with adjuvant tamoxifen for 2 years (cohort I) and from 208 premenopausal lymph node-negative patients, of which 87% were not subjected to any adjuvant systemic treatment (cohort II). GPER1-dependent proapoptotic signaling was analyzed in MCF7 cells with and without GPER1 knockdown, T47D cells, HEK293 cells (HEK), and HEK stably expressing GPER1 (HEK-R).

Results: GPER1 positively correlates with ER and progesterone receptor expression. Multivariate analysis showed that GPER1 is an independent prognostic marker of increased 10-year DDFS in the ER-positive subgroup. HEK-R has higher basal proapoptotic signaling compared with HEK including increased cytochrome C release, caspase-3 cleavage, PARP cleavage, and decreased cell viability. Treating HEK-R with the proteasome inhibitor epoxomicin, to decrease GPER1 degradation, further increases receptor-dependent proapoptotic signaling. Also, GPER1 knockdown decreases basal and agonist-stimulated proapoptotic receptor signaling in MCF7 cells.

Conclusions: GPER1 is a prognostic indicator for increased DDFS in ER-positive breast cancer, which may be associated with constitutive GPER1-dependent proapoptotic signaling in ER-positive breast cancer cells. *Clin Cancer Res; 19(7); 1681–92. ©2013 AACR.*

Introduction

Breast cancer is the most common female cancer constituting about 30% of all cancers in women (1). This cancer is a heterogeneous disease with several subtypes with different biologic characteristics and clinical behaviors, which are traditionally divided on the basis of the presence of 3 receptors, estrogen receptor-α (ER-α), progesterone receptor (PgR), and HER2 (2). The presence of ER and HER2 allows targeted therapeutic intervention by blocking proliferative ER and HER2 signaling. Endocrine therapy with antiestrogens, for example, tamoxifen, has long been a therapeutic choice for all stages of ER-positive breast cancer. Tamoxifen acts by interfering with proliferative genomic estrogen signaling at ER, which functions as a nuclear transcription factor to regulate gene expression (3). However, a significant number of ER-positive breast cancers fail to respond to tamoxifen treatment (4) emphasizing the necessity for other therapeutic targets in this cancer.

G protein–coupled estrogen receptor 1 (GPER1), formerly known as GPR30 as an orphan, is a G protein–coupled receptor (GPCR) structurally distinct from ER that was reported to bind 17β-estradiol (E2) with relatively high affinity and to mediate nongenomic responses to estrogen

Authors' Affiliations: [1]Department of Experimental Medical Science, [2]Department of Clinical Science, Division of Oncology, and [3]Department of Clinical Science, Division of Pathology, Lund University; [4]Skåne Department of Oncology, Skåne University Hospital, Lund, Sweden; and [5]Medical Research Division, Regional Academic Health Center, The University of Texas Health Science Center at San Antonio, Edinburg, Texas

Note: Supplementary data for this article are available at Clinical Cancer Research Online (http://clincancerres.aacrjournals.org/).

S. Broselid, B. Cheng, and M. Sjöström contributed equally as first authors. M. Fernö and L.M.F. Leeb-Lundberg contributed equally as last authors.

Corresponding Author: L.M. Fredrik Leeb-Lundberg, Department of Experimental Medical Science, Lund University, BMC, A12, SE-22184 Lund, Sweden. Phone: 46-46-2223944; Fax: 46-46-2220568; E-mail: fredrik.leeb-lundberg@med.lu.se

doi: 10.1158/1078-0432.CCR-12-2376

Translational Relevance

G protein–coupled estrogen receptor 1 (GPER1) is a novel putative membrane estrogen receptor (ER). Here, we investigated whether GPER1 correlates with any clinicopathologic variables and distant disease-free survival (DDFS) in patients with breast cancer. Two cohorts of patients with breast cancer were studied, one with stage II carcinoma subsequently treated with tamoxifen and another with lymph node-negative carcinoma subsequently mainly not treated with tamoxifen. GPER1 positively correlated with ER-α and progesterone receptor expression and with increased DDFS in ER-positive cancer. GPER1 was constitutively proapoptotic in ER-positive breast cancer cells. Therefore, GPER1 may be a novel prognostic marker in breast cancer, and enhancing GPER1-dependent proapoptotic signaling may be a therapeutic avenue in this disease.

in vivo (5–7) and *in vitro* (8, 9) and to tamoxifen *in vitro* (10, 11). However, the designation of E2 as the cognate GPER1 ligand is debated (12, 13). Nevertheless, GPER1 correlates with ER and PgR expression in breast tumors (14–17) and coimmunoprecipitates with ER in ER- and PgR-positive MCF7 cells (18), suggesting that GPER1 and ER are functionally related. GPER1 knockdown enhances E2-stimulated cell proliferation in MCF7 cells (17), and progestin-promoted GPER1 upregulation is required for the antiproliferative progestin response in these cells (19, 20). Because this occurs apparently independently of E2 (19, 20), GPER1 may be constitutively antiproliferative in ER-positive breast cancer cells. Indeed, GPER1 is constitutively apoptotic in rat cardiac cells (21), and E2-regulated GPER1 activity is either proapoptotic (22, 23) or antiapoptotic (24, 25) depending on the system studied.

Here, we investigated if GPER1 correlates with any clinicopathologic variables and distant disease-free survival (DDFS) in patients with breast cancer, if any prognostic impact of the receptor is dependent on ER status, and if the receptor impacts apoptotic signaling. Our results show that GPER1 correlates positively with ER and PgR expression, but not with HER2 expression, associates with increased DDFS in ER-positive breast cancer and is constitutively apoptotic in ER-positive breast cancer cells. Thus, GPER1 may be an interesting new prognostic marker and therapeutic target in ER-positive breast cancer.

Materials and Methods

Patients

Cohort I consisted of 273 patients, including 56 (21%) premenopausal and 217 (79%) postmenopausal (median age 62 years; range, 26–81), with stage II (pT2pN0pM0, pT1-2pN1pM0) breast carcinoma diagnosed in the South Sweden Health Care Region (1985–1994). The patients had previously been selected from 2 randomized clinical trials (26, 27) to compare methods for evaluation of hormone receptor status (28). All patients were operated with modified radical mastectomy or breast-conserving surgery with axillary lymph node dissection (level I and II). After breast-conserving surgery, radiotherapy (50 Gy) was given to the breast. In patients with axillary lymph node metastases, locoregional radiotherapy was also administered. All patients were treated with tamoxifen for 2 years, irrespective of ER status. The median follow-up was 6.1 years for the endpoint DDFS for patients alive and free from distant metastases at the last review of the patients' records. No patients received any systemic adjuvant therapy besides tamoxifen.

Cohort II consisted of 237 premenopausal women with node-negative breast carcinoma diagnosed in the South Sweden Health Care Region (1991–1994). In 14 cases, no paraffin blocks were retrieved, 6 cases were excluded because of problems in preparation or staining, and 9 cases were excluded as the material only contained normal breast tissue or carcinoma *in situ*. Of the analyzed 208 patients (median age 47; range, 30–57), all patients received breast surgery and in most cases postoperative radiotherapy. Of these, 180 patients received no adjuvant systemic therapy after surgery, 7 patients received tamoxifen (20 mg daily for 5 years), 1 patient was oophorectomized, and 20 patients received chemotherapy (cyclophosphamide, methotrexate, and 5-fluoruracil i.v. 9 cycles). The median follow-up was 10.8 years for the endpoint DDFS for patients alive and free from distant metastases at the last review of the patients' records. Information on clinical outcome and patient- and tumor-related factors were reported previously (29).

Preparation of tissue microarrays

Tissue microarrays (TMA) were prepared from paraffin-embedded blocks using a manual arrayer (Beecher Instruments). Two 0.6-mm cores were taken from representative areas of each primary tumor block and transferred into a recipient paraffin block, constituting the TMA block. Sections (4 μm) were cut from each TMA block and placed on glass slides (Menzel Superfrost Plus) and dried at 60°C for 2 hours.

Immunohistochemical staining

Deparaffinization and pretreatment was conducted in PT-Link (Dako) with Target Retrieval Solution pH 6. After blocking with peroxidase block S2023 (Dako) for 5 minutes, the slides were incubated with GPER1 antibody (R&D System, 1:50) for 60 minutes and then with K0690 (Dako) with a biotinylated secondary antibody followed by streptavidin–horseradish peroxidase (HRP). Peroxidase/DAB was used for visualization. Nuclear staining with Mayer's hematoxylin was done for contrast. These steps were carried out in an Autostainer plus staining machine (Dako). The slides were then washed in tap water for 10 minutes and dehydrated with ethanol and xylene. Glass coverslips were mounted with Pertex mounting medium.

Evaluation of immunohistochemical staining

Immunohistochemical staining was examined by light microscopy without knowledge of clinical and tumor

characteristic data. GPER1 antibody staining was estimated semi-quantitatively as the fraction of stained tumor cells (0%–1%, 2%–10%, 11%–50%, and 51%–100%) and the intensity of stained tumor cells was scored (0, no; 1, very weak; 2, weak; 3, moderate; and 4, strong). Two individuals examined all stained samples and final consensus was reached in any discrepant cases. In cohort I, 24 (8.8%) showed 0%–1% stained cells, 1 (0.4%) 2%–10%, 5 (1.8%) 11%–50%, and 243 (89%) more than 50%. In terms of staining intensity, 24 (8.8%) were judged negative (level 0), 38 (13%) very weak (level 1), 125 (46%) weak (level 2), 75 (28%) moderate (level 3), and 11 (4%) strong (level 4). In cohort II, 20 (9.6%) showed 0%–1% stained cells, 2 (1%) 2%–10%, 0 (0%) 11%–50%, and 186 (89%) more than 50%. In terms of staining intensity, 20 (10%) were level 0, 69 (33%) level 1, 87 (42%) level 2, 23 (11%) level 3, and 9 (4%) level 4.

Cell culture and DNA constructs

HeLa cells [American Type Culture Collection (ATCC)] and cells stably expressing GPER1 were made and grown as previously described (30). HEK293 cells (ATCC; HEK) and HEK stably expressing GPER1 tagged in the N terminus with the FLAG epitope (HEK-R) were made and grown as previously described (31). HEK were transiently transfected with cDNA for GPER1 tagged in the N terminus with the FLAG epitope (FGPER1) using TransIT-293 (Mirus). MCF7 cells (ATCC) were grown in Dulbecco's modified essential medium supplemented with 10% FBS in 5% CO_2 at 37°C. Two days before experimentation, cells were grown in 5% charcoal-treated FBS. MCF7 cells were infected with GPER1 short hairpin RNA (shRNA) lentiviral particles and stable clones were enriched using puromycin as described by the supplier (Santa Cruz).

Immunoblotting

Immunoblotting was done as previously described (32). Membranes were probed with antibodies from R&D Systems (GPER1), Sigma-Aldrich (M2 FLAG, β-actin), Biovision (cytochrome C), Cell Signaling (cleaved caspase-3, PARP, and ubiquitin), and Santa Cruz [p-ERK1/2, extracellular signal–regulated kinase (ERK)1/2, and p53]. Immunoreactive bands were visualized with a chemiluminescence immunodetection kit as described by the supplier (GE Healthcare).

Flow cytometry analysis

For cell surface receptor analysis, cells were collected and washed twice with ice-cold buffer (PBS with Ca^{2+}/Mg^{2+}–containing 10% FBS). Cells were resuspended in cold buffer, counted, and aliquoted at 5×10^5 cells/mL. The cells were then incubated with mouse M1 FLAG antibody (Sigma-Aldrich) at 4°C for 20 minutes, followed by further incubation with goat anti-mouse allophycocyanin (APC)-conjugated antibody (Life Technologies) at 4°C for 30 minutes in the dark. The cells were then fixed in PBS containing 2% formaldehyde before analysis by flow cytometry. The geometric mean fluorescence in the APC channel for stained cells was measured by fluorescence-activated cell sorting (FACS) analysis on an LSRFortessa (BD Biosciences) using FACSDiva software version 6.1.2 (BD Biosciences) for data collection. FlowJo software version 7.6.4 (Tree Star) was used for analysis. For each sample, 3×10^4 events were collected and forward scatter (FSC) and side scatter (SSC) gates were set on the cell population. For all samples, greater than 85% of the events fell within the FSC/SSC gate. Statistical analysis was done using Excel software (Microsoft Office 2007).

For cell-cycle analysis, collected cells were briefly fixed for 30 minutes with 4% formaldehyde on ice. Cells were permeabilized by adding 5 mL of cold 70% ethanol dropwise while vortexing. Samples were stored at −20°C until staining with propidium iodide (PI)/RNase staining buffer (BD Biosciences) for 15 minutes at room temperature. Cell-cycle profiles were collected on 3×10^4 events per sample using the LSRFortessa (BD Biosciences). For data collection, FACSDiva software ver. 6.1.2 (BD Biosciences) was used. Statistical analysis was done using Excel software (Microsoft Office 2007).

Immunofluorescence microscopy

Fixed HEK transiently transfected with FGPER1 cDNA were stained and visualized using M1 FLAG antibody (Sigma-Aldrich) as primary antibody and Alexa488-labeled mouse immunoglobulin G (IgG)2b (Invitrogen) as secondary antibody, and images were collected using a Nikon Eclipse confocal fluorescence microscope as previously described (31). An antibody against endogenously expressed cytokeratin 8 (Sigma-Aldrich) and a secondary Alexa568-labeled mouse IgG1 antibody (Invitrogen) were used to distinguish transfected from untransfected cells.

Cell viability

Morphologic changes and nuclear staining of cells with Hoechst 33342 were determined by phase-contrast and fluorescence microscopy using a Leica 6000 B microscope. Cell viability was monitored by the conversion of MTT to formazan.

Statistical analysis

DDFS was visualized using the Kaplan–Meier method and the influence of GPER1 intensity (on 5 levels) on DDFS was tested using a log-rank test for trend. The Cox proportional hazards model was used for estimation of univariate and multivariate HRs and to investigate interactions between GPER1 and ER. GPER1 intensity on 5 levels (coded as 0–4) and age were used as linear covariates (i.e., test for trend), whereas all other factors were used as dichotomized covariates in the statistical analyses, except for histologic grade (3 groups). The HR for GPER1 as a linear covariate is then a mean change for 1 step on the linear GPER1 intensity scale. Proportional hazards assumptions were checked both graphically and using Schoenfeld test (33). To check the assumptions of linear trend for GPER1, we compared the linear Cox-model with a Cox-model with GPER1 as a factor on 5 levels. For the established prognostic factors, standard

cutoff values were used and were the same as for earlier published patient series (29, 34). Association between GPER1 and the other factors were analyzed using Pearson χ^2 test for trend. All *P* values correspond to 2-sided tests. The statistical calculations were conducted using Stata version 11.0 (StataCorp 2009).

Ethical considerations

This project was approved by the ethical committee at Lund University (Lund, Sweden; LU 240-01). All information and data were handled confidentially. Full consent was obtained from patients involved in the study for patient participation and for publication of study results.

Results

GPER1 expression correlates with ER-positive breast tumors

GPER1 was evaluated by immunohistochemical staining of breast tumors from 2 patient cohorts using a GPER1-specific antibody. The specificity of the receptor antibody was validated in HeLa cells, with naïve cells (HeLa), which do not express GPER1, lacking immunoreactivity, and HeLa cells stably expressing the receptor (HeLa-GPER1) showing an immunoreactive band of a molecular mass (40 kDa) corresponding to the predicted mass of the receptor (Fig. 1A).

Because approximately 90% of the tumor samples had more than 50% stained cells, staining intensity at 5 levels (Fig. 1B, a–e) rather than staining fraction was used for further analysis. In cohort I, consisting of 273 pre- and postmenopausal stage II cases subsequently treated with tamoxifen, tumors with higher GPER1 were more likely to be ER-positive ($P = 0.01$) and PgR-positive ($P = 0.01$) but did not correlate with any other clinicopathologic variable including age, lymph node status, tumor size, histologic grade, HER2 expression, and Ki67 staining (Table 1). In cohort II, consisting of 208 premenopausal node-negative breast cancer cases subsequently mainly not subjected to adjuvant systemic treatment, tumors with higher GPER1 intensity were also more likely to be positive for ER ($P = 0.0005$) and PgR ($P = 0.0004$) and again did not correlate with HER2 (Table 1). However, GPER1 correlated positively with increasing age ($P = 0.003$) and negatively with large tumor size ($P = 0.05$), high histologic grade ($P = 0.0003$), and high Ki67 staining ($P = 0.0007$; Table 1).

GPER1 expression correlates with increased DDFS in patients with ER-positive breast tumors

With 10 years of follow-up for survival and distant metastases, 81 patients were diagnosed with distant recurrences in cohort I. In this cohort, GPER1 significantly correlated with increased DDFS ($P = 0.014$; log-rank test for trend; Fig. 1C). A Cox-model for univariate analysis with GPER1 as a linear covariate gave HR = 0.75 [95% confidence interval (CI), 0.60–0.94], which should be interpreted as the mean HR for an arbitrary step on the scale (0–4). Testing this model against the more flexible model treating GPER1 as a factor on 5 levels, did not contradict this interpretation ($P = 0.3$). Schoenfeld test did not indicate departure from the assumption of proportional hazards. When stratifying for ER status, GPER1 was a significant prognostic factor in the ER-positive subgroup (HR, 0.66; 95% CI, 0.49–0.88; $P = 0.007$; Fig. 1C; Table 2) but not in the ER-negative subgroup (HR, 1.06; 95% CI, 0.76–1.48; $P = 0.7$; Fig. 1C). In a Cox-model allowing for interaction between GPER1 as a linear covariate and ER-status, we achieved moderate evidence of interaction ($P = 0.06$). Consistent with the whole cohort, GPER1 did not correlate with any other clinicopathologic variable in the ER-positive subgroup (Supplementary Table S1). Further multivariate analysis revealed that GPER1 was a significant independent prognostic factor in the ER-positive subgroup (HR, 0.67; 95% CI, 0.50–0.92; $P = 0.01$; Table 2). The HR for GPER1 remained relatively constant and significant in the multivariate analysis regardless of which additional variables indicated in Table 2 that were included in the model (data not shown).

In cohort II, 46 patients were diagnosed with distant recurrences within 10 years. Analysis of this cohort revealed a trend toward increased 10-year DDFS in patients with higher GPER1-expressing tumors ($P = 0.08$; log-rank test for trend; Fig. 1D). A Cox-model for univariate analysis with GPER1 as a linear covariate gave HR = 0.75 (95% CI, 0.55–1.04), and treating GPER1 as a factor on 5 levels did not significantly improve the fit ($P = 0.8$). With GPER1 as a linear covariate, Schoenfeld test gave modest evidence ($P = 0.06$) for departure from the assumption of proportional hazards, in which case the HR should be interpreted as a mean HR over the time-period studied rather than constant at all times. When stratifying for ER status, the trend was again observed in the ER-positive subgroup (HR, 0.62; 95% CI, 0.39–0.99; $P = 0.047$; Fig. 1D; Table 3) but not in the ER-negative subgroup (HR, 0.97; 95% CI, 0.63–1.49; $P = 0.89$; Fig. 1D) but the interaction was not statistically significant ($P = 0.16$). In the ER-positive subgroup, GPER1 remained negatively associated with high histologic grade ($P = 0.02$) and high Ki67 staining ($P = 0.05$) but not with any other clinicopathologic variables (Supplementary Table S1). The prognostic value of GPER1 did not remain significant in multivariate analysis of this subgroup (HR, 0.60; 95% CI, 0.34–1.1; $P = 0.09$; Table 3). Indeed, due to the large number of factors included, and the colinearity between them, no established risk factor was significant in this multivariate model. However, the HR for GPER1 in this subgroup was comparable with that in cohort I and again remained relatively constant regardless of which additional variables indicated in Table 3 that were included in the model (data not shown). This suggests that GPER1 has added prognostic value, and that the lack of significance is due in part to the smaller number of cases and recurrences available for analysis in this subgroup (34 in cohort I and 18 in cohort II). Similar results were obtained when only the 180 systemically untreated patients were analyzed in cohort II (data not shown). However, due to fewer events, the *P* values were higher for this subgroup than for the entire cohort.

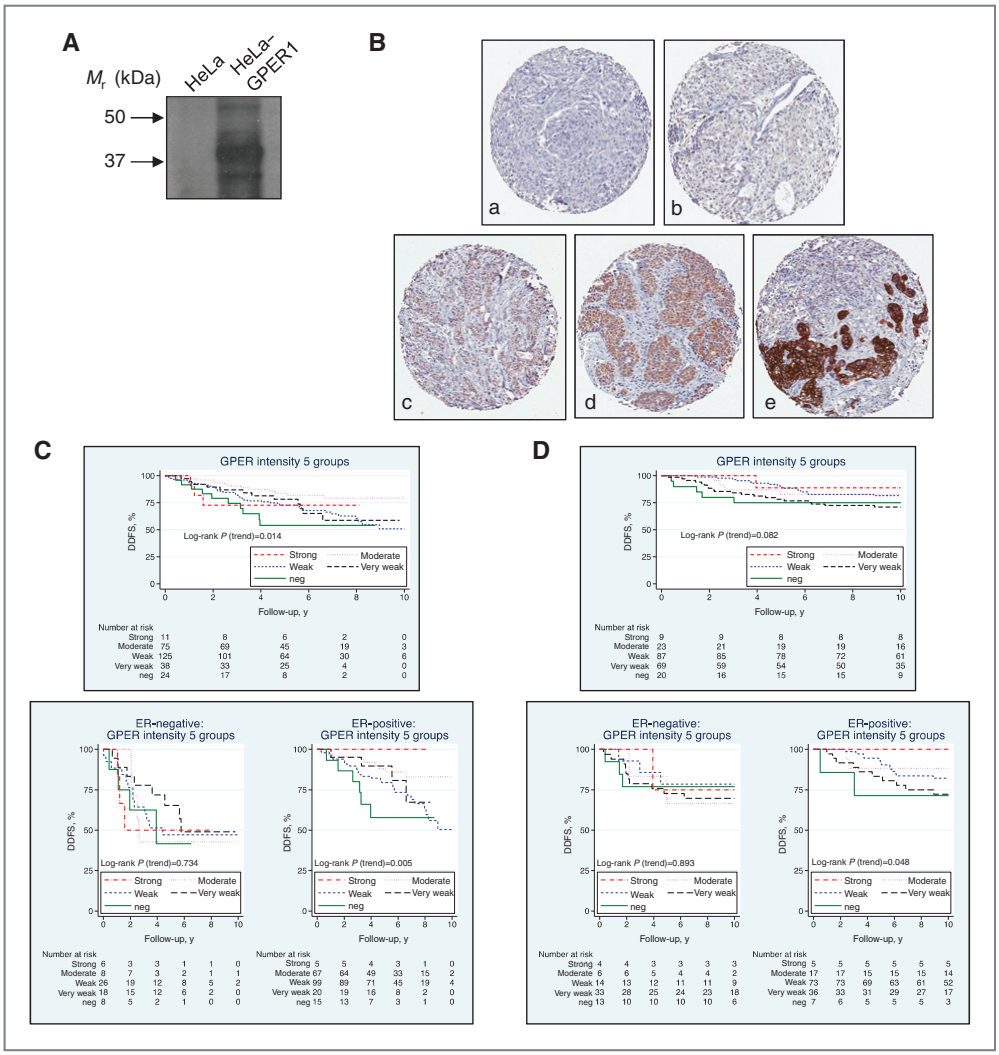

Figure 1. GPER1 expression correlates with increased DDFS in ER-positive breast cancer. A, GPER1 antibody specificity as determined by immunoblotting HeLa cells without (*HeLa*) and with stable expression of human GPER1 (*HeLa-GPER1*). Molecular mass (M_r) standards (kDa; left side arrows) are indicated. B, levels of GPER1 immunostaining intensity in invasive breast cancer in cohort II. Representative images show intensity levels as negative (level 0; a), very weak (level 1; b), weak (level 2; c), moderate (level 3; d), and strong (level 4; e). C, Kaplan–Meier estimates of DDFS for GPER1 status in the whole cohort I and the ER-positive and -negative subgroups of cohort I. D, Kaplan–Meier estimates of DDFS for GPER1 status in the whole cohort II and the ER-positive and ER-negative subgroups of cohort II. *P* values were calculated using the log-rank test for trend. Below each graph is the number of patients remaining at risk in each group at each time.

GPER1 is constitutively proapoptotic in a HEK293 cell model system

Because GPER1 was found to be of clinical benefit both with and without tamoxifen treatment, we first investigated if the receptor constitutively impacts proapoptotic signaling, that is, without added stimulus. To do this requires comparing cells completely lacking GPER1 expression with the same cells stably expressing the receptor. To this end, we

Table 1. Association between GPER1 intensity score and various clinicopathologic variables in cohorts I and II

	Cohort I							Cohort II						
		GPER1 intensity							GPER1 intensity					
Factor	**Patient**	**0**	**1**	**2**	**3**	**4**	***P*[a]**	**Patient**	**0**	**1**	**2**	**3**	**4**	***P*[a]**
	N			*N* (%)				*N*			*N*(%)			
All	273	24 (9)	38 (14)	125 (46)	75 (27)	11 (4)		208	20 (10)	69 (33)	87 (42)	23 (11)	9 (4)	
Age, years							0.18							0.003
Node status														
Negative	89	8 (9)	16 (18)	30 (34)	26 (29)	9 (10)	0.26							
Positive	183	16 (9)	22 (12)	94 (51)	49 (27)	2 (1)								
Missing	1													
Tumor size														
≤20 mm	80	5 (6)	12 (15)	42 (53)	21 (26)	0 (0)	0.56	155	10 (6)	51 (33)	69 (45)	18 (12)	7 (5)	0.05
>20 mm	193	19 (10)	26 (13)	83 (43)	54 (28)	11 (6)		53	10 (19)	18 (34)	18 (34)	5 (9)	2 (4)	
Histologic grade														
1	15	0 (0)	1 (7)	6 (40)	8 (53)	0 (0)	0.88	62	0 (0)	16 (26)	34 (55)	10 (16)	2 (3)	0.0003
2	176	19 (11)	18 (10)	89 (51)	45 (26)	5 (3)		77	5 (6)	25 (32)	39 (51)	6 (8)	2 (3)	
3	73	3 (4)	17 (23)	27 (37)	20 (27)	6 (8)		67	15 (22)	28 (42)	13 (19)	6 (9)	5 (7)	
Missing	9							2						
ER														
Positive	206	15 (7)	20 (10)	99 (48)	67 (33)	5 (2)	0.01	138	7 (5)	36 (26)	73 (53)	17 (12)	5 (4)	0.0005
Negative	66	8 (12)	18 (27)	26 (39)	8 (12)	6 (9)		70	13 (19)	33 (47)	14 (20)	6 (9)	4 (6)	
Missing	1													
PgR														
Positive	164	11 (7)	16 (10)	76 (46)	57 (35)	4 (2)	0.01	151	10 (7)	39 (26)	79 (52)	19 (13)	4 (3)	0.0004
Negative	108	12 (11)	22 (20)	49 (45)	18 (17)	7 (6)		57	10 (18)	30 (53)	8 (14)	4 (7)	5 (9)	
Missing	1													
HER2														
Negative	206	16 (8)	30 (15)	92 (45)	57 (28)	11 (5)	0.76	173	17 (10)	52 (30)	77 (45)	19 (11)	8 (5)	0.45
Positive	34	2 (6)	4 (12)	19 (56)	9 (26)	0 (0)		22	1 (5)	11 (50)	7 (32)	3 (14)	0 (0)	
Missing	43							13						
Ki67														
Low (≤20%)	170	13 (8)	20 (12)	80 (47)	51 (30)	6 (4)	0.24	127	7 (6)	31 (24)	69 (54)	16 (13)	4 (3)	0.0007
High (>20%)	97	9 (9)	17 (18)	44 (45)	23 (24)	4 (4)		60	9 (15)	32 (53)	11 (18)	5 (8)	3 (5)	
Missing	6							21						

[a]Test for zero slope in a linear regression, which equals a χ^2 test for trend for binary variables.

compared naïve HEK293 cells (HEK) with HEK stably expressing GPER1 (HEK-R; Fig. 2A), a well-studied GPCR model system. HEK-R had a 35% ± 2% ($P < 0.001$) decrease in cell viability compared with HEK as determined by the MTT assay (Fig. 2A). Consistent with constitutive proapoptotic receptor signaling, HEK-R also had increased basal mitochondrial cytochrome C release, an early marker of apoptosis (Fig. 2B, EPX: 0 nmol/L). Caspase-3 cleavage was not detected under basal conditions in either HEK or HEK-R, but HEK-R had increased basal PARP cleavage, a product of caspase-3 activity, and increased ERK1/2 phosphorylation (p-ERK1/2; Fig. 2B, EPX: 0 nmol/L).

Epoxomicin (EPX) is a specific proteasomal inhibitor and apoptotic stimulant as shown by increased protein ubiquitination, cytochrome C release, and PARP cleavage in HEK following treatment with 50 and 100 nmol/L epoxomicin for 24 hours (Fig. 2B, epoxomicin: 50,100 nmol/L). Epoxomicin is also expected to increase the level of GPER1 by blocking proteasomal receptor degradation (35). Indeed, epoxomicin treatment of HEK-R increased the level of GPER1 at the cell surface as shown by both flow cytometry (Fig. 2C) and confocal immunofluorescence microscopy (Supplementary Fig. S1). Consistent with constitutive proapoptotic GPER1 signaling, epoxomicin treatment of HEK-R also yielded levels of cytochrome C release, caspase-3 cleavage, and PARP cleavage that were significantly higher than in epoxomicin-treated HEK (Fig. 2B, epoxomicin: 50,100 nmol/L). The higher level of proapoptotic signaling in HEK-R was also evident by the increased morphologic changes and chromatin condensation/nuclear fragmentation in

Table 2. DDFS by Cox univariate and multivariate analysis in the ER-positive subgroup of cohort I

	Univariate DDFS			Multivariate DDFS		
Variable	***N***	**HR (95% CI)**	***P***	***N***	**HR (95% CI)**	***P***
Age (linear, y)	206	0.99 (0.97–1.02)	0.62	199	1.00 (0.97–1.03)	0.93
GPER1 (trend)	206	0.66 (0.49–0.88)	0.007	199	0.67 (0.50–0.92)	0.01
Node status (N+ vs. N0)	206	1.23 (0.66–2.28)	0.52	199	1.60 (0.83–3.07)	0.16
Tumor size (>20 mm vs. ≤20 mm)	206	1.95 (0.95–4.02)	0.05	199	2.22 (1.04–4.72)	0.04
Histologic grade	202		0.18[a]	199		0.46[a]
1 vs. 3		0.22 (0.03–1.76)	0.16		0.45 (0.05–3.80)	0.46
2 vs. 3		0.93 (0.45–1.93)	0.85		1.24 (0.55–2.81)	0.60
HER2 (pos vs. neg)	181	0.96 (0.38–2.46)	0.93	—[b]	—	—
PgR (pos vs. neg)	206	0.84 (0.45–1.59)	0.60	199	0.99 (0.51–1.94)	0.98
Ki67 (>20% vs. ≤20%)	203	2.02 (1.15–3.56)	0.02	199	2.01 (1.05–3.88)	0.04

[a]*P* value for histologic grade as a factor on 3 levels.
[b]HER2 excluded because of a higher frequency of missing data than the other variables.

these cells (Fig. 2D). Thus, GPER1 is constitutively proapoptotic and sensitizes cells to additional apoptotic stimulation in a model system.

GPER1 is proapoptotic in ER-positive breast cancer cells

Next, we evaluated if GPER1 is constitutively proapoptotic in ER-positive breast cancer cells. This was done by comparing naïve MCF7 cells with cells in which GPER1 had been knocked down with shRNA (MCF7-shRNA; Fig. 3A). Consistent with constitutive GPER1 signaling, receptor knockdown decreased basal p53 expression (Fig. 3B, G_1:0 μmol/L), a tumor suppressor protein associated with both increased apoptosis and decreased cell-cycle progression (36). No difference was observed in basal PARP cleavage and ERK1/2 phosphorylation (Fig. 3B). On the other hand, MCF7-shRNA had decreased cytochrome C release (Fig. 3B, 4OHT: 0 μmol/L). We conclude from these results that GPER1 is constitutively proapoptotic in MCF7 cells.

Proapoptotic GPER1 signaling in MCF7 cells was also investigated using G_1, a commercially available synthetic GPER1 agonist, keeping in mind that while this substance has been reported to be a receptor agonist (37), receptor-independent effects on, for example, cell-cycle progression has also been reported (38, 39). Stimulation with 1 μmol/L G_1 for 24 hours increased cytochrome C release, p53, PARP cleavage, and ERK1/2 phosphorylation (Fig. 3B) and decreased cell viability (Fig. 3C), the latter 4 responses clearly attenuated in MCF7-shRNA cells (Fig. 3B and C). We also determined the effect of G_1 in ER-positive T47D cells, which express significantly less GPER1 than MCF7 cells (40). Consistent with GPER1-dependent signaling, T47D cells were also much less sensitive than MCF7 cells to G_1-stimulated cytochrome C release and PARP cleavage

Table 3. DDFS by Cox univariate and multivariate analysis in the ER-positive subgroup of cohort II

	Univariate DDFS			Multivariate DDFS		
Variable	***N***	**HR (95% CI)**	***P***	***N***	**HR (95% CI)**	***P*[b]**
Age (linear, y)	138	0.90 (0.84–0.96)	0.002	120	0.88 (0.82–0.95)	0.001
GPER1 (trend)	138	0.62 (0.39–0.99)	0.05	120	0.60 (0.34–1.1)	0.09
Tumor size (>20 mm vs. ≤20 mm)	138	1.1 (0.44–2.7)	0.85	120	0.78 (0.30–2.0)	0.60
Histologic grade	136		0.02[a]	120		0.59[a]
1 vs. 3		0.28 (0.11–0.73)	0.01		0.65 (0.17–2.6)	0.54
2 vs. 3		0.34 (0.14–0.82)	0.02		0.53 (0.16–1.8)	0.31
HER2 (pos vs. neg)	132	2.4 (0.85–7.1)	0.14	120	0.77 (0.23–2.5)	0.66
PgR (pos vs. neg)	138	0.88 (0.21–3.7)	0.87	120	4.5 (0.81–25.1)	0.09
Ki67 (>20% vs. ≤20%)	124	3.9 (1.8–8.6)	0.002	120	3.3 (1.0–10.6)	0.05

[a]*P* value for histologic grade as a factor on 3 levels.
[b]For some factors, the much higher *P* values in multivariate analysis, compared with univariate analysis, can be explained by a high degree of colinearity between the variables in the model.

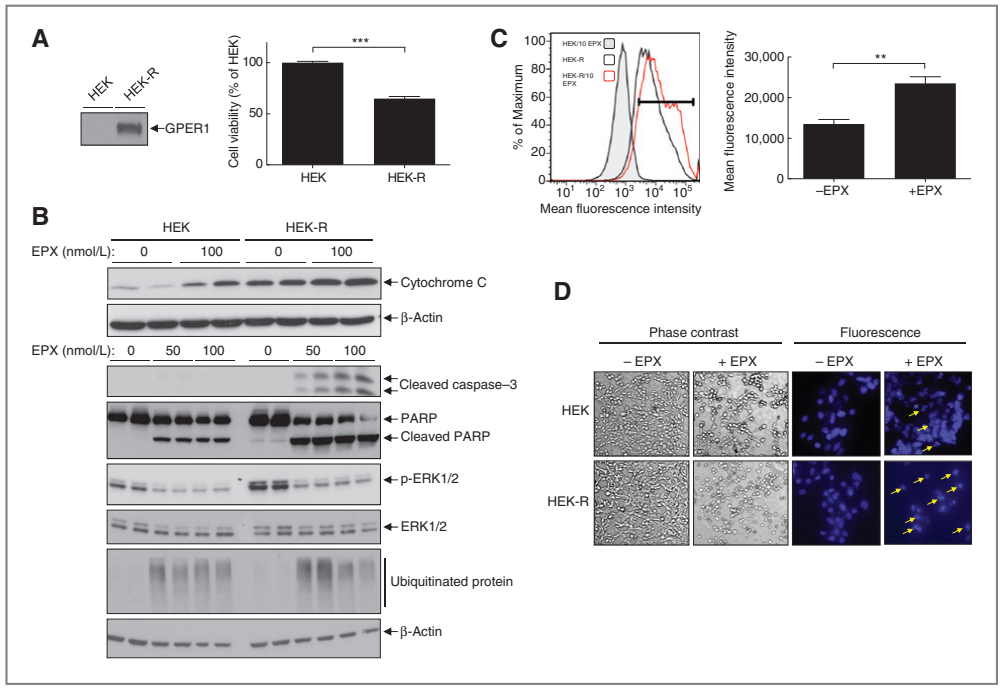

Figure 2. Constitutive proapoptotic GPER1 signaling in a HEK293 cell model system. A, immunoblotting of heterologously expressed GPER1 in HEK-R but not in HEK, and decreased cell viability of HEK-R compared with HEK as determined by the MTT assay (B), immunoblotting of cytochrome C release, cleaved caspase-3, cleaved PARP, phosphorylated ERK1/2 (p-ERK1/2), and ubiquitinated protein in HEK and HEK-R treated without and with different concentrations of epoxomicin for 24 hours as indicated. Duplicate samples were immunoblotted and total ERK1/2 and β-actin serve as loading controls. C, mean fluorescence intensity determined by flow cytometry of HEK and HEK-R labeled with primary mouse M1 FLAG antibody and secondary goat anti-mouse APC-labeled antibody. Before analysis, HEK were treated with 10 nmol/L epoxomicin (*HEK/10 EPX*), and HEK-R were treated without (*HEK-R*) and with 10 nmol/L epoxomicin for 24 hours (*HEK-R/10 EPX*). In this representative experiment, M1 FLAG-positive gate is shown (bar), and the percentage positive cells and mean fluorescence intensity was 1.1% and 5,679, respectively, for HEK/10 epoxomicin, 67.3% and 14,500, respectively, for HEK-R, and 78.4% and 24,500 for HEK-R/10 epoxomicin. Quantification of mean fluorescence intensity is also shown. D, morphologic changes as determined by phase-contrast and chromatin condensation/nuclear fragmentation as determined by Hoechst 33342 staining fluorescence following treatment of HEK and HEK-R without (*–EPX*) and with 50 nmol/L epoxomicin (*+EPX*) for 24 hours. Yellow arrows indicate fragmented nuclei. **, $P < 0.01$; ***, $P < 0.001$.

(Supplemental Fig. S2). Thus, agonist-stimulated GPER1 activity is proapoptotic in MCF7 cells.

G_1 treatment for 24 hours also inhibited MCF7 cell-cycle progression at the G_2–M interphase in a GPER1-dependent manner (Fig. 3D and Supplemental Fig. S3), consistent with GPER1 mediating an increase in the p53 level and p53 blocking the cell cycle at this point (41). G_1 also changed cell morphology and increased the number of cells with fragmented nuclei (Fig. 3D).

We also investigated if GPER1 mediates any proapoptotic tamoxifen effects in MCF7 cells, noting again that this is complicated in an ER-positive environment because tamoxifen is also an ER antagonist, which in turn could impact apoptotic signaling. Nevertheless, 4-hydroxytamoxifen (4OHT), the active metabolite of tamoxifen, dose-dependently increased cytochrome C release and PARP cleavage in naïve MCF7 cells (Fig. 3B). These responses were lower in MCF7-shRNA cells suggesting that they are at least in part GPER1-dependent. In analogy with G_1 and consistent with GPER1-dependence, the 4OHT effects were significantly lower in T47D cells (Supplemental Fig. S2). These results suggest that tamoxifen is proapoptotic in MCF7 cells in part via GPER1.

Discussion

Here, we show that GPER1 positively correlates with ER and PgR expression and with increased DDFS in ER-positive lymph node-negative and stage II breast cancer. GPER1 constitutively promotes proapoptotic signaling as determined in ER- and PgR-positive MCF7 cells and in a HEK model system stably expressing the receptor, which may explain in part the beneficial value of GPER1 on DDFS in ER-positive breast cancer.

More than 80% of breast cancers are positive for ER, emphasizing the importance of this receptor in cancer

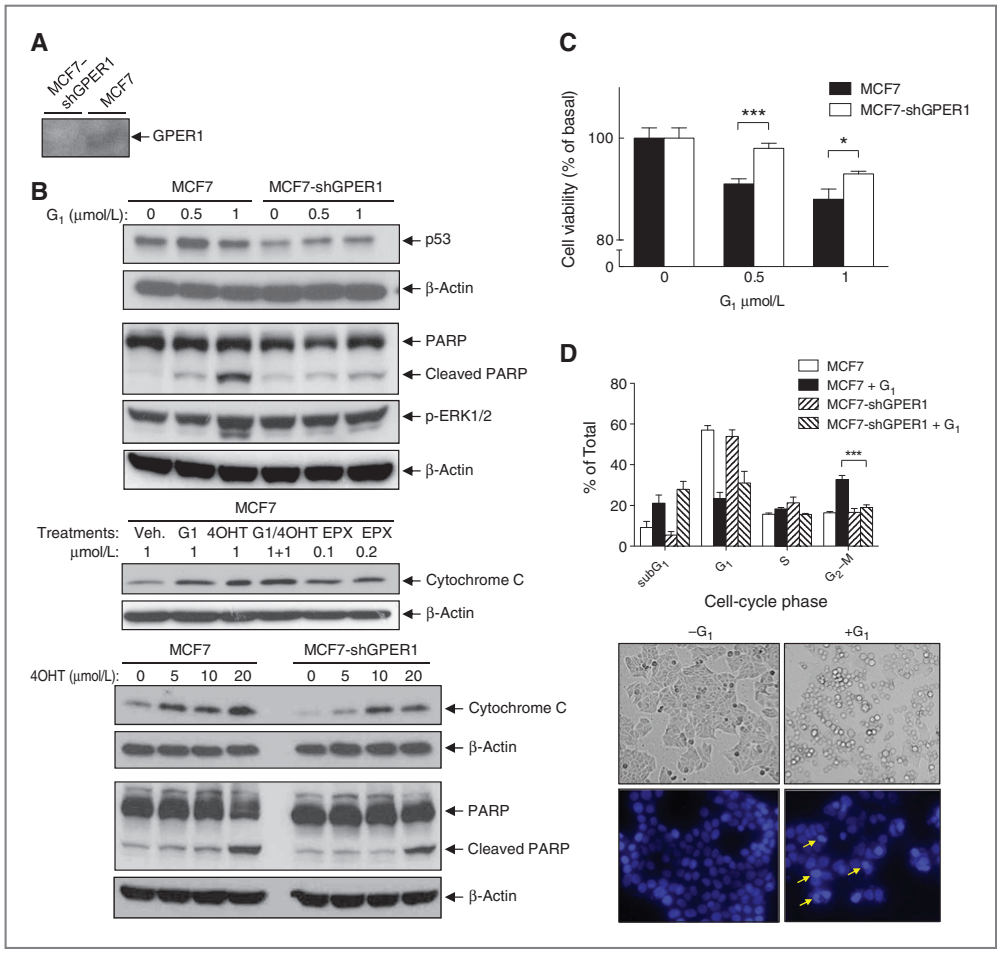

Figure 3. Constitutive and agonist-stimulated proapoptotic GPER1 signaling in MCF7 cells. A, immunoblotting of GPER1 in MCF7 cells without (*MCF7*) and with GPER1 shRNA knockdown (*MCF7-shGPER1*). B, immunobloting of p53, cleaved PARP, phosphorylated ERK1/2 (p-ERK1/2), and cytochrome C release in MCF7 cells without (*MCF7*) and with GPER1 shRNA knockdown (*MCF7-shGPER1*) and treated with different concentrations of G_1 (G_1), *4OHT*, and *EPX* for 24 hours as indicated. β-Actin serves as a loading control. C, viability of MCF7 cells without (*MCF7*) and with GPER1 shRNA knockdown (*MCF7-shGPER1*) and treated without and with increasing concentrations of G_1 for 24 hours as determined with the MTT assay. D, cell-cycle phases in MCF7 cells without (*MCF7*) and with GPER1 shRNA knockdown (*MCF7-shGPER1*) and treated without and with 1 μmol/L G_1 for 24 hours as determined by flow cytometry, and morphologic changes and chromatin condensation/nuclear fragmentation as determined by Hoechst 33342 staining in MCF7 cells following treatment without ($-G_1$) and with 1 μmol/L G_1 ($+G_1$) for 24 hours. Yellow arrows indicate fragmented nuclei. *, $P < 0.05$; ***, $P < 0.001$.

progression. We found a positive correlation of GPER1 with ER and PgR in 2 Swedish breast cancer cohorts, a stage II cohort (cohort I) and a lymph node-negative cohort (cohort II), which is consistent with data obtained on other cohorts by Filardo and colleagues (14) and Liu and colleagues (15) analyzing receptor protein by immunohistochemistry and by Kuo and colleagues (16) and Ariazi and colleagues (17) analyzing receptor transcript. In neither cohort analyzed in our study did GPER1 correlate with HER2 expression. However, in cohort II GPER1 expression correlated negatively with several clinicopathologic markers for advanced disease and metastasis, whereas in cohort I it did not correlate with any of these markers. The reason for this cohort difference is not known but may be related to the menopausal stage because most (79%) patients in cohort I were postmenopausal, whereas all patients in cohort II were

premenopausal. Another difference is that patients in cohort I were diagnosed before the introduction of mammographic screening, mostly with tumors greater than 20 mm, whereas patients in cohort II were diagnosed during the screening period, mostly with tumors smaller than 20 mm. Kuo and colleagues (16) and Tu and colleagues (42) also found no correlation with HER2 and with markers of poor prognosis. On the other hand, Filardo and colleagues (14), Liu and colleagues (15), and Ignatov and colleagues (43) found a positive correlation with HER2 as well as with various indicators of poor prognosis. The reason for this difference is also unknown but may be related to the composition of the various cohorts with patients of different ethnical and lifestyle backgrounds. Nevertheless, an association between GPER1 expression and ER-positive breast cancer is a consistent observation in clinical studies.

Reports that GPER1 associates with indicators of poor prognosis have led some investigators to propose that this receptor is linked to cancer progression (14, 43). However, the *GPER1* gene has not appeared in any gene expression profiles for aggressive breast cancer (44). Indeed, in our study with 2 cohorts, GPER1 correlated with increased DDFS. This correlation was specifically associated with the ER-positive groups. Furthermore, multivariate analysis showed that GPER1 has independent prognostic value in this subgroup. Consistent with our results, Ignatov and colleagues (43) also found that GPER1 significantly correlated with increased relapse-free survival in patients with breast cancer on no adjuvant treatment. Furthermore, Krakstad and colleagues (45) found the loss of GPER1 in a subgroup of ER-positive endometrial cancer to be associated with decreased survival. These results argue that GPER1 expression is a marker for good prognosis in ER-positive cancer.

Therapeutic activation of apoptosis in cancer cells is an attractive anticancer strategy. In HEK, a well-defined model system for studying GPCR function, GPER1 expression yielded increased proapoptotic signaling, whereas GPER1 knockdown in MCF7 cells yielded decreased signaling. These results show not only that GPER1 is proapoptotic in ER-positive breast cancer cells, but also that such receptor signaling occurs constitutively in the absence of any added stimulus, which may explain the beneficial clinical effect of GPER1 both in the absence and presence of adjuvant treatment. GPER1 expression also made HEK cells significantly more sensitive to apoptotic effects by the proteasomal inhibitor epoxomicin. This increased sensitivity was associated with an increased number of functional GPER1 in the plasma membrane rather than with accumulation of overexpressed receptors in the endoplasmic reticulum, a potential artificial cause of cellular stress and apoptosis. Thus, promoting cellular receptor expression and/or stabilizing GPER1 in the plasma membrane for example by decreasing constitutive receptor endocytosis and degradation may be a novel therapeutic avenue in ER-positive breast cancer. Hypoxia upregulates GPER1 expression, which in turn may increase constitutive apoptotic GPER1 signaling as previously described in cardiac cells (21). The GPER1 agonist G_1 stimulated receptor-dependently proapoptotic signaling in MCF7 cells suggesting that direct receptor activation may be an alternative therapeutic approach in this disease.

Some investigators have suggested that GPER1 contributes to tamoxifen resistance based on observations that tamoxifen stimulates GPER1 *in vitro* (10, 11) and that GPER1 is upregulated in tamoxifen-resistant MCF7 cells (46). However, GPER1 has not appeared in functional screens for genes contributing to tamoxifen-resistance in breast cancer cells (47, 48). In our study, the prognostic value of GPER1 for increased DDFS was significant in both the tamoxifen-treated cohort I and the mainly untreated cohort II. Thus, no clear predictive value for the outcome of tamoxifen treatment can be assigned to GPER1 based on our study. Nevertheless, we found that tamoxifen stimulates proapoptotic signaling in MCF7 cells in part through GPER1, suggesting that it could potentially contribute to the beneficial clinical effects in our study. However, Ignatov and colleagues (43) found a negative correlation of GPER1 with relapse-free survival in patients treated with tamoxifen that was significantly different from their control group on no adjuvant treatment. Thus, assignment of GPER1 as a predictive factor for the outcome of tamoxifen treatment needs to be further investigated.

In summary, we show that GPER1 positively correlates with ER and PgR expression and with increased DDFS in ER-positive lymph node-negative and stage II breast cancer. Furthermore, GPER1 is proapoptotic in several cell types including ER-positive breast cancer cells. Therefore, expression of GPER1 may be a novel prognostic factor in this breast cancer, and enhancing GPER1 signaling in ER-positive breast tumors may present a novel therapeutic avenue to increase survival of patients with this disease.

Disclosure of Potential Conflicts of Interest

No potential conflicts of interest were disclosed.

Authors' Contributions

Conception and design: S. Broselid, B. Cheng, M. Sjöström, M. Belting, B. Olde, P.-O. Bendahl, M. Fernö, L.M.F. Leeb-Lundberg
Development of methodology: B. Cheng, M. Fernö
Acquisition of data (provided animals, acquired and managed patients, provided facilities, etc.): S. Broselid, M. Sjöström, H.L.P. Klug-De Santiago, K. Jirström, P. Malmström, M. Fernö
Analysis and interpretation of data (e.g., statistical analysis, biostatistics, computational analysis): S. Broselid, B. Cheng, M. Sjöström, H.L.P. Klug-De Santiago, P.-O. Bendahl, L. Hartman, M. Fernö, L.M.F. Leeb-Lundberg
Writing, review, and/or revision of the manuscript: S. Broselid, B. Cheng, M. Sjöström, H.L.P. Klug-De Santiago, M. Belting, K. Jirström, P. Malmström, B. Olde, P.-O. Bendahl, L. Hartman, M. Fernö, L.M.F. Leeb-Lundberg
Administrative, technical, or material support (i.e., reporting or organizing data, constructing databases): B. Cheng, K. Lövgren, M. Belting, M. Fernö
Study supervision: M. Fernö, L.M.F. Leeb-Lundberg

Acknowledgments

The authors thank the participating departments of the South Sweden Breast Cancer Group for providing us with breast cancer samples and clinical follow-up data. The expert technical assistance by J. Daszkiewicz-Nilsson is highly appreciated.

Grant Support

The study was supported by funds from the Swedish Research Council, Swedish Cancer Society, Gunnar, Arvid, and Elisabeth Nilsson Foundation, Mrs. Berta Kamprad Foundation, the University Hospital of Lund Research Foundation, the Anna and Edwin Bergers Foundation, Skåne County Council's Research and Development Foundation, Governmental Funding of Clinical Research within the National Health Service, and Regional Academic Health Center, The University of Texas Health Science Center at San Antonio.

The costs of publication of this article were defrayed in part by the payment of page charges. This article must therefore be hereby marked *advertisement* in accordance with 18 U.S.C. Section 1734 solely to indicate this fact.

Received July 18, 2012; revised December 21, 2012; accepted January 7, 2013; published online April 3, 2013.

References

1. Kamangar F, Dores GM, Anderson WF. Patterns of cancer incidence, mortality, and prevalence across five continents: defining priorities to reduce cancer disparities in different geographic regions of the world. J Clin Oncol 2006;24:2137–50.
2. Weigelt B, Peterse JL, van 't Veer LJ. Breast cancer metastasis: markers and models. Nat Rev Cancer 2005;5:591–602.
3. Heldring N, Pike A, Andersson S, Matthews J, Cheng G, Hartman J, et al. Estrogen receptors: how do they signal and what are their targets. Physiol Rev 2007;87:905–31.
4. Early Breast Cancer Trialists' Collaborative Group (EBCTCG)Davies C, Godwin J, Gray R, Clarke M, Cutter D, et al. Relevance of breast cancer hormone receptors and other factors to the efficacy of adjuvant tamoxifen: patient-level meta-analysis of randomised trials. Lancet 2011;378:771–84
5. Mårtensson UEA, Salehi SA, Windahl S, Gomez MF, Swärd K, Wendt A, et al. Deletion of the G protein-coupled receptor GPR30 impairs glucose tolerance, reduces bone growth, increases blood pressure, and eliminates estradiol-stimulated insulin release in female mice. Endocrinology 2009;150:687–98.
6. Windahl SH, Andersson N, Chagin AS, Mårtensson UEA, Carlsten H, Olde B. The role of the G protein-coupled receptor GPR30 in the effects of estrogen in ovariectomized mice. Am J Physiol 2009;296:E490–6.
7. Olde B, Leeb-Lundberg LMF. GPR30/GPER1: searching for a role in estrogen physiology. Trends Endocrinol Metab 2009;20:409–16.
8. Thomas P, Pang Y, Filardo EJ, Dong J. Identity of an estrogen membrane receptor coupled to a G protein in human breast cancer cells. Endocrinology 2005;146:624–32.
9. Revankar CM, Cimino DF, Sklar LA, Arterburn JB, Prossnitz ER. A transmembrane intracellular estrogen receptor mediates rapid cell signaling. Science 2005;307:1625–30.
10. Maggiolini M, Vivacqua A, Fasanella G, Recchia AG, Sisci D, Pezzi V, et al. The G protein-coupled receptor GPR30 mediates c-fos up-regulation by 17beta-estradiol and phytoestrogens in breast cancer cells. J Biol Chem 2004;279:27008–16.
11. Vivacqua A, Bonofiglio D, Recchia AG, Musti AM, Picard D, Andò S, et al. The G protein-coupled receptor GPR30 mediates the proliferative effects induced by 17beta-estradiol and hydroxytamoxifen in endometrial cancer cells. Mol Endocrinol 2006;20:631–46.
12. Langer G, Bader B, Meoli L, Isensee J, Delbeck M, Noppinger PR, et al. A critical review of fundamental controversies in the field of GPR30 research. Steroids 2010;75:603–10.
13. Levin ER. G protein-coupled receptor 30: estrogen receptor or collaborator? Endocrinology 2009;150:1563–5.
14. Filardo EJ, Graeber CT, Quinn JA, Resnick MB, Giri D, DeLellis RA, et al. Distribution of GPR30, a seven membrane-spanning estrogen receptor, in primary breast cancer and its association with clinicopathologic determinants of tumor progression. Clin Cancer Res 2006;12:6359–66.
15. Liu Q, Li JG, Zheng XY, Jin F, Dong HT. Expression of CD133, PAX2, ESA, and GPR30 in invasive ductal breast carcinomas. Chin Med J (Engl) 2009;122:2763–9.
16. Kuo WH, Chang LY, Liu DL, Hwa HL, Lin JJ, Lee PH, et al. The interactions between GPR30 and the major biomarkers in infiltrating ductal carcinoma of the breast in an Asian population. Taiwan J Obstet Gynecol 2007;46:135–45.
17. Ariazi EA, Brailoiu E, Yerrum S, Shupp HA, Slifker MJ, Cunliffe HE, et al. The G protein-coupled receptor GPR30 inhibits proliferation of estrogen receptor-positive breast cancer cells. Cancer Res 2010;70:1184–94.
18. Vivacqua A, Lappano R, De Marco P, Sisci D, Aquila S, De Amicis F, et al. G protein-coupled receptor 30 expression is up-regulated by EGF and TGF alpha in estrogen receptor alpha-positive cancer cells. Mol Endocrinol 2009;23:1815–26.
19. Ahola TM, Purmonen S, Pennanen P, Zhuang YH, Tuohimaa P, Ylikomi T. Progestin upregulates G-protein-coupled receptor 30 in breast cancer cells. Eur J Biochem 2002;269:2485–90.
20. Ahola TM, Manninen T, Alkio N, Ylikomi T. G protein-coupled receptor 30 is critical for a progestin-induced growth inhibition in MCF-7 breast cancer cells. Endocrinology 2002;143:3376–84.
21. Kimura M, Mizukami Y, Miura T, Fujimoto K, Kobayashi S, Matsuzaki M. Orphan G protein-coupled receptor, GPR41, induces apoptosis via a p53/Bax pathway during ischemic hypoxia and reoxygenation. J Biol Chem 2001;276:26453–60.
22. Ding Q, Gros R, Limbird LE, Chorazyczewski J, Feldman RD. Estradiol-mediated ERK phosphorylation and apoptosis in vascular smooth muscle cells requires GPR30. Am J Physiol Cell Physiol 2009;297:C1178–87.
23. Chan QK, Lam HM, Ng CF, Lee AY, Chan ES, Ng HK, et al. Activation of GPR30 inhibits the growth of prostate cancer cells through sustained activation of Erk1/2, c-jun/c-fos-dependent upregulation of p21, and induction of G(2) cell-cycle arrest. Cell Death Differ 2010;17:1511–23.
24. Recchia AG, De Francesco EM, Vivacqua A, Sisci D, Panno ML, Andò S, et al. The G protein-coupled receptor 30 is up-regulated by hypoxia-inducible factor-1alpha (HIF-1alpha) in breast cancer cells and cardiomyocytes. J Biol Chem 2011;286:10773–82.
25. Kanda N, Watanabe S. 17Beta-estradiol inhibits oxidative stress-induced apoptosis in keratinocytes by promoting Bcl-2 expression. J Invest Dermatol 2003;121:1500–9.
26. Swedish Breast Cancer Cooperative Group. Randomized trial of two versus five years of adjuvant tamoxifen for postmenopausal early stage breast cancer. J Natl Cancer Inst 1996;88:1543–9.
27. Rydén L, Jönsson PE, Chebil G, Dufmats M, Fernö M, Jirström K, et al. Two years of adjuvant tamoxifen in premenopausal patients with breast cancer: a randomised, controlled trial with long-term follow-up. Eur J Cancer 2005;41:256–64.
28. Chebil G, Bendahl PO, Idvall I, Fernö M. Comparison of immunohistochemical and biochemical assay of steroid receptors in primary breast cancer—clinical associations and reasons for discrepancies. Acta Oncol 2003;42:719–25.
29. Malmström P, Bendahl PO, Boiesen P, Brunner N, Idvall I, Fernö M. S-phase fraction and urokinase plasminogen activator are better markers for distant recurrences than Nottingham Prognostic Index and histologic grade in a prospective study of premenopausal lymph node-negative breast cancer. J Clin Oncol 2001;19:2010–9.
30. Kotarsky K, Owman C, Olde B. A chimeric reporter gene allowing for clone selection and high-throughput screening of reporter cell lines expressing G-protein-coupled receptors. Anal Biochem 2001;288:209–15.
31. Sanden C, Broselid S, Cornmark L, Andersson K, Daszkiewicz-Nilsson J, Mårtensson UEA, et al. G protein-coupled estrogen receptor 1/G protein-coupled receptor 30 localizes in the plasma membrane and traffics intracellularly on cytokeratin intermediate filaments. Mol Pharmacol 2011;79:400–10.
32. Cheng B, Maffi SK, Martinez AA, Acosta YP, Morales LD, Roberts JL. Insulin-like growth factor-I mediates neuroprotection in proteasome inhibition-induced cytotoxicity in SH-SY5Y cells. Mol Cell Neurosci 2011;47:181–90.

33. Schoenfeld D. Partial residuals for the proportional hazards regression model. Biometrika 1982;69:239–41.
34. Klintman M, Bendahl PO, Grabau D, Lövgren K, Malmström P, Fernö M, et al. The prognostic value of Ki67 is dependent on estrogen receptor status and histological grade in premenopausal patients with node-negative breast cancer. Mod Pathol 2010;23:251–9.
35. Cheng SB, Quinn JA, Graeber CT, Filardo EJ. Down-modulation of the G-protein-coupled estrogen receptor, GPER, from the cell surface occurs via a trans-Golgi-proteasome pathway. J Biol Chem 2011;286: 22441–55.
36. Junttila MR, Evan GI. p53—a Jack of all trades but master of none. Nat Rev Cancer 2009;9:821–9.
37. Bologa CG, Revankar CM, Young SM, Edwards BS, Arterburn JB, Kiselyov AS, et al. Virtual and biomolecular screening converge on a selective agonist for GPR30. Nat Chem Biol 2006;2:207–12.
38. Holm A, Grände PO, Ludueña RF, Olde B, Prasad V, Leeb-Lundberg LM, et al. The G protein-coupled oestrogen receptor 1 agonist G-1 disrupts endothelial cell microtubule structure in a receptor-independent manner. Mol Cell Biochem 2012;366:239–49.
39. Wang C, Lv X, Jiang C, Davis JS. The putative G-protein coupled estrogen receptor agonist G-1 suppresses proliferation of ovarian and breast cancer cells in a GPER-independent manner. Am J Transl Res 2012;4:390–402.
40. Carmeci C, Thompson DA, Ring HZ, Francke U, Weigel RJ. Identification of a gene (GPR30) with homology to the G-protein-coupled receptor superfamily associated with estrogen receptor expression in breast cancer. Genomics 1997;45:607–17.
41. Agarwal ML, Agarwal A, Taylor WR, Stark GR. p53 controls both the G_2 /M and the G_1 cell cycle checkpoints and mediates reversible growth arrest in human fibroblasts. Proc Natl Acad Sci U S A 1995;92:8493–7.
42. Tu G, Hu D, Yang G, Yu T. The correlation between GPR30 and clinicopathologic variables in breast carcinomas. Technol Cancer Res Treat 2009;8:231–4.
43. Ignatov A, Ignatov T, Weissenborn C, Eggemann H, Bischoff J, Semczuk A, et al. G-protein-coupled estrogen receptor GPR30 and tamoxifen resistance in breast cancer. Breast Cancer Res Treat 2011; 128:457–66.
44. Miller LD, Liu ET. Expression genomics in breast cancer research: microarrays at the crossroads of biology and medicine. Breast Cancer Res 2007;9:206.
45. Krakstad C, Trovik J, Wik E, Engelsen IB, Werner HM, Birkeland E, et al. Loss of GPER identifies new targets for therapy among a subgroup of ERα-positive endometrial cancer patients with poor outcome. Br J Cancer 2012;106:1682–8.
46. Ignatov A, Ignatov T, Roessner A, Costa SD, Kalinski T. Role of GPR30 in the mechanisms of tamoxifen resistance in breast cancer MCF-7 cells. Breast Cancer Res Treat 2010;123:87–96.
47. Meijer D, van Agthoven T, Bosma PT, Nooter K, Dorssers LC. Functional screen for genes responsible for tamoxifen resistance in human breast cancer cells. Mol Cancer Res 2006;4:379–86.
48. van Agthoven T, Sieuwerts AM, Meijer-van Gelder ME, Look MP, Smid M, Veldscholte J, et al. Relevance of breast cancer antiestrogen resistance genes in human breast cancer progression and tamoxifen resistance. J Clin Oncol 2009;27:542–9.

Paper III

G-protein-coupled receptor 30 interacts with receptor activity-modifying protein 3 and confers sex-dependent cardioprotection

Patricia M Lenhart, Stefan Broselid[1], Cordelia J Barrick, L M Fredrik Leeb-Lundberg[1] and Kathleen M Caron

Department of Cell Biology and Physiology, The University of North Carolina, CB #7545, 6340B MBRB, 111 Mason Farm Road, Chapel Hill, North Carolina 27599, USA
[1]Department of Experimental Medical Science, Lund University, SE-22184 Lund, Sweden

Correspondence should be addressed to K M Caron
Email
kathleen_caron@med.unc.edu

Journal of Molecular Endocrinology

Abstract

Receptor activity-modifying protein 3 (RAMP3) is a single-pass transmembrane protein known to interact with and affect the trafficking of several G-protein-coupled receptors (GPCRs). We sought to determine whether RAMP3 interacts with GPR30, also known as G-protein-coupled estrogen receptor 1. GPR30 is a GPCR that binds estradiol and has important roles in cardiovascular and endocrine physiology. Using bioluminescence resonance energy transfer titration studies, co-immunoprecipitation, and confocal microscopy, we show that GPR30 and RAMP3 interact. Furthermore, the presence of GPR30 leads to increased expression of RAMP3 at the plasma membrane in HEK293 cells. *In vivo*, there are marked sex differences in the subcellular localization of GPR30 in cardiac cells, and the hearts of *Ramp3*$^{-/-}$ mice also show signs of GPR30 mislocalization. To determine whether this interaction might play a role in cardiovascular disease, we treated *Ramp3*$^{+/+}$ and *Ramp3*$^{-/-}$ mice on a heart disease-prone genetic background with G-1, a specific agonist for GPR30. Importantly, this *in vivo* activation of GPR30 resulted in a significant reduction in cardiac hypertrophy and perivascular fibrosis that is both RAMP3 and sex dependent. Our results demonstrate that GPR30–RAMP3 interaction has functional consequences on the localization of these proteins both *in vitro* and *in vivo* and that RAMP3 is required for GPR30-mediated cardioprotection.

Key Words
- G-protein-coupled receptors
- estradiol
- cardiac hypertrophy
- cardioprotection

Journal of Molecular Endocrinology
(2013) **51**, 191–202

Introduction

Receptor activity-modifying proteins (RAMPs) are single-pass transmembrane-accessory proteins that interact with G-protein-coupled receptors (GPCRs) to modulate their trafficking, ligand-binding specificity, and downstream signaling. The RAMPs were first identified in association with calcitonin receptor-like receptor (CLR; McLatchie *et al*. 1998, Bomberger *et al*. 2012) – a discovery that clarified considerable controversy over CLR function and has since been exploited by the pharmaceutical industry for the development of small-molecule drugs that specifically target the RAMP–CLR interface (Sexton *et al*. 2009). Several additional GPCRs have been shown to interact with RAMPs (Christopoulos *et al*. 2003, Harikumar *et al*. 2009). Therefore, there remains great interest in understanding the pharmacological and biochemical properties of the RAMPs and in continuing to identify novel GPCR

http://jme.endocrinology-journals.org
DOI: 10.1530/JME-13-0021

Published by Bioscientifica Ltd.

targets for these proteins, with the ultimate goal of manipulating the RAMP–GPCR interface for treatment of human disease.

RAMP3 is unique among the RAMP family members in that it is transcriptionally induced by estradiol (E_2; Hewitt *et al.* 2005, Watanabe *et al.* 2006) and has been shown to play a sex-dependent role in the development of cardiac hypertrophy and transition to heart failure (Barrick *et al.* 2012). For these reasons, we considered that GPR30, or G-protein-coupled estrogen receptor 1, might be a candidate RAMP3-binding GPCR. GPR30 binds E_2 with high affinity, eliciting rapid intracellular signaling (Carmeci *et al.* 1997, Filardo *et al.* 2007), and mediates pleiotropic functions in the cardiovascular, endocrine, immune, and central nervous systems (Olde & Leeb-Lundberg 2009, Nilsson *et al.* 2011, Prossnitz & Barton 2011).

There is substantial evidence for GPR30-mediated cardioprotection. GPR30 is expressed in the rodent and human hearts (Deschamps & Murphy 2009, Patel *et al.* 2010), and using male rats, Filice *et al.* (2009) showed that GPR30 is involved in mediating the effects of E_2 in the heart. Numerous studies have explored the effects of pharmacological activation of GPR30 with G-1, a synthetic agonist for GPR30 that specifically activates GPR30 but does not activate the steroid E_2 receptors (Bologa *et al.* 2006). Administration of G-1 is directly cardioprotective, reducing infarct size in rat and mouse hearts exposed to ischemia–reperfusion (Deschamps & Murphy 2009, Bopassa *et al.* 2010). Furthermore, chronic G-1 treatment reduces left ventricular wall thickness and myocyte hypertrophy without significant effects on blood pressure or fibrosis in a rat model of salt-induced hypertension (Jessup *et al.* 2010) and attenuates heart failure (Kang *et al.* 2012) and diastolic dysfunction independent of blood pressure in ovariectomized female rats (Wang *et al.* 2012). Based on these preclinical studies, pharmacological activation of GPR30 as a potential therapeutic intervention could have utility in the treatment of cardiovascular disease.

Despite what is known about GPR30, there remains intense controversy regarding the trafficking and subcellular localization of GPR30, in addition to many conflicting reports regarding its downstream signaling and even ligand-binding specificity. As RAMPs serve to modulate these aspects of GPCR behavior, we hypothesized that an interaction with RAMPs could potentially clarify some of the controversies surrounding GPR30. Specifically, we sought to determine whether RAMP3, an E_2-induced accessory protein known to be important in cardiovascular disease, could interact with and modulate the function of GPR30, as an E_2 receptor with protective roles in cardiac and vascular biology.

Materials and methods

Animals

Ramp3$^{-/-}$ animals were generated as described previously (Dackor *et al.* 2007) and *Ramp3*$^{+/+}$ and *Ramp3*$^{-/-}$ mice were crossed to heterozygous RenTgMK mice (Barrick *et al.* 2012). Experimental animals were 8 weeks of age and maintained on an isogenic 129S6/SvEv genetic background. All experiments were approved by the Institutional Animal Care and Use Committee of the University of North Carolina at Chapel Hill.

Bioluminescence resonance energy transfer

Bioluminescence resonance energy transfer (BRET) titration studies to test the molecular association between GPR30 and RAMP3 were carried out as described previously (Heroux *et al.* 2007). Briefly, the calcium phosphate precipitation method was used to transfect HEK293 cells with a constant amount of hGPR30-*R*Luc, hCLR-*R*Luc (positive control), hB2AR-*R*Luc, or hD1R-*R*Luc (negative controls) and increasing doses of hRAMP3–YFP. Cells were treated with the luciferase substrate coelenterazine H for 10 min and read using a Berthold Technologies Mithras (Bad Wildbad, Germany) LB940 plate reader. BRET signal was calculated as the ratio of light emitted from YFP (530 nm) to light emitted from *R*Luc (485 nm). Total fluorescence emission was measured at 530 nm from wells not treated with coelenterazine H that were excited at 485 nm to control for the expression level of hRAMP3–YFP, and total luminescence was determined to control for the expression level of the receptors. Results were analyzed using GraphPad Prism. Results shown are representative of at least three replicate BRET experiments that were performed with similar results.

Co-immunoprecipitation

HEK293 cells were transfected with HA-RAMP3 and FLAG-GPR30 using TransIT-293 (Mirus, Madison, WI, USA), and GPR30 was immunoprecipitated by incubating the cleared cell lysates overnight at 4 °C with M2 FLAG antibody beads (Sigma–Aldrich). The precipitate was washed extensively and sequentially in lysis buffer and in 10 mM Tris–HCl, pH 7.4. For immunoblotting, proteins were denatured in SDS–PAGE sample buffer including 6% β-mercaptoethanol for 30 min at 37 °C, fractionated by SDS–PAGE, transferred

http://jme.endocrinology-journals.org
DOI: 10.1530/JME-13-0021

Published by Bioscientifica Ltd.

to a nitrocellulose membrane, and the membrane was blocked for at least 45 min in Tris-buffered saline and 10% nonfat milk. The proteins were stained by incubating with rabbit anti-HA antibody (Invitrogen; 1:1000) for 1 h at room temperature. Immunoreactive bands were visualized with a chemiluminescence kit using anti-rabbit peroxidase-labeled secondary antibody according to the procedure described by the supplier (PerkinElmer Life (Waltham, MA, USA) and Analytical Sciences (Petaluma, CA, USA)).

Confocal imaging

HEK293 cells were transfected with HA-RAMP3 and FLAG-GPR30 using TransIT-293 (Mirus). Transfected cells were grown on glass coverslips coated with poly(D-lysine) and then incubated in serum- and phenol-free media for at least 1 h at 37 °C. For live cell staining, cells were then incubated in serum- and phenol-free media containing IgG1 monoclonal anti-HA (1:100; Covance, Raleigh, NC, USA) and IgG2b monoclonal anti-M1 FLAG (1:500; Sigma–Aldrich) primary antibodies for 30 min at 37 °C. Cells were fixed with 3.7% formaldehyde in PBS and permeabilized, then washed with PBS, and incubated with anti-IgG1-488 and anti-IgG2b-568 secondary antibodies (Invitrogen). Alternatively, for dead cell staining, cells were incubated with both primary and secondary antibodies after fixation. Cells were also stained with 4′,6-diamidino-2-phenylindole (DAPI). Images were collected using a Nikon Eclipse confocal fluorescence microscope (Nikon, Tokyo, Japan) and analyzed with Nikon EC-Z1 3.90 Software.

Gene expression analysis

mGpr30 and *mRamp3* gene expression was analyzed by quantitative RT-PCR with the Applied Biosystems StepOne Plus machine. The primer/probe set for *Ramp3* has been described previously (Dackor *et al.* 2007). For *Gpr30*, we used a pre-designed Assay on Demand primer/probe set (#Mm02620446_s1, Applied Biosystems). Mouse eukaryotic translation elongation factor 1 alpha 1 was used as the internal control for all samples; the primer/probe set has been described previously (Barrick *et al.* 2012). RNA was isolated from adult tissues with TRIzol reagent (Life Technologies) and subsequently DNase treated. Two micrograms of total RNA was used to generate cDNA with the MMLV Reverse Transcriptase Kit (Life Technologies). The $\Delta\Delta C$t method was used to determine the relative levels of gene expression and was shown as a fold increase over wild-type male controls. Estrus cycle phase was determined by microscopic examination of mouse vaginal smears stained with the Kwik Diff Stain Kit (Thermo Scientific). For the ovariectomized samples, mice were 21–28 days old at the time of ovariectomy. Mice were anesthetized with avertin (0.2–0.4 ml/10 g body weight (BW) of 1.25% solution) and placed on a warm heating pad to maintain body temperature throughout the surgical procedure. Hair was removed from the abdomen and a small (<1 cm) incision was made through the abdominal wall about 1 cm to the left of the spinal cord. The ovary was exteriorized and placed on a sterile drape. Silk sutures were used to ligate the oviduct and anterior connective tissue before excising the ovary. The body wall was then sutured with dissolvable sutures and wound clips were used to close the skin. The procedure was repeated on the animal's right side. Wound clips were removed 4–5 days after surgery; 4 weeks later, the ovariectomized mice were dissected and the heart tissue was used for RT-PCR.

Subcellular fractionation and western blotting

Homogenized lysates were prepared from heart tissue of *Ramp3*$^{+/+}$, *Ramp3*$^{-/-}$, RenTgMK;*Ramp3*$^{+/+}$, and RenTgMK; *Ramp3*$^{-/-}$ male and female mice. The nuclear pellet was removed by centrifuging at 1300 ***g*** for 1 h. Membrane-enriched fractions of cardiac lysates were isolated by subsequent ultracentrifugation at 20 000 ***g*** for 1 h, and the remaining supernatant was designated as the cytosolic fraction. Lysates were denatured in SDS–PAGE sample buffer including 6% β-mercaptoethanol for 5 min at 100 °C, fractionated by SDS–PAGE, transferred to a nitrocellulose membrane, and the membrane was blocked for 1 h in casein (Thermo Scientific). The membrane was stained using rabbit anti-GPR30 primary antibody (MBL International, Woburn, MA, USA) or mouse anti-actin (Sigma–Aldrich) as a loading control, followed by goat anti-rabbit 680 or goat anti-mouse 800 secondary antibody (Thermo Scientific). Membranes were imaged via LI-COR, and quantitation of integrated density normalized to actin was performed using the free ImageJ software. The Student's *t*-test was used to compare the ratio of plasma membrane to cytosolic GPR30 protein relative to actin, and a value of $P<0.05$ was considered statistically significant. Results shown are representative of at least three replicate fractionation experiments that were performed with similar results.

G-1 treatment and histology

Male and female RenTgMK;*Ramp3*$^{+/+}$ and RenTgMK; *Ramp3*$^{-/-}$ mice at 8 weeks of age were anesthetized with

http://jme.endocrinology-journals.org
DOI: 10.1530/JME-13-0021

Published by Bioscientifica Ltd.

avertin (0.2–0.4 ml/10 g BW of 1.25% solution) and injected with a s.c., continuous release pellet (Innovative Research of America, Sarasota, FL, USA) containing 6 mg G-1 (Tocris, Bristol, UK) or placebo similar to a previously described method (Wang *et al*. 2009). After 40 days of treatment, the mice were killed. To determine the left ventricle to BW (LV:BW) ratio, the heart chambers were dissected and the LV was weighed. The Mann–Whitney *U* test was used to compare LV:BW data; a value of $P<0.05$ was considered statistically significant. Subsequently, the LV was fixed in 4% paraformaldehyde and 5 μm sections were prepared for staining. Masson's trichrome-stained slides imaged at 10× were used to analyze interstitial and perivascular cardiac fibrosis. Interstitial fibrosis was quantified by blinded scoring of the extent of interstitial fibrosis in one representative field per mouse. Perivascular fibrosis was quantified by measuring the area of fibrosis surrounding a vessel normalized to the vessel lumen area, using ImageJ Software. Three vessels were measured per mouse. Cardiomyocyte area was determined by measuring the cross-sectional area of five cardiomyocytes in each of two fields per mouse from hematoxylin and eosin-stained slides at 25×, using ImageJ Software. For analysis of fibrosis and cardiomyocyte area, the Student's *t*-test was used to compare data and a value of $P<0.05$ was considered statistically significant.

Blood pressure measurements

Male and female RenTgMK;*Ramp3*$^{+/+}$ and RenTgMK; *Ramp3*$^{-/-}$ mice at 2–5 months of age were injected with a s.c., continuous release pellet containing 6 mg of G-1 or placebo as described earlier. Blood pressures were measured on unanesthetized mice using a Coda computerized volume pressure recording tail cuff system (Kent Scientific, Torrington, CA, USA). After a 5-day period of acclimation to the tail cuff system, blood pressures were measured daily for 5 days on each mouse during the third week following pellet injection. The Student's *t*-test was used to compare data; a value of $P<0.05$ was considered statistically significant.

Results

To directly test whether GPR30 and RAMP3 interact in living cells, we utilized BRET (Heroux *et al*. 2007) titration studies. HEK293 cells were transfected with a constant dose of hGPR30-*R*Luc and increasing doses of hRAMP3–YFP. We observed a robust increase in the BRET signal with increasing amounts of hRAMP3 (ΔBRET=0.664), indicating a specific interaction between the two proteins (Fig. 1A). Almost no change in BRET signal was seen with the negative controls, β2-adrenergic receptor (ΔBRET=0.061), and dopamine-1 receptor (ΔBRET=0.079). The positive increase in BRET signal observed for hGPR30 and hRAMP3 was an order of magnitude greater than the negative controls and comparable to that seen with the positive control, hCLR (ΔBRET=0.728).

To further confirm that hGPR30 and hRAMP3 interact, we performed co-immunoprecipitation. In cells transfected with either FLAG-hGPR30 alone or with HA-hRAMP3, we immunoprecipitated with M2-FLAG beads and immunoblotted for HA (Fig. 1B). The M2-FLAG beads pull down HA material only when FLAG-hGPR30 and HA-hRAMP3 are co-expressed, indicating by a second technique that GPR30 and RAMP3 interact.

The ability of GPCRs to enhance the localization of RAMPs in the plasma membrane is the standard method in the field by which the association of receptors with RAMPs has been tested (Harikumar *et al*. 2009). Therefore, we imaged the interaction of GPR30 and RAMP3 by confocal microscopy of HEK293 cells transiently transfected with HA-hRAMP3 and FLAG-hGPR30 and stained with epitope-specific antibodies. The top row of Fig. 2A shows cells stained following fixation to identify total cellular proteins. In this representative field, cells are present

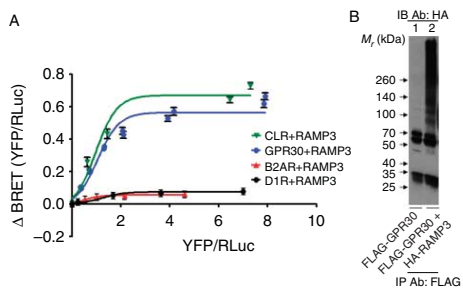

Figure 1

In vitro analysis of GPR30–RAMP3 protein–protein interaction. (A) BRET analysis of the hGPR30–hRAMP3 interaction. hGPR30+hRAMP3 (blue) shows a robust increase in BRET signal with increasing doses of hRAMP3–YFP, as does the positive control, hCLR+hRAMP3 (green). The negative controls, β2-adrenergic receptor (hB2AR, red) and dopamine-1 receptor (D1R, black), which are not expected to interact with RAMPs, show negligible change in the BRET signal. Results shown are representative of at least three replicate experiments that were performed with similar results. (B) Immunoprecipitation with M2 FLAG beads and immunoblotting with anti-HA primary antibody. M2 FLAG pulls down HA immunoreactivity specifically when FLAG-hGPR30 and HA-hRAMP3 are co-expressed. Nonspecific bands at 25 and 50 kDa are IgG bands. The experiment was repeated three times with similar results.

http://jme.endocrinology-journals.org
DOI: 10.1530/JME-13-0021

Published by Bioscientifica Ltd.

expressing HA-hRAMP3 alone and together with FLAG-hGPR30. When expressed alone, diffuse RAMP3 staining occurs throughout the cell. On the other hand, co-expression with GPR30 organizes RAMP3 staining and extensive co-localization occurs in the plasma membrane and intracellularly on filamentous structures and in puncta. Figure 2B shows cells stained live and imaged after fixation to identify cell surface proteins. In this representative field, cells are present expressing HA-hRAMP3 and FLAG-hGPR30 individually and together. When expressed alone, RAMP3 is primarily in intracellular puncta. On the other hand, co-expression with GPR30 increases the relative amount of RAMP3 staining at the cell surface and extensive co-localization occurs. Thus, the formation of a GPR30–RAMP3 complex within the cell increases RAMP3 localization to the plasma membrane.

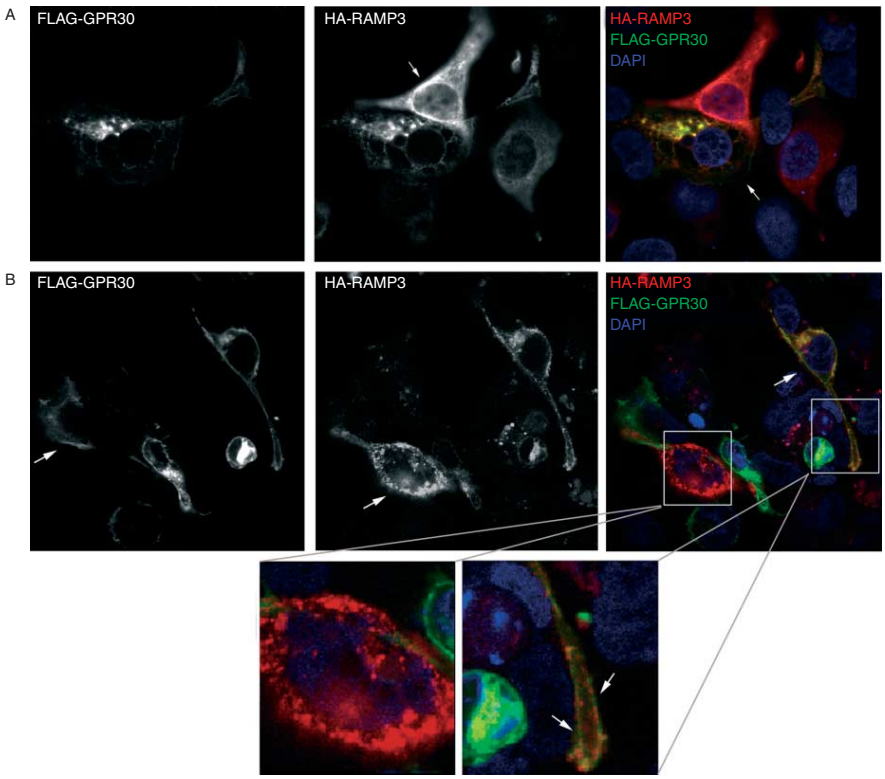

Figure 2

Localization of GPR30 and RAMP3 *in vitro*. (A) Fixed cell staining, confocal microscopy of HEK293 cells transfected with HA-hRAMP3 (green in merged panel) and FLAG-hGPR30 (red in merged panel) stained fixed with M1 FLAG antibody and anti-HA antibody and then with secondary antibody. Left panel shows the FLAG-hGPR30 channel alone, the middle panel shows the HA-hRAMP3 channel alone (arrow indicates a cell expressing only HA-hRAMP3), and the right panel shows the two channels merged with DAPI nuclear stain in blue (arrow indicates a cell expressing both FLAG-hGPR30 and HA-hRAMP3). (B) Live cell staining, HEK293 cells were similarly transfected and stained live with M1 FLAG antibody and anti-HA antibody followed by fixing and staining with secondary antibody. The left panel shows the FLAG-hGPR30 channel alone (arrow indicates a cell expressing only FLAG-hGPR30), the middle panel shows the HA-hRAMP3 channel alone (arrow indicates a cell expressing only HA-hRAMP3), and the right panel shows the two channels merged with DAPI nuclear stain in blue (arrow indicates a cell expressing both FLAG-hGPR30 and HA-hRAMP3). The regions indicated by the white boxes are enlarged in the corresponding panels below and arrows indicate co-localization at the plasma membrane. The experiment was repeated three times with similar results.

http://jme.endocrinology-journals.org
DOI: 10.1530/JME-13-0021

Published by Bioscientifica Ltd.

We next sought to determine whether the interaction of GPR30 and RAMP3 has functional consequences *in vivo*. First, we determined the gene expression levels of *Gpr30* and *Ramp3* in the hearts of wild-type mice. Expression of both *Ramp3* (Fig. 3A) and *Gpr30* (Fig. 3B) was detected in the hearts of male mice, female mice in diestrus and estrus, and female mice that have been ovariectomized to deplete endogenous E_2. For both genes, we observed modest increases in females in estrus compared with diestrus. Ovariectomized females had a statistically significant reduction in both *Gpr30* and *Ramp3* expression compared with intact females in diestrus. Though the differences in expression between males and females in the phases of the estrus cycle are modest, these findings, particularly the reduced gene expression in the ovariectomized females, indicate that cardiac *Gpr30* and *Ramp3* gene expression levels correlate with endogenous E_2.

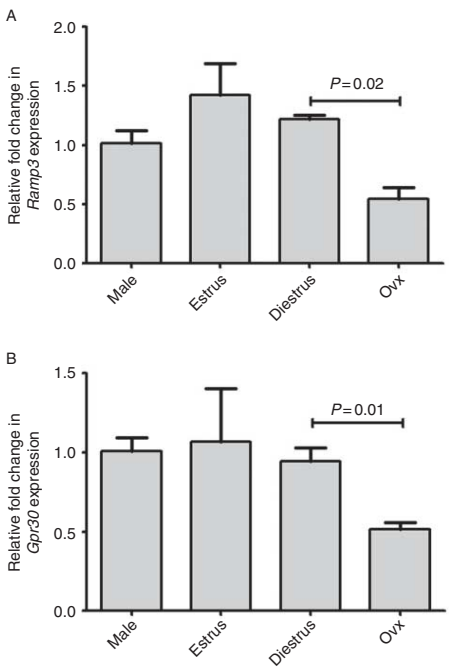

Figure 3
Cardiac expression of *Gpr30* and *Ramp3*. Quantitative PCR was used to compare the expression of (A) *Ramp3* and (B) *Gpr30* in the hearts of male mice, female mice in estrus or diestrus, and ovariectomized (Ovx) females; $n=3$–4 animals per group. Depletion of endogenous estradiol by ovariectomy in female mice resulted in a statistically significant reduction in expression of both *Ramp3* and *Gpr30* in the heart.

Using heart tissue from $Ramp3^{+/+}$ and $Ramp3^{-/-}$ mice, we investigated GPR30 protein levels and localization by performing subcellular fractionation and western blots for GPR30. In pooled heart lysates ($n=3$) from $Ramp3^{+/+}$ mice, we detected robust expression of GPR30 protein at the expected molecular size (50 kD) in the membrane fraction and very little in the cytosolic fraction (Fig. 4A). By contrast, pooled $Ramp3^{-/-}$ heart lysates ($n=3$) showed reduced membrane GPR30 levels (GPR30-integrated density at membrane relative to actin, $Ramp3^{-/-}=0.27$ compared to $Ramp3^{+/+}=1.0$). The $Ramp3^{-/-}$ hearts also show a concomitant increase in cytosolic GPR30 protein relative to wild-type (Fig. 4A). To determine whether cardiac expression and localization of GPR30 protein differ by sex, we performed the same experiment using male and female hearts side-by-side. Figure 4B shows the membrane fraction from these samples. These data show that $Ramp3^{+/+}$ hearts have more membrane-localized GPR30 than $Ramp3^{-/-}$ hearts in both sexes. Furthermore, female hearts have more overall GPR30 at the membrane compared with males, a difference that was statistically significant for wild-type animals (relative GPR30-integrated density at membrane: females, $Ramp3^{+/+}=1.0$ and $Ramp3^{-/-}=0.43$; males, $Ramp3^{+/+}=0.41$ and $Ramp3^{-/-}=0.10$).

To explore the effect of RAMP3 on GPR30 localization in the setting of cardiovascular disease, we utilized RenTgMK mice. The RenTgMK mouse is a well-described model of angiotensin II-mediated chronic hypertension and cardiac hypertrophy (Caron *et al.* 2002, 2004, 2005). We have previously shown that *Ramp3* gene expression is increased in the hearts of RenTgMK mice of both sexes compared with wild-type, and this heart disease-related upregulation of *Ramp3* is greatest in females (Barrick *et al.* 2012). For the current study, we generated RenTgMK mice lacking *Ramp3* (RenTgMK;$Ramp3^{-/-}$) and RenTgMK mice with intact RAMP3 (RenTgMK;$Ramp3^{+/+}$), isolated heart tissue, and performed subcellular fractionation and western blotting to determine GPR30 localization in this model of heart disease. Consistent with our findings in wild-type animals, we detected more GPR30 protein at the membrane in RenTgMK females than in males (relative GPR30-integrated density at membrane: females=1.0, males=0.58; Fig. 4C). Using replicate samples, we also observed that RenTgMK;$Ramp3^{-/-}$ mice had reduced GPR30 at the plasma membrane compared with RenTgMK;$Ramp3^{+/+}$ mice (relative GPR30-integrated

Journal of Molecular Endocrinology

http://jme.endocrinology-journals.org
DOI: 10.1530/JME-13-0021

Published by Bioscientifica Ltd.

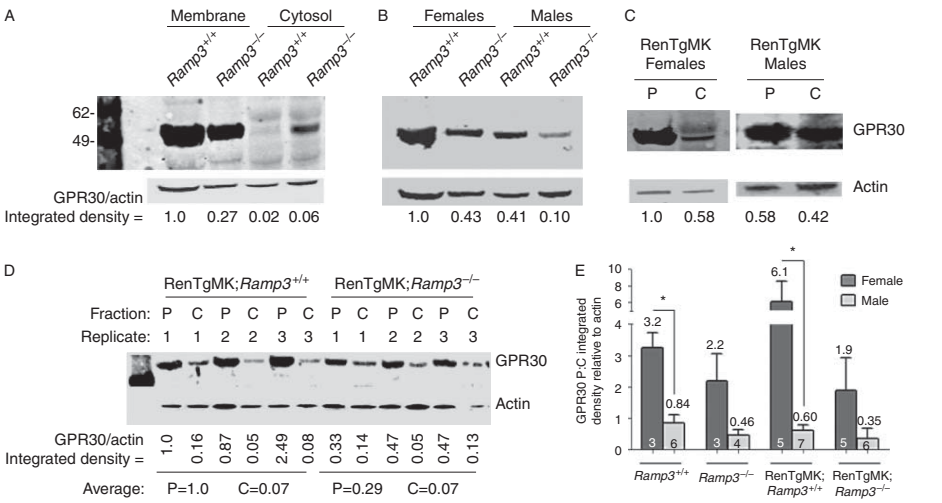

Figure 4

Localization of GPR30 and RAMP3 *in vivo*. (A, B, C and D) GPR30 immunoblots of fractionated cardiac lysates. Membrane-enriched and cytosolic fractions were prepared by ultracentrifugation, and western blotting for GPR30 protein was performed. The integrated density of GPR30 normalized to actin for each lane is listed below each blot, with the first lane set equal to 1.0. (A) GPR30 western blot of cardiac lysates of *Ramp3*$^{+/+}$ and *Ramp3*$^{-/-}$ mice ($n=3$ animals per genotype). GPR30 is reduced in the membrane fraction and increased in the cytosolic fraction in *Ramp3*$^{-/-}$ vs *Ramp3*$^{+/+}$ hearts. (B) GPR30 western blot of the plasma membrane fraction of cardiac lysates from male and female *Ramp3*$^{+/+}$ and *Ramp3*$^{-/-}$ mice ($n=3$ animals per group). Females have more membrane-localized GPR30 than males, and loss of *Ramp3* reduces membrane GPR30 levels in both sexes. (C) Western blot of the plasma membrane (P) and cytosolic (C) fractions of pooled RenTgMK male and female hearts ($n=3$ animals per group). In this heart disease model, females have increased membrane-localized GPR30 compared with males. (D) Western blot of the plasma membrane (P) and cytoplasmic (C) fractions of cardiac lysates from replicate samples of RenTgMK;*Ramp3*$^{+/+}$ ($n=3$) and RenTgMK;*Ramp3*$^{-/-}$ ($n=3$) mice. Each replicate number represents a separate animal. The average densities for the P and C fraction for each genotype are listed below the blot. Loss of *Ramp3* on the RenTgMK background reduces plasma membrane GPR30. (E) Quantitation of immunoblot data showing the normalized ratio of GPR30 protein in the plasma membrane and cytosolic fractions (P:C) in male and female hearts across genotypes. *Ramp3*$^{+/+}$ and RenTgMK;*Ramp3*$^{+/+}$ females have significantly higher GPR30 P:C ratios compared with males of the same genotype. Numbers inside bars represent *n* for each group, numbers above bars represent the average P:C ratio for each group; $*P<0.05$.

density at membrane: RenTgMK;*Ramp3*$^{+/+}=1.0$, RenTgMK;*Ramp3*$^{-/-}=0.29$; Fig. 4D). Figure 4E summarizes the quantitative findings and statistical analysis from each of these experiments. For both sexes, there is a robust trend of reduced membrane to cytosolic (P:C) ratio of GPR30 protein in disease-free and RenTgMK hearts in the absence of *Ramp3*. Female mice have a higher P:C ratio of GPR30 protein compared with males across all conditions, and this sex difference is statistically significant in *Ramp3*$^{+/+}$ and RenTgMK;*Ramp3*$^{+/+}$ hearts. Thus, female mice have significantly increased membrane-localized GPR30 protein compared with males, and there is a trend of GPR30 protein mislocalization in male and female *Ramp3*$^{-/-}$ and RenTgMK;*Ramp3*$^{-/-}$ heart tissues.

Finally, we investigated whether pharmacological activation of GPR30 is cardioprotective in the RenTgMK model of heart disease and whether these effects are dependent on RAMP3. We treated male and female RenTgMK;*Ramp3*$^{+/+}$ and RenTgMK;*Ramp3*$^{-/-}$ mice with G-1, the specific agonist for GPR30, or a placebo for a period of 40 days and then performed cardiovascular phenotyping. First, we measured blood pressure to determine whether G-1 treatment affected the hypertensive phenotype of the RenTgMK mice. We found no significant change in blood pressure with G-1 treatment in male mice (RenTgMK;*Ramp3*$^{+/+}$ placebo$=145.6\pm$ 22.4 mmHg, RenTgMK;*Ramp3*$^{+/+}$ G-1$=148.7\pm25.9$ mmHg and RenTgMK;*Ramp3*$^{-/-}$ placebo$=150.3\pm38.6$ mmHg, RenTgMK;*Ramp3*$^{-/-}$ G-1$=159.5\pm25.1$ mmHg) or female mice (RenTgMK;*Ramp3*$^{+/+}$ placebo$=128.5\pm25.6$ mmHg, RenTgMK;*Ramp3*$^{+/+}$ G-1$=118.0\pm25.0$ mmHg and Ren TgMK;*Ramp3*$^{-/-}$ placebo$=135.8\pm27.4$ mmHg, RenTgMK;*Ramp3*$^{-/-}$ G-1$=140.1\pm38.8$ mmHg).

http://jme.endocrinology-journals.org
DOI: 10.1530/JME-13-0021

Published by Bioscientifica Ltd.

Next, we examined cardiac fibrosis. Consistent with other studies (Jessup *et al*. 2010), we found that there were no overt differences in interstitial fibrosis between the genotypes or with G-1 treatment in male mice (Fig. 5A and B). However, G-1 treatment did result in a statistically significant reduction in perivascular fibrosis (Fig. 5C and D) in the hearts of RenTgMK;*Ramp3*$^{+/+}$, but not RenTgMK;*Ramp3*$^{-/-}$, male mice. We also examined female hearts and found no significant differences in either perivascular or interstitial fibrosis.

We also found interesting changes in the LV:BW ratio of these mice. The LV:BW ratio of RenTgMK;*Ramp3*$^{+/+}$ male mice was significantly reduced with G-1 treatment compared with placebo (Fig. 6A). RenTgMK;*Ramp3*$^{-/-}$ males, on the other hand, had no reduction in their LV:BW ratio with G-1 treatment. Female mice of both genotypes had no significant response to G-1 treatment. BWs did not differ by genotype or treatment condition for males (RenTgMK;*Ramp3*$^{+/+}$ placebo$=24.36\pm4.19$ g, RenTgMK;*Ramp3*$^{+/+}$ G-1$=23.79\pm2.98$ g and RenTgMK;*Ramp3*$^{-/-}$ placebo$=23.19\pm2.73$ g, RenTgMK;*Ramp3*$^{-/-}$ G-1$=23.96\pm3.39$ g) or females (RenTgMK;*Ramp3*$^{+/+}$ placebo$=18.44\pm1.60$ g, RenTgMK;*Ramp3*$^{+/+}$ G-1$=19.23\pm2.21$ g and RenTgMK;*Ramp3*$^{-/-}$ placebo$=20.05\pm1.77$ g, RenTgMK;*Ramp3*$^{-/-}$ G-1$=20.15\pm1.75$ g). In addition to determining LV:BW ratios, we measured cardiomyocyte cross-sectional area, which revealed results consistent with the heart weight findings. Only male RenTgMK mice with intact *Ramp3* showed a significant reduction in cardiomyocyte area with G-1 treatment, while females or males lacking *Ramp3* did not respond to G-1 treatment (Fig. 6B and C).

Discussion

The identification of novel GPCR–RAMP interactions is of great interest because this complex forms a pharmacologically tractable interface, which could potentially be manipulated for the treatment of human disease (Sexton *et al*. 2009). In the current study, we identified GPR30, an E_2 receptor with important functions in the cardiovascular system (Olde & Leeb-Lundberg 2009, Nilsson *et al*. 2011, Prossnitz & Barton 2011), as a novel target for RAMP3, a modifying protein also known for its sex-dependent cardioprotective effects (Barrick *et al*. 2012). The association of GPR30 with a RAMP is of particular interest because this has the potential to clarify much of the controversy that still surrounds GPR30's cellular localization, ligand-binding specificity, and function. Furthermore, GPR30 is the first family A GPCR to be shown to interact with an RAMP.

In this study, we have made use of both standard and newly available techniques in the field to provide compelling evidence for the GPR30–RAMP3 interaction. BRET, already well described for its utility in testing protein–protein interactions in general, has recently been used as an elegant and quantitative method to interrogate GPCR–RAMP interactions (Heroux *et al*. 2007, Harikumar *et al*. 2009). Here, we use this method to reveal a robust interaction between GPR30 and RAMP3 that is equivalent to that observed with CLR, the canonical RAMP-associated receptor. Co-immunoprecipitation of the epitope-tagged GPR30 and RAMP3 proteins further supports this conclusion. In the past, the use of confocal microscopy to test the ability of GPCRs to enhance the localization of RAMPs in the plasma membrane was the standard method by which the association of receptors with RAMPs had been tested (Harikumar *et al*. 2009). Similarly, with this technique, we found that GPR30 and RAMP3 co-localize, and expression of GPR30 enhances RAMP3 localization to the cell surface. This provides further evidence for an interaction between the two proteins and shows that the association of GPR30 and RAMP3 alters the localization of this complex.

In addition to the localization effects observed *in vitro*, RAMP3 may also affect localization of GPR30 *in vivo*, as absence of RAMP3 results in a trend of mislocalized GPR30 in both normal mouse heart tissue and in heart tissue on a background of cardiovascular disease. Sex differences in GPR30 localization were also observed, as the hearts of female mice have a significantly increased proportion of GPR30 protein at the plasma membrane compared with males when *Ramp3*, an estrogen regulated gene, is present. Most importantly, these *in vivo* differences have functional consequences, as pharmacological activation of GPR30 reduces cardiac hypertrophy and perivascular fibrosis in male mice with intact *Ramp3*, while genetic loss of *Ramp3* eliminates this cardioprotective effect. These effects were independent of blood pressure, which is consistent with previous studies showing that chronic G-1 treatment does not affect blood pressure under hypertensive conditions in intact male or female rats (Lindsey *et al*. 2009, 2011, Jessup *et al*. 2010, Wang *et al*. 2012). Thus, it is likely that this cardioprotection is due to direct effects of GPR30–RAMP3 function in the heart, which is influenced by the localization of the protein complex.

Interestingly, we found that the reduction of cardiac hypertrophy and perivascular fibrosis is only observed in male mice, indicating that the protective effect of GPR30

http://jme.endocrinology-journals.org
DOI: 10.1530/JME-13-0021

Published by Bioscientifica Ltd.

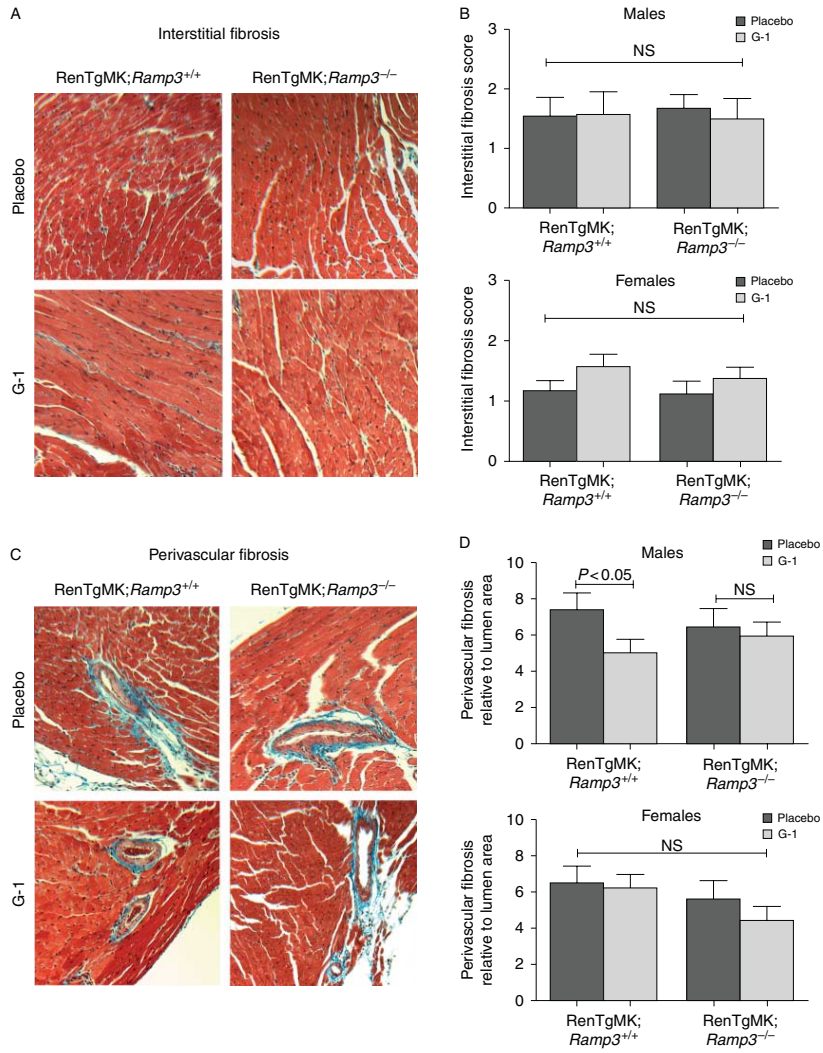

Figure 5

The effect of *in vivo* activation of GPR30 on cardiac fibrosis. (A) Masson's trichrome staining of interstitial fibrosis in the left ventricle of male RenTgMK;*Ramp3*$^{+/+}$ and RenTgMK;*Ramp3*$^{-/-}$ mice treated with 6 mg continuous release pellets of G-1 or placebo for 40 days, (B) with quantitation. No overt differences in interstitial fibrosis were observed between the genotypes or with G-1 treatment. (C) Masson's trichrome staining of perivascular fibrosis in the left ventricle of male RenTgMK; *Ramp3*$^{+/+}$ and RenTgMK;*Ramp3*$^{-/-}$ mice treated with G-1 or placebo, (D) with quantitation. G-1 treatment resulted in a statistically significant reduction in perivascular fibrosis in RenTgMK;*Ramp3*$^{+/+}$ males but not in RenTgMK;*Ramp3*$^{-/-}$ males or female mice of either genotype. $n = 5–9$ animals per group.

http://jme.endocrinology-journals.org
DOI: 10.1530/JME-13-0021

Published by Bioscientifica Ltd.

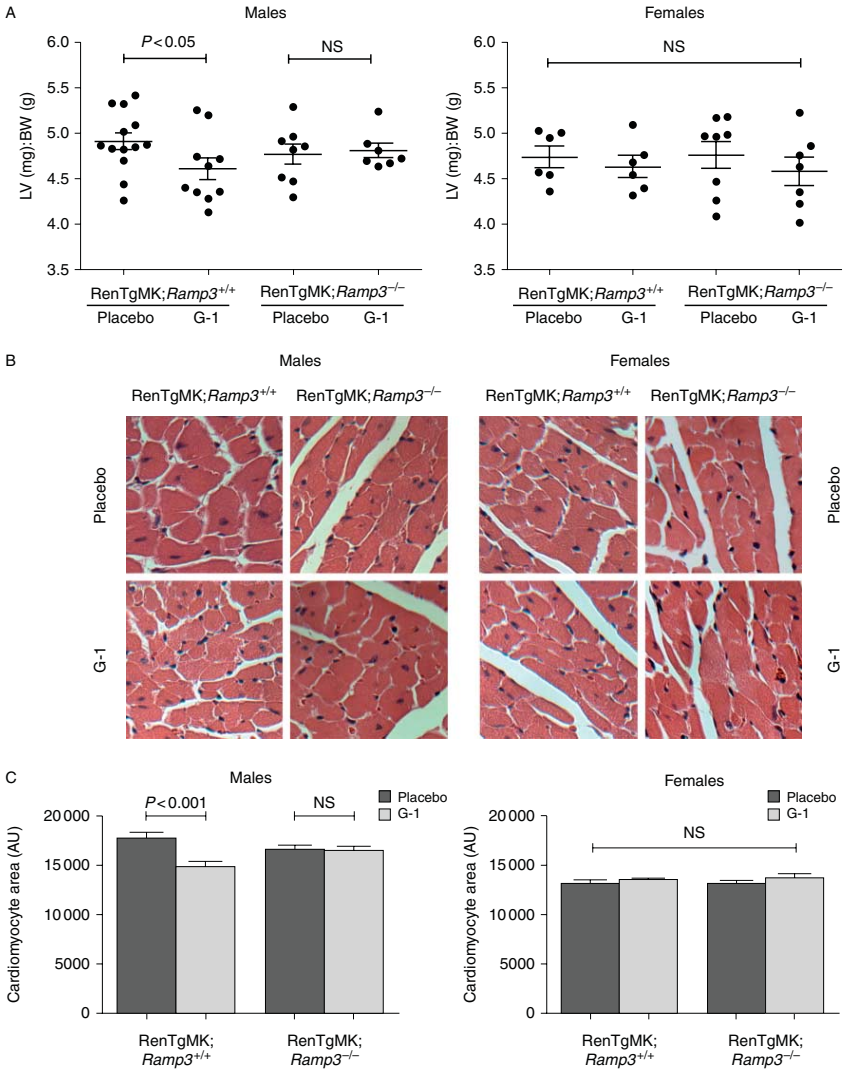

Figure 6

The effect of *in vivo* activation of GPR30 on left ventricular hypertrophy. (A) Left ventricle to body weight (LV:BW) ratios of male and female RenTgMK;*Ramp3*$^{+/+}$ and RenTgMK;*Ramp3*$^{-/-}$ mice treated with the G-1 or placebo. Male RenTgMK;*Ramp3*$^{+/+}$ mice show a statistically significant reduction in LV:BW ratio with G-1 treatment ($P<0.05$). (B) Hematoxylin and eosin staining of the left ventricles of male and female RenTgMK;*Ramp3*$^{+/+}$ and RenTgMK;*Ramp3*$^{-/-}$ mice. (C) Cardiomyocyte cross-sectional area measurements of male and female RenTgMK; *Ramp3*$^{+/+}$ and RenTgMK;*Ramp3*$^{-/-}$ mice. Male RenTgMK;*Ramp3*$^{+/+}$ mice show a statistically significant reduction in cardiomyocyte area with G-1 treatment ($P<0.001$). $n=5$–9 animals per group.

http://jme.endocrinology-journals.org
DOI: 10.1530/JME-13-0021

Published by Bioscientifica Ltd.

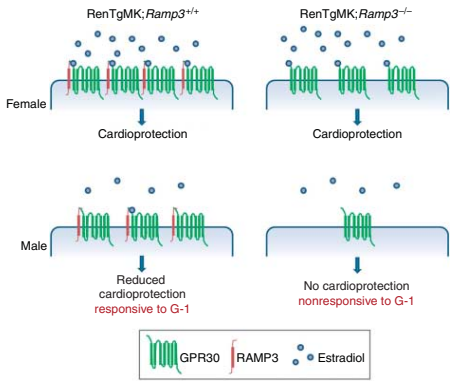

Figure 7
A model of GPR30- and RAMP3-mediated cardioprotection. Female mice have increased GPR30 at the cell membrane compared with males and high levels of the estradiol (E_2). Therefore, regardless of G-1 treatment, females may remain cardioprotected even when *Ramp3* is absent. Males have reduced membrane GPR30 and low E_2 levels and thus lack the natural cardioprotection seen in females. G-1 treatment can improve the cardiovascular phenotype only if the male expresses *Ramp3*, which may maintain GPR30 localization at the cell membrane, allowing for efficient response to ligand treatment.

in the heart is both RAMP3 and sex dependent. Our previously published work has demonstrated that RenTgMK;*Ramp3*$^{-/-}$ males at 5–6 months of age have exacerbated cardiac hypertrophy. We intentionally performed our cardiovascular phenotyping experiments in mice beginning at 2 months of age, and as expected at this early time point, the LV:BW ratios and cardiomyocyte areas did not differ in mice lacking *Ramp3*. Thus, *Ramp3* genotype-dependent effects do not confound the interpretation of our results from the G-1 treatment experiments. Figure 7 models our proposed explanation for why the effectiveness of G-1 treatment was dependent on sex and *Ramp3* genotype. We hypothesize that because female mice have increased GPR30 at the cell membrane compared with males and high levels of the endogenous GPR30 ligand, E_2, they remain cardioprotected even when *Ramp3* is absent, regardless of G-1 treatment. However, males have reduced membrane GPR30 and low E_2 levels. This leads to a worsened cardiovascular phenotype that can be ameliorated with G-1 treatment only if the males express *Ramp3*, which may maintain GPR30 localization at the cell membrane, allowing for efficient response to ligand treatment. The requirement of intact *Ramp3* for GPR30 cardioprotection may also depend on RAMP-mediated effects in addition to localization, such as downstream signaling. Future studies will be directed at determining whether and how RAMP3 alters GPR30-mediated cell signaling.

Our results are consistent with our previous studies showing a sex-dependent cardioprotective role for RAMP3 (Barrick *et al*. 2012), and our findings also complement studies by others including Jessup *et al*. (2010) showing that G-1 treatment significantly reduces cardiomyocyte hypertrophy in intact female rats with salt-sensitive hypertension. Although G-1 treatment reduces interstitial fibrosis in ovariectomized female rats (Kang *et al*. 2012, Wang *et al*. 2012), the reduction in perivascular fibrosis with G-1 treatment in male mice shown here is unique. To our knowledge, this is the first report of GPR30 agonist-induced cardioprotection in a genetic mouse model of cardiovascular disease, with the additional discovery of sex differences. The requirement for RAMP3 to mediate these effects is entirely novel.

Our results demonstrate for the first time that GPR30 and RAMP3 interact. This interaction has functional consequences on the localization of these proteins, and we show that RAMP3 plays a critical and sex-dependent role in GPR30-mediated cardioprotection. GPR30–RAMP3 is a novel pathway that may contribute to sex differences in cardiovascular disease susceptibility and progression, and ultimately, this pathway could potentially be targeted for sex-tailored treatment for cardiovascular disease.

Declaration of interest
The authors declare that there is no conflict of interest that could be perceived as prejudicing the impartiality of the research reported.

Funding
This work was supported by funds from the National Institutes of Health (NIH/NHLBI HL091973 and NIH/NICHD HD060860 and HD035041 to K M C and F30HL104778 to P M L), an American Heart Association Established Investigator Award (to K M C), the Swedish Research Council (VR2009-4077 to L M F L-L), the Swedish Cancer Society (CAN2011/628 to L M F L-L), and the Swedish Research School for Drug Science FLÄK to S B.

Author contribution statement
P M L, S B, and C D B designed and performed experiments and analyzed the results. P M L wrote the manuscript with input from all coauthors. L M F L-L and K M C designed experiments, analyzed data, and provided the conceptual framework for the research.

Acknowledgements
The authors thank James Barwell, Dan Rathbone, and David Poyner for their helpful discussions and insights. They also thank Manyu Li for assistance with cloning, and Kim Fritz-Six and Mahita Kadmiel for assistance with experiments.

http://jme.endocrinology-journals.org
DOI: 10.1530/JME-13-0021

Published by Bioscientifica Ltd.

References

Barrick CJ, Lenhart PM, Dackor RT, Nagle E & Caron KM 2012 Loss of receptor activity-modifying protein 3 exacerbates cardiac hypertrophy and transition to heart failure in a sex-dependent manner. *Journal of Molecular and Cellular Cardiology* **52** 165–174. (doi:10.1016/j.yjmcc.2011.10.021)

Bologa CG, Revankar CM, Young SM, Edwards BS, Arterburn JB, Kiselyov AS, Parker MA, Tkachenko SE, Savchuck NP, Sklar LA *et al.* 2006 Virtual and biomolecular screening converge on a selective agonist for GPR30. *Nature Chemical Biology* **2** 207–212. (doi:10.1038/nchembio775)

Bomberger JM, Parameswaran N & Spielman WS 2012 Regulation of GPCR trafficking by RAMPs. *Advances in Experimental Medicine and Biology* **744** 25–37. (doi:10.1007/978-1-4614-2364-5_3)

Bopassa JC, Eghbali M, Toro L & Stefani E 2010 A novel estrogen receptor GPER inhibits mitochondria permeability transition pore opening and protects the heart against ischemia–reperfusion injury. *American Journal of Physiology. Heart and Circulatory Physiology* **298** H16–H23. (doi:10.1152/ajpheart.00588.2009)

Carmeci C, Thompson DA, Ring HZ, Francke U & Weigel RJ 1997 Identification of a gene (GPR30) with homology to the G-protein-coupled receptor superfamily associated with estrogen receptor expression in breast cancer. *Genomics* **45** 607–617. (doi:10.1006/geno.1997.4972)

Caron KM, James LR, Kim HS, Morham SG, Sequeira Lopez ML, Gomez RA, Reudelhuber TL & Smithies O 2002 A genetically clamped renin transgene for the induction of hypertension. *PNAS* **99** 8248–8252. (doi:10.1073/pnas.112222199)

Caron KM, James LR, Kim HS, Knowles J, Uhlir R, Mao L, Hagaman JR, Cascio W, Rockman H & Smithies O 2004 Cardiac hypertrophy and sudden death in mice with a genetically clamped renin transgene. *PNAS* **101** 3106–3111. (doi:10.1073/pnas.0307333101)

Caron KM, James LR, Lee G, Kim HS & Smithies O 2005 Lifelong genetic minipumps. *Physiological Genomics* **20** 203–209. (doi:10.1152/physiolgenomics.00221.2004)

Christopoulos A, Christopoulos G, Morfis M, Udawela M, Laburthe M, Couvineau A, Kuwasako K, Tilakaratne N & Sexton PM 2003 Novel receptor partners and function of receptor activity-modifying proteins. *Journal of Biological Chemistry* **278** 3293–3297. (doi:10.1074/jbc.C200629200)

Dackor R, Fritz-Six K, Smithies O & Caron K 2007 Receptor activity-modifying proteins 2 and 3 have distinct physiological functions from embryogenesis to old age. *Journal of Biological Chemistry* **282** 18094–18099. (doi:10.1074/jbc.M703544200)

Deschamps AM & Murphy E 2009 Activation of a novel estrogen receptor, GPER, is cardioprotective in male and female rats. *American Journal of Physiology. Heart and Circulatory Physiology* **297** H1806–H1813. (doi:10.1152/ajpheart.00283.2009)

Filardo E, Quinn J, Pang Y, Graeber C, Shaw S, Dong J & Thomas P 2007 Activation of the novel estrogen receptor G protein-coupled receptor 30 (GPR30) at the plasma membrane. *Endocrinology* **148** 3236–3245. (doi:10.1210/en.2006-1605)

Filice E, Recchia AG, Pellegrino D, Angelone T, Maggiolini M & Cerra MC 2009 A new membrane G protein-coupled receptor (GPR30) is involved in the cardiac effects of 17β-estradiol in the male rat. *Journal of Physiology and Pharmacology* **60** 3–10.

Harikumar KG, Simms J, Christopoulos G, Sexton PM & Miller LJ 2009 Molecular basis of association of receptor activity-modifying protein 3 with the family B G protein-coupled secretin receptor. *Biochemistry* **49** 11773–11785. (doi:10.1021/bi901326k)

Heroux M, Breton B, Hogue M & Bouvier M 2007 Assembly and signaling of CRLR and RAMP1 complexes assessed by BRET. *Biochemistry* **46** 7022–7033. (doi:10.1021/bi0622470)

Hewitt SC, Collins J, Grissom S, Deroo B & Korach KS 2005 Global uterine genomics *in vivo*: microarray evaluation of the estrogen receptor α-growth factor cross-talk mechanism. *Molecular Endocrinology* **19** 657–668. (doi:10.1210/me.2004-0142)

Jessup JA, Lindsey SH, Wang H, Chappell MC & Groban L 2010 Attenuation of salt-induced cardiac remodeling and diastolic dysfunction by the GPER agonist G-1 in female mRen2.Lewis rats. *PLoS ONE* **5** e15433. (doi:10.1371/journal.pone.0015433)

Kang S, Liu Y, Sun D, Zhou C, Liu A, Xu C, Hao Y, Li D, Yan C & Sun H 2012 Chronic activation of the G protein-coupled receptor 30 with agonist G-1 attenuates heart failure. *PLoS ONE* **7** e48185. (doi:10.1371/journal.pone.0048185)

Lindsey SH, Cohen JA, Brosnihan KB, Gallagher PE & Chappell MC 2009 Chronic treatment with the G protein-coupled receptor 30 agonist G-1 decreases blood pressure in ovariectomized mRen2.Lewis rats. *Endocrinology* **150** 3753–3758. (doi:10.1210/en.2008-1664)

Lindsey SH, Yamaleyeva LM, Brosnihan KB, Gallagher PE & Chappell MC 2011 Estrogen receptor GPR30 reduces oxidative stress and proteinuria in the salt-sensitive female mRen2.Lewis rat. *Hypertension* **58** 665–671. (doi:10.1161/HYPERTENSIONAHA.111.175174)

McLatchie LM, Fraser NJ, Main MJ, Wise A, Brown J, Thompson N, Solari R, Lee MG & Foord SM 1998 RAMPs regulate the transport and ligand specificity of the calcitonin-receptor-like receptor. *Nature* **393** 333–339. (doi:10.1038/30666)

Nilsson BO, Olde B & Leeb-Lundberg LM 2011 G protein-coupled oestrogen receptor 1 (GPER1)/GPR30: a new player in cardiovascular and metabolic oestrogenic signalling. *British Journal of Pharmacology* **163** 1131–1139. (doi:10.1111/j.1476-5381.2011.01235.x)

Olde B & Leeb-Lundberg LM 2009 GPR30/GPER1: searching for a role in estrogen physiology. *Trends in Endocrinology and Metabolism* **20** 409–416. (doi:10.1016/j.tem.2009.04.006)

Patel VH, Chen J, Ramanjaneya M, Karteris E, Zachariades E, Thomas P, Been M & Randeva HS 2010 G-protein coupled estrogen receptor 1 expression in rat and human heart: protective role during ischaemic stress. *International Journal of Molecular Medicine* **26** 193–199. (doi:10.3892/ijmm_00000452)

Prossnitz ER & Barton M 2011 The G-protein-coupled estrogen receptor GPER in health and disease. *Nature Reviews. Endocrinology* **7** 715–726. (doi:10.1038/nrendo.2011.122)

Sexton PM, Poyner DR, Simms J, Christopoulos A & Hay DL 2009 Modulating receptor function through RAMPs: can they represent drug targets in themselves? *Drug Discovery Today* **14** 413–419. (doi:10.1016/j.drudis.2008.12.009)

Wang C, Dehghani B, Li Y, Kaler LJ, Proctor T, Vandenbark AA & Offner H 2009 Membrane estrogen receptor regulates experimental autoimmune encephalomyelitis through up-regulation of programmed death 1. *Journal of Immunology* **182** 3294–3303. (doi:10.4049/jimmunol.0803205)

Wang H, Jessup JA, Lin MS, Chagas C, Lindsey SH & Groban L 2012 Activation of GPR30 attenuates diastolic dysfunction and left ventricle remodelling in oophorectomized mRen2.Lewis rats. *Cardiovascular Research* **94** 96–104. (doi:10.1093/cvr/cvs090)

Watanabe H, Takahashi E, Kobayashi M, Goto M, Krust A, Chambon P & Iguchi T 2006 The estrogen-responsive adrenomedullin and receptor-modifying protein 3 gene identified by DNA microarray analysis are directly regulated by estrogen receptor. *Journal of Molecular Endocrinology* **36** 81–89. (doi:10.1677/jme.1.01825)

Received in final form 8 May 2013
Accepted 14 May 2013
Accepted Preprint published online 14 May 2013

http://jme.endocrinology-journals.org
DOI: 10.1530/JME-13-0021

Published by Bioscientifica Ltd.

Paper IV

THE JOURNAL OF BIOLOGICAL CHEMISTRY VOL. 289, NO. 32, pp. 22117–22127, August 8, 2014

G protein-coupled Receptor 30 (GPR30) Forms a Plasma Membrane Complex with Membrane-associated Guanylate Kinases (MAGUKs) and Protein Kinase A-anchoring Protein 5 (AKAP5) That Constitutively Inhibits cAMP Production*

Received for publication, March 19, 2014, and in revised form, June 19, 2014 Published, JBC Papers in Press, June 24, 2014, DOI 10.1074/jbc.M114.566893

Stefan Broselid[‡], Kelly A. Berg[§], Teresa A. Chavera[§], Robin Kahn[¶], William P. Clarke[§], Björn Olde[‖], and L. M. Fredrik Leeb-Lundberg[‡1]

From the Departments of [‡]Experimental Medical Science, [¶]Nephrology, and [‖]Cardiology, Lund University, 22184 Lund, Sweden and the [§]Department of Pharmacology, University of Texas Health Science Center, San Antonio, Texas 78229

Background: GPR30 plays important roles in cardiometabolic regulation and cancer.
Results: GPR30 forms a complex with a MAGUK and AKAP5 that constitutively inhibits cAMP production independently of $G_{i/o}$ and retains receptors in the plasma membrane.
Conclusion: The GPR30-MAGUK-AKAP5 complex mediates receptor signaling.
Significance: These results present a new mechanism by which a receptor inhibits cAMP production.

GPR30, or G protein-coupled estrogen receptor, is a G protein-coupled receptor reported to bind 17β-estradiol (E_2), couple to the G proteins G_s and $G_{i/o}$, and mediate non-genomic estrogenic responses. However, controversies exist regarding the receptor pharmacological profile, effector coupling, and subcellular localization. We addressed the role of the type I PDZ motif at the receptor C terminus in receptor trafficking and coupling to cAMP production in HEK293 cells and CHO cells ectopically expressing the receptor and in Madin-Darby canine kidney cells expressing the native receptor. GPR30 was localized both intracellularly and in the plasma membrane and subject to limited basal endocytosis. E_2 and G-1, reported GPR30 agonists, neither stimulated nor inhibited cAMP production through GPR30, nor did they influence receptor localization. Instead, GPR30 constitutively inhibited cAMP production stimulated by a heterologous agonist independently of $G_{i/o}$. Moreover, siRNA knockdown of native GPR30 increased cAMP production. Deletion of the receptor PDZ motif interfered with inhibition of cAMP production and increased basal receptor endocytosis. GPR30 interacted with membrane-associated guanylate kinases, including SAP97 and PSD-95, and protein kinase A-anchoring protein (AKAP) 5 in the plasma membrane in a PDZ-dependent manner. Knockdown of AKAP5 or St-Ht31 treatment, to disrupt AKAP interaction with the PKA RIIβ regulatory subunit, decreased inhibition of cAMP production, and St-Ht31 increased basal receptor endocytosis. Therefore, GPR30 forms a plasma membrane complex with a membrane-associated guanylate kinase and AKAP5, which constitutively attenuates cAMP production in response to heterologous agonists independently of $G_{i/o}$ and retains receptors in the plasma membrane.

GPR30 is a G protein-coupled receptor (GPCR)[2] that is currently attracting considerable attention for important roles in cardiometabolic regulation and cancer. The receptor was named G protein-coupled estrogen receptor following reports that it binds 17β-estradiol (E_2) with high affinity (1, 2) and mediates non-genomic estrogenic responses via the G proteins G_s (3) and $G_{i/o}$ *in vitro* (1–5). However, the receptor pharmacological profile, effector coupling, and subcellular localization are controversial (6–10), indicating that a number of receptor details are missing.

PDZ domains are protein-protein recognition modules present in some proteins that bind C-terminal short, linear sequences that may be divided into three types, including type I (*X*-(S/T)-*X*-Ø), type II (*X*-Ø-*X*-Ø), and type III (*X*(D/E)-*X*-Ø) (11). Some GPCRs contain PDZ motifs at their C termini that regulate receptor signaling and trafficking (12). GPR30 contains a conserved C-terminal canonical type I PDZ motif, -SSAV, and this motif has been shown recently to interact with postsynaptic density 95 (PSD-95) and to be important for receptor plasma membrane localization (13). PSD-95 is a neuronal protein and the most studied member of the membrane-associated guanylate kinase (MAGUK) family of PDZ domain proteins. These proteins serve as scaffolds to organize events in signal transduction, cell adhesion, and membrane trafficking at specialized cell-cell junctions (14). Several MAGUKs also interact via a unique domain with protein kinase A-anchoring protein (AKAP) 79/150 or AKAP5 (15, 16), which is known to interact with the RII regulatory subunit of PKA (17). Furthermore, AKAP5-RII interacts with, phosphorylates, and inhibits adenylate cyclase (AC) (17, 18). Therefore, AKAP5 exists in complexes that compartmentalize the regulation of cAMP production and signaling.

* This work was supported by the Swedish Cancer Foundation, the Swedish Research Council, the NovoNordisk Foundation, the Alfred Österlund Foundation, and the Gunnar Nilsson Cancer Foundation (to L. M. F. L. L.).
[1] To whom correspondence should be addressed: Dept. of Experimental Medical Science, Lund University, BMC A12, 22184 Lund, Sweden. Tel.: 46-46-2223944; Fax: 46-46-2220568; E-mail: fredrik.leeb-lundberg@med.lu.se.

[2] The abbreviations used are: GPCR, G protein-coupled receptor; MAGUK, membrane-associated guanylate kinase; AKAP, A kinase-anchoring protein; AC, adenylate cyclase; MDCK, Madin-Darby canine kidney; β1AR, β1 adrenergic receptor; RIA, radioimmunoassay; FSK, forskolin; PGE_2, prostaglandin E_2; ISO, isoproterenol; Ab, antibody.

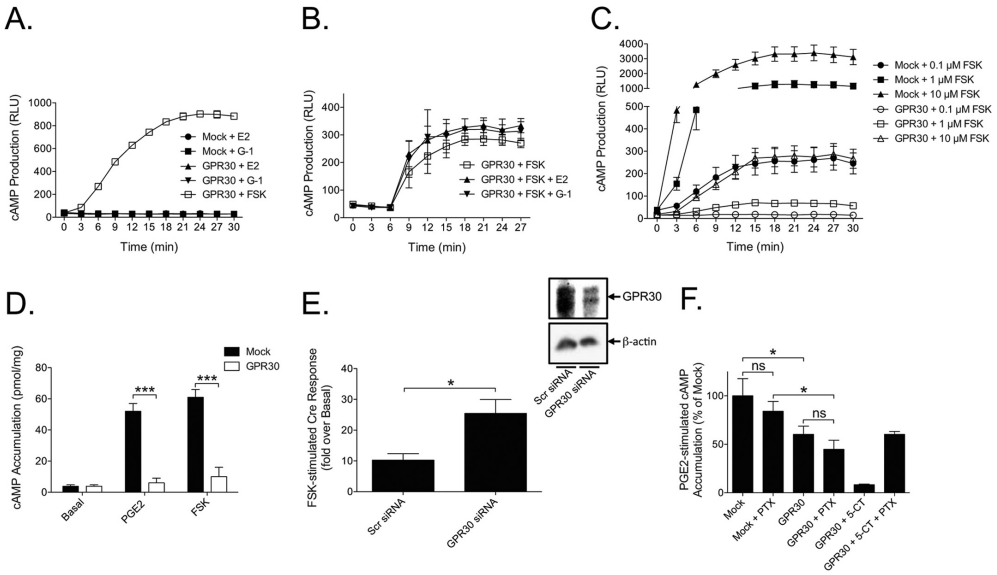

FIGURE 1. **GPR30 constitutively inhibits cAMP production.** *A* and *B*, HEK cells transfected without (*Mock*) and with GPR30 were treated with 0.1 μM E_2, 1 μM G-1, and/or 1 μM FSK. *C*, HEK cells transfected without and with GPR30 were treated with increasing concentrations of FSK. *D*, CHO cells transfected without and with GPR30 were treated with 1 μM PGE2 or 1 μM FSK for 30 min. *E*, MDCK-Cre cells transfected with scrambled (*Scr siRNA*) and GPR30-specific siRNA (*GPR30 siRNA*) were treated with 1 μM FSK and immunoblotted for GPR30 and β-actin. *F*, CHO cells transfected without and with GPR30 were treated without and with 100 ng/ml pertussis toxin (*PTX*) for 24 h and then with 1 μM PGE2 without or with 100 nM 5-carboxamidotryptamine (*5-CT*) for 30 min. *A–C*, cAMP was measured in real time with the GloSensor assay, and the results, shown as relative light units (*RLU*), are representative of at least six experiments, with each data point being the mean ± S.E. of 8–16 measurements. In *D* and *F*, cAMP was measured with RIA, and in *E*, cAMP was measured with the Cre reporter assay, and the values are means ± S.E. of at least three independent experiments, with each data point representing 3–16 measurements. *, $p < 0.05$; ***, $p < 0.001$; *ns*, not significant.

Here we investigated the role of the GPR30 PDZ motif in receptor plasma membrane localization and regulation of cAMP production and addressed the involvement of MAGUKs and AKAP5 in these events. Our results show that GPR30 forms a PDZ motif-dependent plasma membrane complex with a MAGUK and AKAP5 that constitutively inhibits cAMP production independently of $G_{i/o}$ and retains the receptor in the plasma membrane.

EXPERIMENTAL PROCEDURES

Cell Culture and DNA Constructs—HEK293 cells, MDCK cells, and CHO-K1 cells (ATCC) were grown in phenol red-free DMEM supplemented with 10% FBS in 5% or 10% CO_2 at 37 °C. In some experiments, FBS was replaced with charcoal-stripped FBS. N-terminally FLAG- and HA-tagged human GPR30 cDNA in pcDNA3.1 were made as described previously (19). A GPR30 cDNA construct, in which the four C-terminal residues in GPR30 (-SSAV) were deleted (GPR30ΔSSAV), was produced by PCR. Human FLAG-tagged PSD-95, human FLAG-tagged β1-adrenergic receptor (β1AR), and PKA RIIβ-GFP cDNAs were obtained from Addgene (Cambridge, MA). Canine GPR30-specific and scrambled siRNAs were obtained from Eurofins MWG Operon (Edelsberg, Germany), and human AKAP5-specific and scrambled shRNAs in pcDNA6.1 vectors were obtained from Dr. S. Bahouth (University of Tennessee Health Science Center, Memphis, TN).

TransIT-LT1 (Mirus Bio LLC, Madison, WI) was used to transiently transfect HEK293 cells and MDCK-Cre cells, and a nucleofection protocol (Amaxa Inc., Gaithersburg, MD) was used to transiently transfect HEK293 cells and CHO-K1 cells. Cells transiently transfected with a plasmid-containing receptor construct were always compared with cells transfected with empty plasmid alone (mock). HEK293 cells stably expressing FLAG-tagged mouse GPR30 were generated and maintained as described previously (19). MDCK cells were transfected with the p6CRE/luc vector using Lipofectamine reagent (Invitrogen). Single colonies were chosen and propagated in the presence of selection-containing medium (medium plus hygromycin B) to generate a clonal stable cell line (MDCK-Cre).

Immunoprecipitation and Immunoblotting—Immunoprecipitation and immunoblotting were done as described previously (19). Proteins were immunoprecipitated with mouse M2 FLAG antibody-agarose (Sigma-Aldrich, St. Louis, MO) and goat GPR30 antibody (R&D Systems, Minneapolis, MN), pan-MAGUK antibody (Merck Millipore, Billerica, MA), AKAP5 antibody (BD Biosciences), and SAP97 antibody (Santa Cruz Biotechnology) coupled to protein G-Sepharose (GE Healthcare). Proteins were immunoblotted with mouse M2 FLAG

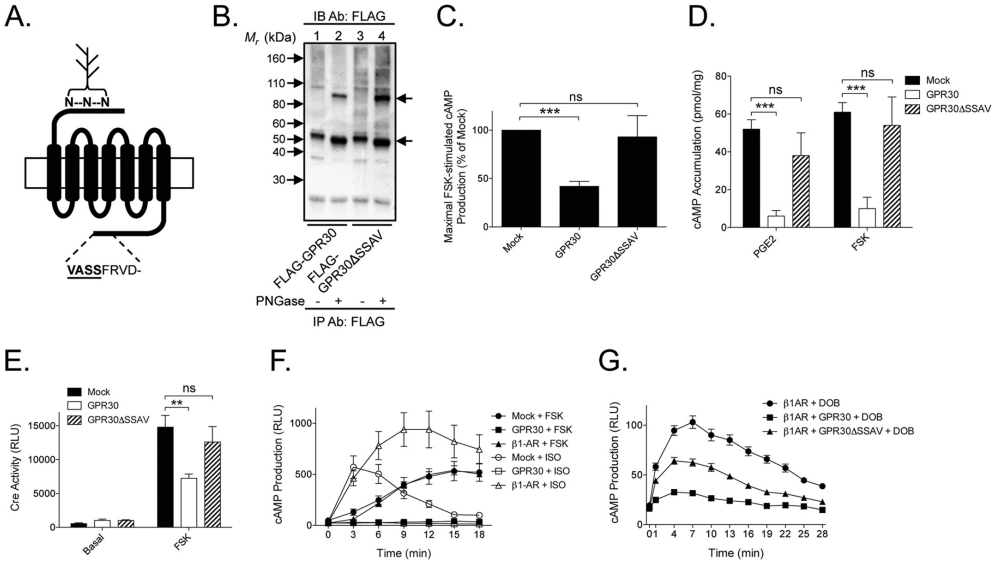

FIGURE 2. **Constitutive GPR30 inhibition of cAMP production requires the receptor C-terminal PDZ motif.** *A*, schematic of the GPR30 structure indicating the C-terminal PDZ motif and N-terminal N-glycosylation sites. *B*, HEK cells transfected with GPR30 or GPR30ΔSSAV were immunoprecipitated (*IP*) with M2 FLAG antibody (*Ab*) beads, treated without (−) and with (+) PNGase, and immunoblotted (*IB*) with M2 FLAG Ab. Molecular weight (M_r) standards (*arrows* on the *left*) and major receptor species, as described by Sanden *et al.* (19), are indicated (*arrows* on the *right*), and the results are representative of experiments performed at least three times. *C*, HEK cells transfected without (*Mock*) and with GPR30 or GPR30ΔSSAV were treated with 1 μM FSK, and cAMP production was measured in real time with the GloSensor assay. *D*, CHO cells transfected without and with GPR30 or GPR30ΔSSAV were treated with 1 μM PGE2 or 1 μM FSK, and cAMP production was measured with RIA. *E*, MDCK-Cre cells transfected without and with GPR30 or GPR30ΔSSAV were treated with 1 μM FSK, and cAMP production was measured with the Cre promoter reporter assay. *F*, HEK cells transfected without and with GPR30 or β1AR were treated with 1 μM FSK or 10 μM ISO, and cAMP production was measured in real time with the GloSensor assay. *G*, HEK cells transfected with β1AR without and with GPR30 or GPR30ΔSSAV were treated with 0.1 μM dobutamine, and cAMP production was measured in real time with the GloSensor assay. *C–E*, the values are mean ± S.E. of at least three independent experiments, with each data point performed in at least triplicates. *F* and *G*, the results are representative of at least three independent experiments, with each data point being the mean ± S.E. of 16 measurements. *E–G*, the results are shown as relative light units (*RLU*). **, $p < 0.01$; ***, $p < 0.001$; *ns*, not significant.

antibody (Sigma-Aldrich, 1:1000), goat GPR30 antibody (1:200), pan-MAGUK antibody (1:2000), SAP97 antibody (1:200), and AKAP5 antibody (1:1000).

Enzymatic Deglycosylation—Deglycosylation was done by treating immunoprecipitates with 500 units PNGase F (New England Biolabs, Ipswich, MA) in 10 mM Tris-HCl (pH 7.4) for 2 h at 37 °C.

Immunofluorescence Microscopy—Immunofluorescence microscopy of HEK293 cells was done as described previously (19, 20). In live antibody staining, we took advantage of the fact that mouse M1 FLAG antibody (Sigma-Aldrich, 1:500) and goat GPR30 antibody (1:100) specifically label the receptor extracellular N-terminal FLAG epitope and N-terminal domain, respectively. Therefore, "feeding" live cells with these antibodies for 30 min at 37 °C monitored exclusively cell surface receptor-antibody complexes and complexes that had undergone endocytosis. Cells were then fixed and permeabilized. In fixed staining, to monitor total cellular receptors, cells were fixed and permeabilized and then incubated with mouse M1 FLAG antibody (1:500) or goat GPR30 antibody (1:100) for 1 h at 22 °C. In all experiments, receptors were then visualized by incubating fixed cells with secondary Alexa Fluor 488-labeled goat antibodies or mouse IgG2b antibodies (Invitrogen). For colocalization, fixed and permeabilized cells were also incubated with rabbit early endosomal antigen 1 (EEA1) antibody (Sigma-Aldrich, 1:200), pan-MAGUK antibody (1:2000), and AKAP5 antibody (1:1000) and then with secondary Alexa Fluor 568-labeled anti-mouse IgG1 or anti-rabbit antibodies (Invitrogen). DAPI was used for nuclear staining. Images were collected using a Nikon Eclipse confocal fluorescence microscope.

Flow Cytometry—Resuspended HEK293 cells were incubated with mouse anti-M1 FLAG antibody (1:200) or mouse IgG (DAKO, Glostrup, Denmark) for 20 min with or without 0.1% saponin/PBS (Sigma-Aldrich) at room temperature to detect the intracellular and cell surface expression of receptors, respectively. Cells were then washed with PBS with Ca^{2+}/Mg^{2+} and resuspended in PBS with phycoerythrin-labeled goat anti-mouse antibody (DAKO, 1:2000) as a secondary antibody, with or without 0.1% saponin/PBS for 20 min at room temperature in the dark. The cells were then washed with PBS, centrifuged at 2000 × *g* for 5 min, and then the pellet was resuspended in PBS and analyzed directly by flow cytometry. The specificity of the secondary antibody was tested by omitting the primary antibody. The cells were analyzed using a BD FACSCanto

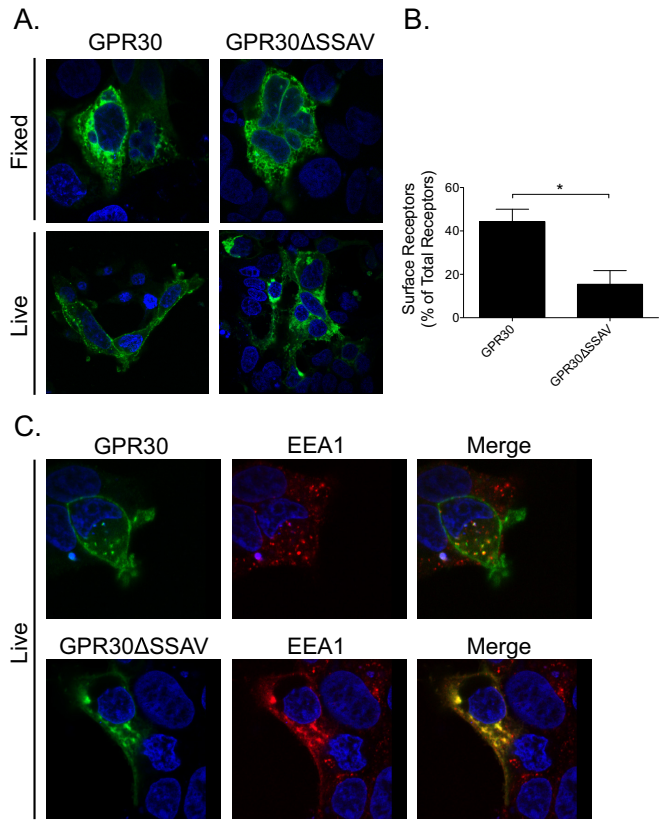

FIGURE 3. **GPR30 requires the C-terminal PDZ motif for plasma membrane retention.** *A*, HEK cells transfected with GPR30 or GPR30ΔSSAV were subjected to fixed staining (*Fixed*) and live staining (*Live*) with M1 FLAG antibodies. *B*, HEK cells transfected with GPR30 or GPR30ΔSSAV were stained live (*Surface Receptors*) and following permeabilization (*Total Receptors*) with M1 FLAG antibodies and then subjected to flow cytometry. The values are means ± S.E. of at least three independent experiments with each data point performed in at least triplicates. *C*, HEK cells transfected with GPR30 or GPR30ΔSSAV were subjected to live staining with M1 FLAG antibodies. Following fixation and permeabilization, cells were stained with EEA1 antibodies. *A* and *C*, the results are representative of experiments performed at least three times. The individual and merged images (*Merge*) were collected using a Nikon Eclipse confocal microscope, ×60 objective, and 50-μm zoom. *Yellow* indicates colocalization in merged images. *, $p < 0.05$.

cytometer and FACSDiva software (BD Biosciences). Forward and side scatter measurements were attained with gain settings in linear mode. In all experiments, binding was calculated after subtracting the background fluorescence of the control antibody.

cAMP Production—Accumulation of cAMP in CHO-K1 cells and HEK293 cells was measured by radioimmunoassay (RIA) as described previously by us (21). Briefly, cells in 24-well plates were washed twice with Hanks' balanced salt solution containing 20 mM HEPES (pH 7.4). Cells were then incubated with the phosphodiesterase inhibitor rolipram (25 μM) with or without stimulus for 15 min. Incubations were terminated by aspiration and addition of 500 μl of ice-cold absolute ethanol. The ethanol extracts from individual wells were then dried under a gentle air stream and reconstituted in 100 μl of 50 mM sodium acetate (pH 6.2). The cAMP content of each 100-μl sample was determined by RIA.

Production of cAMP in HEK293 cells was also measured using the GloSensor cAMP assay according to the instructions of the manufacturer (Promega, Madison, WI). Briefly, cells in 96-well plates (20,000 cells/well) were incubated with the GloSensor cAMP reagent. Following addition of the stimulus, cAMP production was measured as luminescence.

Cre Promoter Activity—Cre activity was measured in MDCK-Cre cells. Cells in 96-well plates (20,000 cells/well) were grown in medium overnight and then in serum-free medium for ~20 h. After washing in the same medium, cells were incubated with 25 μM rolipram for 5 min, after which various stimuli were added for 22 h. Incubations were terminated by aspiration and addition of 10 μl/well reporter lysis buffer (Promega). Follow-

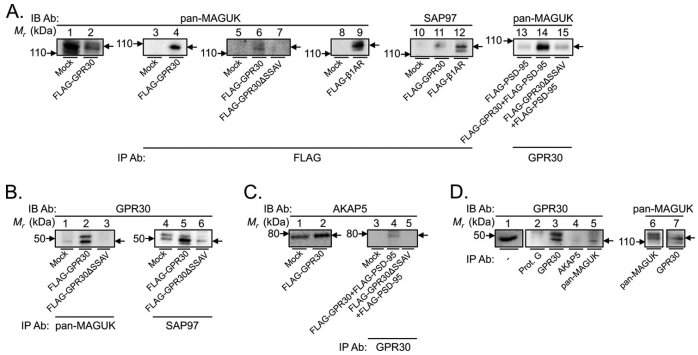

FIGURE 4. **The GPR30 C-terminal PDZ motif forms a complex with MAGUKs and AKAP5.** *A*, lysates of naïve HEK cells (*Mock*, *lane 1*) and HEK cells stably expressing mouse GPR30 (*FLAG-GPR30*, *lane 2*) were immunoblotted (*IB*) with pan-MAGUK antibody or first immunoprecipitated (*IP*) with M2 FLAG Ab beads and then IB with pan-MAGUK Ab (*lanes 3* and *4*). Lysates of HEK cells transfected without (*Mock*, *lanes 5*, *8*, and *10*) and with human GPR30 (*lanes 6* and *11*), GPR30ΔSSAV (*lane 7*), or β1-AR (*lanes 9* and *12*) were immunoprecipitated with M2 FLAG Ab beads and then immunoblotted with pan MAGUK Ab (*lanes 5–9*) or SAP97 Ab (*lanes 10–12*). Lysates of HEK cells transfected with PSD-95 without (*lane 13*) and with human GPR30 (*lane 14*) or GPR30ΔSSAV (*lane 15*) were immunoprecipitated with GPR30 Ab-protein G beads and then immunoblotted with pan-MAGUK Ab. *B*, lysates of HEK cells transfected without (*lane 1*) and with GPR30 (*lane 2*) or GPR30ΔSSAV (*lane 3*) were immunoprecipitated with pan-MAGUK Ab-protein G beads and then immunoblotted with GPR30 Ab. *C*, lysates of naïve HEK cells (*lane 1*) and HEK cells stably expressing mouse GPR30 (*lane 2*) were immunoblotted with AKAP5 antibody. Lysates of HEK cells transfected with PSD-95 without (*lane 3*) and with human GPR30 (*lane 4*) or GPR30ΔSSAV (*lane 5*) were immunoprecipitated with M2 FLAG Ab beads and then immunoblotted with AKAP5 antibody. *D*, lysates of MDCK cells were immunoblotted with GPR30 antibody (*lane 1*) or first immunoprecipitated with protein G beads (*lane 2*) or protein G beads bound with GPR30 Ab (*lanes 3* and *7*), AKAP5 Ab (*lane 4*), or pan-MAGUK Ab (*lanes 5* and *6*) and then immunoblotted with GPR30 Ab (*lanes 2–5*) or pan-MAGUK Ab (*lanes 6* and *7*). Molecular weight (M_r) standards (in kilodaltons) are indicated (*arrows* on the *left*). MAGUKs (*A* and *D*, *lanes 6* and *7*), GPR30 (*B* and *D*, *lanes 1–5*), and AKAP5 (*C*) are indicated (*arrows* on the *right*). The results are representative of experiments performed at least three times.

ing addition of 35 μl/well luciferin reagent (Biothema, Handen, Sweden) and ATP, Cre promoter activity was measured as luminescence.

Data Analysis—Data are presented as mean ± S.E. Where appropriate, paired analysis with Student's *t* test or one-way analysis of variance with Bonferroni's post hoc test was used for statistical comparisons. $p < 0.05$ was regarded as statistically significant. Data analysis was performed using the Prizm program (GraphPad, La Jolla, CA).

RESULTS

GPR30 Constitutively Inhibits cAMP Production—To investigate whether GPR30 regulates cAMP production, we transiently expressed N-terminally FLAG-tagged human GPR30 (GPR30) in HEK293 cells and CHO cells, two well described model systems. First, we assessed GPR30-dependent effects by treating HEK293 cells with the proposed GPR30 agonists E_2 (0.1 μM) and G-1 (1 μM) (22). Neither agonist increased cAMP production (Fig. 1*A*) nor decreased cAMP production stimulated by forskolin (FSK) (1 μM) (Fig. 1*B*) in either GPR30- or mock-transfected cells. The same results were obtained with CHO cells transiently expressing the receptor (data not shown).

Next, we took an unbiased approach and assessed whether GPR30 regulated cAMP production constitutively, *i.e.* in the absence of agonist. To do so, cAMP production in cells expressing the receptor was compared with that in mock-transfected cells. GPR30 expression had no effect on basal cAMP production in either HEK293 cells or CHO cells (data not shown). On the other hand, GPR30 drastically decreased FSK-stimulated cAMP production, as determined in HEK293 cells (Fig. 1*C*). The inhibition was not caused by a serum-derived factor because the same effect was observed after growing cells in phenol red-free and charcoal-stripped serum or keeping them in serum-free medium for 24 h (data not shown). GPR30 also decreased both prostaglandin E_2 (PGE_2)- and FSK-stimulated cAMP production in CHO cells (Fig. 1*D*). Consistent with these observations, siRNA knockdown of native GPR30 in MDCK cells stably expressing a p6CRE/luc construct (MDCK-Cre) significantly increased FSK-stimulated Cre promoter activity (Fig. 1*E*). Pretreatment of CHO cells expressing GPR30 with 100 ng/ml pertussis toxin for 24 h had no effect on GPR30 inhibition of cAMP production, whereas pertussis toxin reversed the inhibitory effect of 100 nM 5-carboxyamidotryptamine through endogenous G_i-coupled 5-HT1B receptors (Fig. 1*F*), as reported previously (21). Therefore, GPR30 constitutively inhibits cAMP production independently of $G_{i/o}$.

Constitutive GPR30 Inhibition of cAMP Production Requires the Receptor C-terminal PDZ Motif—To address the functional role of the type I PDZ binding motif (-SSAV) at the receptor C terminus (Fig. 2*A*), an N-terminally FLAG-tagged receptor construct lacking this motif (GPR30ΔSSAV) was expressed and compared with GPR30. Both constructs expressed equally well with the same peptide profile in HEK293 cells (Fig. 2*B*, *lanes 1* and *3*). Furthermore, the constructs exhibited the same unique peptide profile as that observed previously with the mouse receptor following receptor *N*-deglycosylation with PNGase (Fig. 2*B*, *lanes 2* and *4*) (19).

Interestingly, deletion of the PDZ motif in GPR30 blunted the ability of this receptor to inhibit cAMP production, regardless of whether cAMP production had been increased with FSK in HEK293 cells (Fig. 2*C*), FSK or PGE_2 in CHO cells (Fig. 2*D*),

or FSK in MDCK-Cre cells (Fig. 2*E*). Furthermore, deletion of the PDZ motif did not introduce either E_2- or G-1 stimulation or inhibition of cAMP production (data not shown). In contrast to GPR30, FLAG-tagged β1AR, a G_s-coupled GPCR that also contains a C-terminal type I PDZ motif (-ESKV), did not constitutively inhibit FSK-stimulated cAMP production in HEK293 cells (Fig. 2*F*). Furthermore, although GPR30 inhibited cAMP production in response to isoproterenol (ISO) stimulation of endogenous β2AR in these cells, β1AR enhanced the ISO response, as expected (Fig. 2*F*). Also, when GPR30 and β1AR were coexpressed, GPR30 inhibited cAMP production in response to the β1-selective agonist dobutamine, whereas GPR30ΔSSAV was less efficacious (Fig. 2*G*). Therefore, GPR30 constitutively inhibits cAMP production in a PDZ-dependent manner.

GPR30 Requires the C-terminal PDZ Motif for Plasma Membrane Retention—To determine the role of the GPR30 PDZ motif in receptor subcellular localization, HEK293 cells expressing GPR30 or GPR30ΔSSAV were stained with M1 FLAG antibodies or GPR30 antibodies, both directed toward extracellular N-terminal receptor epitopes, and then imaged by confocal immunofluorescence microscopy. Fixed staining, in which receptors were stained following cell fixation to monitor all cellular receptors, showed that GPR30 and GPR30ΔSSAV distributed similarly both intracellularly and in the plasma membrane (Fig. 3*A*, *Fixed*), and neither distribution was influenced by E_2 or G-1 (data not shown). Live staining, in which live cells were fed primary antibody for 30 min at 37 °C prior to cell fixation to selectively monitor cell surface receptor-antibody complexes and complexes that had internalized during this time period, showed that GPR30 was present primarily in the plasma membrane with limited basal endocytosis (Fig. 3*A*, *Live*). On the other hand, live staining of GPR30ΔSSAV was primarily intracellular, indicating that, although this construct also reached the cell surface, it was subject to considerably higher basal endocytosis compared with GPR30 (Fig. 3*A*, *Live*). Flow cytometry analysis confirmed that the steady-state cell surface level of GPR30ΔSSAV was significantly lower than that of GPR30 (Fig. 3*B*). Therefore, the GPR30 PDZ motif is also important for retaining receptors in the plasma membrane.

Fig. 3*C* shows that the limited amount of internalized GPR30 observed following live staining partially colocalized with the early endosomal marker EEA1, indicating that it proceeds via typical receptor-mediated endocytosis. Interestingly, deletion of the PDZ motif increased colocalization with this marker, suggesting that this motif may also participate in postendocytic receptor sorting.

The GPR30 C-terminal PDZ Motif Forms a Complex with MAGUKs and AKAP5—Immunoblotting of HEK293 cell lysates shows that these cells express MAGUKs with which the GPR30 PDZ motif could potentially interact (Fig. 4*A*, *lanes 1* and *2*). Immunoprecipitation of mouse GPR30 from HEK293 cells stably expressing this receptor specifically coprecipitated a native MAGUK of about 110 kDa (Fig. 4*A*, *lane 4*). Transiently expressed human GPR30 coprecipitated a MAGUK of a slightly larger size (Fig. 4*A*, *lane 6*) that was not observed when expressing GPR30ΔSSAV (Fig. 4*A*, *lane 7*). The size of this MAGUK

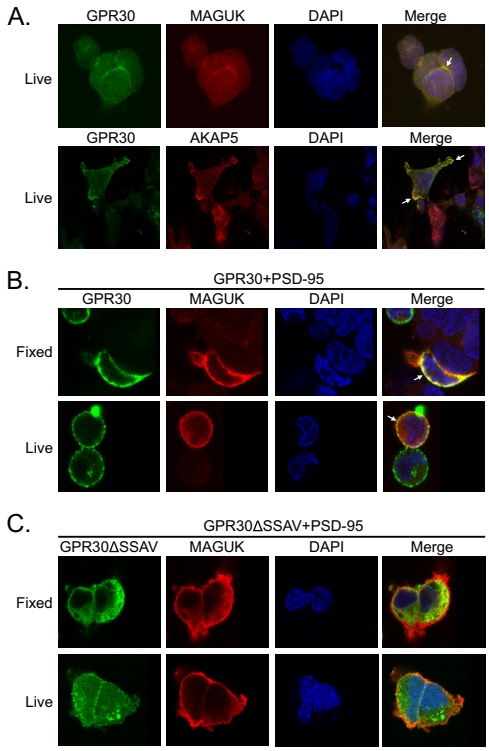

FIGURE 5. **The GPR30-MAGUK-AKAP5 complex is localized in the plasma membrane.** *A*, HEK cells transfected with GPR30 were subjected to live staining (*Live*) with GPR30 antibodies. Following fixation and permeabilization, cells were stained with pan-MAGUK antibodies, AKAP5 antibodies, or DAPI. *B*, HEK cells transfected with GPR30 and PSD-95 were subjected to fixed staining (*Fixed*) and live staining (*Live*) with GPR30 antibodies. Following fixation and permeabilization, cells were stained with pan-MAGUK antibodies (*MAGUK*) or DAPI. *C*, HEK cells transfected with GPR30ΔSSAV and PSD-95 were subjected to fixed staining and live staining with GPR30 antibodies. Following fixation and permeabilization, cells were stained with pan-MAGUK antibodies or DAPI. The results are representative of experiments performed at least three times, and the individual and merged images (*Merge*) were collected using a Nikon Eclipse confocal microscope, ×60 objective, and 50-μm zoom. The *arrows* indicate protein colocalization (*yellow*).

was very similar to that coprecipitated by human β1AR in these cells, which was reported to interact through its PDZ motif with SAP97 (Fig. 4*A*, *lane 9*) (23). Indeed, both human GPR30 and β1AR coprecipitated SAP97 from these cells (Fig. 4*A*, *lanes 11* and *12*). Although the prototypic neuronal MAGUK PSD-95 is not expressed in HEK293 cells (23), this protein also coprecipitated with GPR30 in a PDZ motif-dependent manner when coexpressed with the receptor (Fig. 4*A*, *lanes 14* and *15*). Consistent with the above results, immunoprecipitation of native MAGUKs and, specifically, SAP97 coprecipitated GPR30 (Fig. 4*B*, *lanes 2* and *5*) but not GPR30ΔSSAV (Fig. 4*B*, *lanes 3* and *6*). HEK293 cells also express AKAP5 (Fig. 4*C*, *lanes 1* and *2*), and GPR30 also co-precipitated this protein (Fig. 4*C*, *lane 4*),

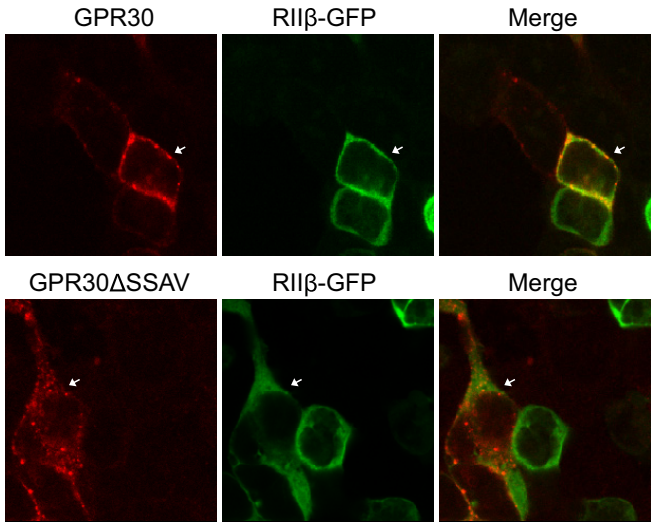

FIGURE 6. **The GPR30-MAGUK-AKAP5 complex is colocalized with the PKA RIIβ regulatory subunit in the plasma membrane.** HEK cells transfected with PKA RIIβ-GFP (*RIIβ-GFP*) together with GPR30 or GPR30ΔSSAV were subjected to live staining with M1 FLAG antibodies. The results are representative of experiments performed at least three times. The individual and merged images (*Merge*) were collected using a Nikon Eclipse confocal microscope, ×60 objective, and 50-μm zoom. The *arrows* indicate cells coexpressing PKA RIIβ-GFP either with GPR30 or GPR30ΔSSAV.

whereas GPR30ΔSSAV did not (Fig. 4*C*, *lane 5*). Therefore, GPR30 forms a PDZ-dependent complex with both a MAGUK and AKAP5.

We also assessed whether native GPR30 in MDCK cells (Fig. 4*D*, *lanes 1* and *3*) forms a complex with a native MAGUK and AKAP5. Indeed, immunoprecipitation of native MAGUKs and AKAP5 from these cells coprecipitated a small but significant amount of native GPR30 (Fig. 4*D*, *lanes 4* and *5*). Consistent with these results, immunoprecipitation of native GPR30 coprecipitated native MAGUKs (Fig. 4*D*, *lanes 6* and *7*). Therefore, both recombinant and native GPR30 form complexes with a MAGUK and AKAP5.

The GPR30-MAGUK-AKAP5 Complex Is Localized in the Plasma Membrane—To address the subcellular localization of the GPR30-MAGUK-AKAP5 complex, the proteins were imaged by confocal microscopy in HEK293 cells. Ectopically expressed GPR30 colocalized with native MAGUKs and AKAP5 specifically in the plasma membrane (Fig. 5*A*, *arrows*). To improve imaging of MAGUKs, GPR30 was coexpressed with PSD-95. Both fixed and live staining showed that GPR30 colocalized with MAGUK/PSD-95 exclusively in plasma membrane (Fig. 5*B*, *arrows*). In contrast, only limited, if any, colocalization was observed between GPR30ΔSSAV and MAGUK/PSD-95 following either fixed or live staining (Fig. 5*C*). Therefore, the GPR30-MAGUK-AKAP5 complex is localized in the plasma membrane. Consistent with these results, a PKA regulatory subunit IIβ (RIIβ)-GFP fusion protein (24) colocalized with GPR30 in the plasma membrane, whereas it did not colocalize with GPR30ΔSSAV (Fig. 6, *arrows*).

The GPR30-MAGUK-AKAP5 Complex Inhibits cAMP Production—We then investigated whether AKAP5 mediates GPR30 inhibition of cAMP production. To this end, HEK293 cells were nucleofected with an AKAP5-specific shRNA vector to knock down the protein, as described previously (25), or with scrambled shRNA. AKAP5 shRNA completely prevented GPR30 inhibition of FSK- and PGE2-stimulated cAMP production 48 and 96 h post-nucleofection, respectively, whereas GPR30 inhibition still occurred with scrambled shRNA (Fig. 7*A*). AKAP5 shRNA had no effect on the response to either FSK or PGE2 in the absence of GPR30 (Fig. 7*A*). Therefore, AKAP5 mediates GPR30 inhibition of cAMP production. We then determined the effect of pretreating cells with St-Ht31 (Promega), a stearated peptide that permeates the membrane and disrupts the interaction between AKAPs and PKA RII (26, 27). Consistent with the above results, 50 μM St-Ht31 attenuated GPR30 inhibition of FSK-stimulated cAMP production over that observed with 50 μM control peptide St-Ht31P (Fig. 7, *B* and *C*). By contrast, St-Ht31 had no effect over that of St-Ht31P on basal or FSK-stimulated cAMP production in the absence of GPR30 (Fig. 7*C*, *Mock*).

The GPR30-MAGUK-AKAP5 Complex Retains GPR30 in the Plasma Membrane—To address whether AKAP also regulates GPR30 cell surface localization, live staining of GPR30 was done on HEK293 cells pretreated with St-Ht31 or the control peptide St-Ht31P. Treatment with 50 μM St-Ht31 increased basal receptor endocytosis, whereas treatment with St-Ht31P (50 μM) had no effect (Fig. 8*A*). These results show that AKAP-RII mediates the retention of GPR30 in the plasma membrane.

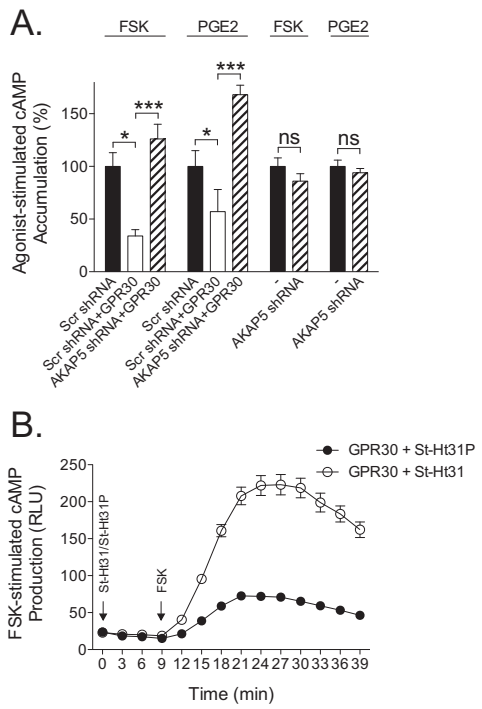

FIGURE 7. **AKAP-RII mediates GPR30 inhibition of cAMP production.** *A*, HEK cells were transfected by nucleofection without or with GPR30, scrambled (*Scr*) shRNA, or AKAP5 shRNA. After 48 h, cells were stimulated with 1 μM FSK for 30 min and, after 96 h, with 1 μM PGE_2 for 30 min. cAMP was measured with RIA, and the values are mean ± S.E. of at least three independent experiments, with each data point representing 3–16 measurements. *, $p < 0.05$; ***, $p < 0.001$. *B*, HEK cells were transfected with GPR30 and treated with 50 μM St-Ht31 or St-Ht31P and 1 μM FSK. The result, shown as relative light units (*RLU*), is representative of three experiments, with each data point being the mean ± S.E. of 24 measurements. *C*, HEK cells were transfected without (*Mock*) and with GPR30 and treated with 50 μM St-Ht31 or St-Ht31P and 10 μM FSK. *B* and *C*, cAMP was measured in real time with the GloSensor assay. The effect of St-Ht31 was determined. *I.e.* each measurement was normalized to basal (time = 0 min), and each data point was the mean ± S.E. of 24 measurements, with measurements including St-Ht31 normalized to those including St-Ht31P.

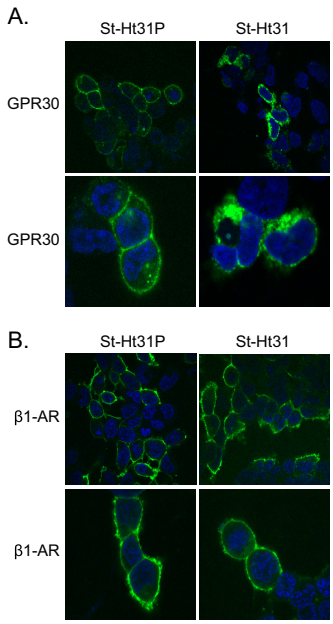

FIGURE 8. **AKAP-RII retains GPR30 in the plasma membrane.** *A* and *B*, HEK cells transfected with GPR30 (*A*) or β1AR (*B*) were preincubated with 50 μM St-Ht31 or St-Ht31P for 30 min and then subjected to live staining with M1 FLAG antibodies. In each panel, the bottom rows show enlarged cell images. The results are representative of experiments performed at least three times. The images were collected using a Nikon Eclipse confocal microscope, ×60 objective, and 50-μm zoom.

St-Ht31 had no effect on basal β1AR endocytosis (Fig. 8*A*), consistent with this receptor requiring AKAP5 for recycling following agonist stimulation (28).

DISCUSSION

Cyclic AMP is a central second messenger in cell signaling and physiology that is regulated by GPCRs through their coupling to G_s and $G_{i/o}$, mediating stimulation and inhibition of AC, respectively. This study outlines a new receptor mechanism for inhibiting cAMP production (Fig. 9) where the GPR30 C-terminal type I PDZ motif enables the receptor to form a plasma membrane complex with a MAGUK and AKAP5. Through AKAP5, this complex constitutively inhibits cAMP production in response to a heterologous agonist (*e.g.* PGE2, ISO, and FSK) independently of $G_{i/o}$ and retains the receptor in the plasma membrane. This is the first observation of a GPCR constitutively inhibiting cAMP production through such a protein complex, and, therefore, this presents a new mechanism of receptor coupling. Considering that this protein complex is capable of recruiting numerous signaling proteins, including protein kinases and phosphatases, this discovery opens up new opportunities to study receptor-regulated cAMP signaling in general as well as to resolve controversies currently surrounding GPR30 specifically.

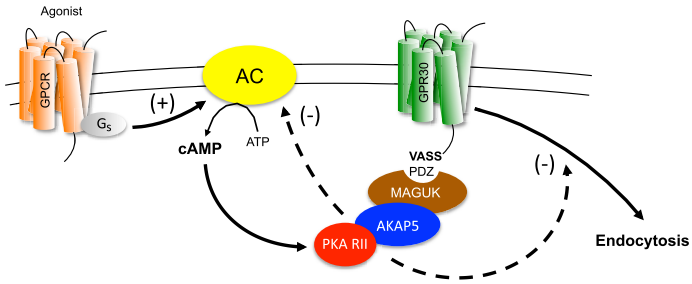

FIGURE 9. **Model of GPR30-MAGUK-AKAP5-mediated inhibition of cAMP production.** GPR30 (*green*) constitutively interacts via its C-terminal PDZ motif (SSAV) with one of the PDZ domains of a MAGUK (*brown*), and the MAGUK interacts with AKAP5 (*blue*). AKAP5, in turn, binds the PKA RII regulatory subunit (*red*). Agonist stimulation of a heterologous G_s-coupled GPCR (*orange*) stimulates (+) cAMP production, which leads to activation of AKAP5-RII in the GPR30 complex. This, in turn, leads to PKA phosphorylation and inhibition (−) of AC (*yellow*) and attenuation of cAMP production. AKAP5-RII also causes PKA phosphorylation of GPR30, which leads to inhibition (−) of basal receptor endocytosis and retention of the receptor in the plasma membrane.

We identified SAP97 as one endogenous MAGUK with which GPR30 interacts in a PDZ-dependent manner in HEK293 cells. Although PSD-95 is not expressed endogenously in HEK293 cells (23), we found that GPR30 also interacts with this MAGUK when coexpressed ectopically with GPR30 in these cells, as reported previously (13). Therefore, GPR30 is able to interact with more than one type of MAGUK. GPR30 adds to a growing list of GPCRs that form PDZ-dependent plasma membrane complexes with MAGUKs, including β1AR (23, 29, 30), β2AR (31), the 5HT2A receptor (32), the 5HT2C receptor (33), corticotropin-releasing factor receptor 1 (34), and the somatostatin subtype 1 receptor (35).

The GPR30-MAGUK complex also contains AKAP5. AKAPs constitute a family of proteins that share the ability to bind the PKA RII regulatory subunit (36). AKAP5 is also known to interact with SAP97 via an alternatively spliced polybasic sequence, termed i3 (37). Therefore, SAP97 potentially bridges the interaction of receptors containing type I PDZ motifs with AKAP5. Through such coupling, AKAP5 could bring PKA into close proximity with GPCRs and their effectors to regulate local cAMP signaling (17, 18). β1AR and β2AR are the only GPCR that have, so far, been shown to form such a complex, which interacts with AKAP5 via SAP97 and PSD-95 (23, 31). The ionotropic AMPA-type glutamate receptor subunit GluR1 also forms a PDZ motif-dependent complex with MAGUKs and AKAP5 (15, 16). Here we show that GPR30 is an additional GPCR with such coupling.

Deletion of the GPR30 PDZ motif reduced the ability of the receptor to inhibit cAMP production. The same effect was observed by knocking down AKAP5 and by dissociating AKAP and RII with St-HT31. Therefore, we believe that it is AKAP5-RII in the receptor complex that is responsible for this inhibitory effect. The timeframe in which St-Ht31 interrupted the inhibitory coupling suggests that this effect involves protein-protein interaction and/or covalent modification. AKAP5 is known to directly interact with AC5 and AC6 and scaffold them to AMPA receptors (39), and AKAP5-bound RII causes phosphorylation and inhibition of these enzymes (40). Furthermore, AKAP9/Yotiao directly inhibits AC2 and AC3 (41). Therefore, AKAP5 may bring AC into close proximity with GPR30 for the receptor complex to inhibit cAMP production.

Deletion of the PDZ motif in GPR30 and treatment with St-Ht31 also increased basal receptor endocytosis. Again, the timeframe in which St-Ht31 caused the loss of membrane receptors suggests that this effect also involves protein-protein interaction and/or covalent modification. In β1AR, AKAP5-RII mediates agonist-promoted phosphorylation of the receptor at Ser-312 in the third intracellular loop, which is necessary for the receptor to enter a recycling pathway and resensitize the receptor following agonist-promoted internalization (28). A similar mechanism occurs with AMPA receptors where AKAP5-RII mediates phosphorylation of Ser-845 in GluR1, and this phosphorylation also favors recycling of the receptor following endocytosis (42, 43). GPR30 contains a PKA phosphorylation consensus motif at Ser-166 in the second intracellular loop. However, if GPR30 is a substrate for AKAP-RII, the consequence of such phosphorylation may be different from β1AR because St-Ht31 increased basal internalization of GPR30, whereas it had no effect on the basal localization of β1AR.

The GPR30 PDZ motif may also participate in postendocytic receptor sorting because deleting the motif apparently increased the amount of receptors colocalized with the endosomal marker EEA1. Cheng *et al.* (44) showed that constitutively internalized GPR30 reached recycling compartments. However, these receptors did not recycle but, instead, targeted the trans-Golgi network and proteasomal degradation.

Our results have direct implications on several of the controversies surrounding GPR30. First, the interaction of GPR30 with AKAP5 opens up new ways to try to understand receptor coupling to cAMP signaling. Second, our results address the specificity and efficacy of receptor agonists reported currently and present new avenues by which this receptor system may be targeted therapeutically. Third, we show that deleting the PDZ motif influences GPR30 subcellular localization, a clear issue of contention with some investigators claiming that GPR30 is localized exclusively in the endoplasmic reticulum (2), whereas others have shown that receptors can clearly be identified in the plasma membrane (13, 19, 45–47). Interestingly, endoplasmic reticulum localization was concluded using a GPR30 construct fused at the C terminus with GFP (2), a modification that has been shown previously to alter trafficking of both GPR30 (46) and GluR1 from this compartment (38) and that we show here

would likely interfere specifically with PDZ-dependent GPR30 trafficking. Whether this has any implications for G-1, a substance selected using a GPR30-GFP construct (22) and used frequently used to define GPR30 specificity, remains to be determined.

In summary, we show that GPR30 exists in a complex with a MAGUK and AKAP5 and that this complex allows AKAP5-RII to constitutively inhibit cAMP production in response to heterologous agonists and independently of $G_{i/o}$ and retain receptors in the plasma membrane (Fig. 9). These results present a new mechanism by which a receptor can inhibit cAMP production and, therefore, could possibly impact several cAMP-elevating agonists. Considering that GPR30 has been implicated in cancer, cardiometabolic disease, and the central nervous system, this discovery is likely to present new therapeutic opportunities in these systems.

Acknowledgments—We thank Dr. Suleyman Bahouth for sharing AKAP5 and scrambled shRNA vectors and J. Daszkiewicz-Nilsson for expert technical assistance.

REFERENCES

1. Thomas, P., Pang, Y., Filardo, E. J., and Dong, J. (2005) Identity of an estrogen membrane receptor coupled to a G protein in human breast cancer cells. *Endocrinology* **146,** 624–632
2. Revankar, C. M., Cimino, D. F., Sklar, L. A., Arterburn, J. B., and Prossnitz, E. R. (2005) A transmembrane intracellular estrogen receptor mediates rapid cell signaling. *Science* **307,** 1625–1630
3. Filardo, E. J., Quinn, J. A., Frackelton, A. R., Jr., and Bland, K. I. (2002) Estrogen action via the G protein-coupled receptor, GPR30: stimulation of adenylyl cyclase and cAMP-mediated attenuation of the epidermal growth factor receptor-to-MAPK signaling axis. *Mol. Endocrinol.* **16,** 70–84
4. Filardo, E. J., Quinn, J. A., Bland, K. I., Frackelton, A. R., Jr. (2000) Estrogen-induced activation of Erk-1 and Erk-2 requires the G protein-coupled receptor homolog, GPR30, and occurs via trans-activation of the epidermal growth factor receptor through release of HB-EGF. *Mol. Endocrinol.* **14,** 1649–1660
5. Maggiolini, M., Vivacqua, A., Fasanella, G., Recchia, A.G., Sisci, D., Pezzi, V., Montanaro, D., Musti, A.M., Picard, D., and Andò, S. (2004) The G protein-coupled receptor GPR30 mediates c-fos up-regulation by 17β-estradiol and phytoestrogens in breast cancer cells. *J. Biol. Chem.* **279,** 27008–27016
6. Pedram, A., Razandi, M., and Levin, E. R. (2006) Nature of functional estrogen receptors at the plasma membrane. *Mol. Endocrinol.* **20,** 1996–2009
7. Otto, C., Rohde-Schulz, B., Schwarz, G., Fuchs, I., Klewer, M., Brittain, D., Langer, G., Bader, B., Prelle, K., Nubbemeyer, R., and Fritzemeier, K. H. (2008) G protein-coupled receptor 30 localizes to the endoplasmic reticulum and is not activated by estradiol. *Endocrinology* **149,** 4846–4856
8. Langer, G., Bader, B., Meoli, L., Isensee, J., Delbeck, M., Noppinger, P. R., and Otto, C. (2010) A critical review of fundamental controversies in the field of GPR30 research. *Steroids* **75,** 603–610
9. Kang, L., Zhang, X., Xie, Y., Tu, Y., Wang, D., Liu, Z., and Wang, Z. Y. (2010) Involvement of estrogen receptor variant ER-α36, not GPR30, in nongenomic estrogen signaling. *Mol. Endocrinol.* **24,** 709–721
10. Gros, R., Ding, Q., Sklar, L. A., Prossnitz, E. E., Arterburn, J. B., Chorazyczewski, J., and Feldman, R. D. (2011) GPR30 expression is required for the mineralocorticoid receptor-independent rapid vascular effects of aldosterone. *Hypertension* **57,** 442–451
11. Songyang, Z., Fanning, A. S., Fu, C., Xu, J., Marfatia, S. M., Chishti, A. H., Crompton, A., Chan, A. C., Anderson, J. M., and Cantley, L. C. (1997) Recognition of unique carboxyl-terminal motifs by distinct PDZ domains. *Science* **275,** 73–77
12. Romero, G., von Zastrow, M., and Friedman, P. A. (2011) Role of PDZ proteins in regulating trafficking, signaling, and function of GPCRs: means, motif, and opportunity. *Adv. Pharmacol.* **62,** 279–314
13. Akama, K. T., Thompson, L. I., Milner, T. A., and McEwen, B. S. (2013) Post-synaptic density-95 (PSD-95) binding capacity of G-protein-coupled receptor 30 (GPR30), an estrogen receptor that can be identified in hippocampal dendritic spines. *J. Biol. Chem.* **288,** 6438–6450
14. Funke, L., Dakoji, S., and Bredt, D. S. (2005) Membrane-associated guanylate kinases regulate adhesion and plasticity at cell junctions. *Annu. Rev. Biochem.* **74,** 219–245
15. Colledge, M., Dean, R. A., Scott, G. K., Langeberg, L. K., Huganir, R. L., and Scott, J. D. (2000) Targeting of PKA to glutamate receptors through a MAGUK-AKAP complex. *Neuron* **27,** 107–119
16. Bhattacharyya, S., Biou, V., Xu, W., Schlüter, O., and Malenka, R. C. (2009) A critical role for PSD-95/AKAP interactions in endocytosis of synaptic AMPA receptors. *Nat. Neurosci.* **12,** 172–181
17. Scott, J. D., Dessauer, C. W., and Taskén, K. (2013) Creating order from chaos: cellular regulation by kinase anchoring. *Annu. Rev. Pharmacol. Toxicol.* **53,** 187–210
18. Dessauer, C. W. (2009) Adenylyl cyclase-A-kinase anchoring protein complexes: the next dimension in cAMP signaling. *Mol. Pharmacol.* **76,** 935–941
19. Sandén, C., Broselid, S., Cornmark, L., Andersson, K., Daszkiewicz-Nilsson, J., Mårtensson, U. E., Olde, B., and Leeb-Lundberg, L. M. (2011) G protein-coupled estrogen receptor 1/G protein-coupled receptor 30 localizes in the plasma membrane and traffics intracellularly on cytokeratin intermediate filaments. *Mol. Pharmacol.* **79,** 400–410
20. Enquist, J., Skröder, C., Whistler, J. L., and Leeb-Lundberg, L. M. (2007) Kinins promote B_2 receptor endocytosis and delay constitutive B_1 receptor endocytosis. *Mol. Pharmacol.* **71,** 494–507
21. Berg, K. A., Clarke, W. P., Sailstad, C., Saltzman, A., and Maayani, S. (1994) Signal transduction differences between 5-hydroxytryptamine type 2A and type 2C receptor systems. *Mol. Pharmacol.* **46,** 477–484
22. Bologa, C. G., Revankar, C. M., Young, S. M., Edwards, B. S., Arterburn, J. B., Kiselyov, A. S., Parker, M. A., Tkachenko, S. E., Savchuck, N. P., Sklar, L. A., Oprea, T. I., and Prossnitz, E. R. (2006) Virtual and biomolecular screening converge on a selective agonist for GPR30. *Nat. Chem. Biol.* **2,** 207–212
23. Gardner, L. A., Naren, A. P., and Bahouth, S. W. (2007) Assembly of an SAP97-AKAP79-cAMP-dependent protein kinase scaffold at the type 1 PSD-95/DLG/ZO1 motif of the human β(1)-adrenergic receptor generates a receptosome involved in receptor recycling and networking. *J. Biol. Chem.* **282,** 5085–5099
24. Zhong, H., Sia, G. M., Sato, T. R., Gray, N. W., Mao, T., Khuchua, Z., Huganir, R. L., and Svoboda K. (2009) Subcellular dynamics of type II PKA in neurons. *Neuron* **62,** 363–374
25. Li, X., Nooh, M. M., and Bahouth, S. W. (2013) Role of AKAP79/150 protein in β1-adrenergic receptor trafficking and signaling in mammalian cells. *J. Biol. Chem.* **288,** 33797–33812
26. Carr, D. W., Stofko-Hahn, R. E., Fraser, I. D., Bishop, S. M., Acott, T. S., Brennan, R. G., and Scott, J. D. (1991) Interaction of the regulatory subunit (RII) of cAMP-dependent protein kinase with RII-anchoring proteins occurs through an amphipathic helix binding motif. *J. Biol. Chem.* **266,** 14188–14192
27. Vijayaraghavan, S., Goueli, S. A., Davey, M. P., and Carr, D. W. (1997) Protein kinase A-anchoring inhibitor peptides arrest mammalian sperm motility. *J. Biol. Chem.* **272,** 4747–4752
28. Gardner, L. A., Tavalin, S. J., Goehring, A. S., Scott, J. D., and Bahouth, S. W. (2006) AKAP79-mediated targeting of the cyclic AMP-dependent protein kinase to the β1-adrenergic receptor promotes recycling and functional resensitization of the receptor. *J. Biol. Chem.* **281,** 33537–33553
29. Hu, L. A., Tang, Y., Miller, W. E., Cong, M., Lau, A. G., Lefkowitz, R. J., and Hall, R. A. (2000) β 1-Adrenergic receptor association with PSD-95: inhibition of receptor internalization and facilitation of β 1-adrenergic receptor interaction with *N*-methyl-D-aspartate receptors. *J. Biol. Chem.* **275,** 38659–38666
30. He, J., Bellini, M., Inuzuka, H., Xu, J., Xiong, Y., Yang, X., Castleberry,

A. M., and Hall, R. A. (2006) Proteomic analysis of β1-adrenergic receptor interactions with PDZ scaffold proteins. *J. Biol. Chem.* **281,** 2820–2827
31. Joiner, M. L., Lisé, M. F., Yuen, E. Y., Kam, A. Y., Zhang, M., Hall, D. D., Malik, Z. A., Qian, H., Chen, Y., Ulrich, J. D., Burette, A. C., Weinberg, R. J., Law, P. Y., El-Husseini, A., Yan, Z., and Hell, J. W. (2010) Assembly of a β2-adrenergic receptor-GluR1 signalling complex for localized cAMP signalling. *EMBO J.* **29,** 482–495
32. Xia, Z., Gray, J. A., Compton-Toth, B. A., and Roth, B. L. (2003) A direct interaction of PSD-95 with 5-HT2A serotonin receptors regulates receptor trafficking and signal transduction. *J. Biol. Chem.* **278,** 21901–21908
33. Gavarini, S., Bécamel, C., Altier, C., Lory, P., Poncet, J., Wijnholds, J., Bockaert, J., and Marin, P. (2006) Opposite effects of PSD-95 and MPP3 PDZ proteins on serotonin 5-hydroxytryptamine2C receptor desensitization and membrane stability. *Mol. Biol. Cell* **17,** 4619–4631
34. Dunn, H. A., Walther, C., Godin, C. M., Hall, R. A., and Ferguson, S. S. (2013) Role of SAP97 protein in the regulation of corticotropin-releasing factor receptor 1 endocytosis and extracellular signal-regulated kinase 1/2 signaling. *J. Biol. Chem.* **288,** 15023–15034
35. Cai, C., Li, H., Kangasniemi, A., Pihlajamaa, T., Von Ossowski, L., Kerkelä, K., Schulz, S., Rivera, C., and Keinänen, K. (2008) Somatostatin receptor subtype 1 is a PDZ ligand for synapse-associated protein 97 and a potential regulator of growth cone dynamics. *Neuroscience* **157,** 833–843
36. Beene, D. L., and Scott, J. D. (2007) A-kinase anchoring proteins take shape. *Curr. Opin. Cell Biol.* **19,** 192–198
37. Nikandrova, Y. A., Jiao, Y., Baucum, A. J., Tavalin, S. J., and Colbran, R. J. (2010) Ca^{2+}/calmodulin-dependent protein kinase II binds to and phosphorylates a specific SAP97 splice variant to disrupt association with AKAP79/150 and modulate α-amino-3-hydroxy-5-methyl-4-isoxazole-propionic acid-type glutamate receptor (AMPAR) activity. *J. Biol. Chem.* **285,** 923–934
38. Sans, N., Prybylowski, K., Petralia, R. S., Chang, K., Wang, Y. X., Racca, C., Vicini, S., and Wenthold, R. J. (2003) NMDA receptor trafficking through an interaction between PDZ proteins and the exocyst complex. *Nat. Cell Biol.* **5,** 520–530
39. Efendiev, R., Samelson, B. K., Nguyen, B. T., Phatarpekar, P. V., Baameur, F., Scott, J. D., and Dessauer, C. W. (2010) AKAP79 interacts with multiple adenylyl cyclase (AC) isoforms and scaffolds AC5 and -6 to α-amino-3-hydroxyl-5-methyl-4-isoxazole-propionate (AMPA) receptors. *J. Biol. Chem.* **285,** 14450–14458
40. Bauman, A. L., Soughayer, J., Nguyen, B. T., Willoughby, D., Carnegie, G. K., Wong, W., Hoshi, N., Langeberg, L. K., Cooper, D. M., Dessauer, C. W., and Scott, J. D. (2006) Dynamic regulation of cAMP synthesis through anchored PKA-adenylyl cyclase V/VI complexes. *Mol. Cell.* **23,** 925–931
41. Piggott, L. A., Bauman, A. L., Scott, J. D., and Dessauer, C. W. (2008) The A-kinase anchoring protein Yotiao binds and regulates adenylyl cyclase in brain. *Proc. Natl. Acad. Sci. U.S.A.* **105,** 13835–13840
42. Ehlers, M. D. (2000) Reinsertion or degradation of AMPA receptors determined by activity-dependent endocytic sorting. *Neuron* **28,** 511–525
43. Oh, M. C., Derkach, V. A., Guire, E. S., and Soderling, T. R. (2006) Extrasynaptic membrane trafficking regulated by GluR1 serine 845 phosphorylation primes AMPA receptors for long-term potentiation. *J. Biol. Chem.* **281,** 752–758
44. Cheng, S. B., Quinn, J. A., Graeber, C. T., and Filardo, E. J. (2011) Down-modulation of the G-protein-coupled estrogen receptor, GPER, from the cell surface occurs via a trans-Golgi-proteasome pathway. *J. Biol. Chem.* **286,** 22441–22455
45. Filardo, E., Quinn, J., Pang, Y., Graeber, C., Shaw, S., Dong, J., and Thomas, P. (2007) Activation of the novel estrogen receptor G protein-coupled receptor 30 (GPR30) at the plasma membrane. *Endocrinology* **148,** 3236–3245
46. Funakoshi, T., Yanai, A., Shinoda, K., Kawano, M.M., and Mizukami, Y. (2006) G protein-coupled receptor 30 is an estrogen receptor in the plasma membrane. *Biochem. Biophys. Res. Commun.* **346,** 904–910
47. Lenhart, P. M., Broselid, S., Barrick, C. J., Leeb-Lundberg, L. M., and Caron, K. M. (2013) G-protein-coupled receptor 30 interacts with receptor activity-modifying protein 3 and confers sex-dependent cardioprotection. *J. Mol. Endocrinol.* **51,** 191–202